Developing and Refining the Use of Water Isotope Tracers in Hydrology and Paleohydrology

by

Yi YI

A thesis
presented to the University of Waterloo
in fulfillment of the
thesis requirement for the degree of
Doctor of Philosophy
in
Earth Sciences

Waterloo, Ontario, Canada, 2008

AUTHOR'S DECLARATION

I hereby declare that I am the sole author of this thesis. This is a true copy of the thesis, including any required final revisions, as accepted by my examiners.

I understand that my thesis may be made electronically available to the public.

Abstract

This thesis investigates stable isotope signals (i.e. $\delta^{18}O$ and $\delta^{2}H$) in various information carriers such as lake water and lacustrine sediments, aiming to develop and refine the use of isotope tracers in hydrology and paleohydrology studies.

Located at the confluence of the Peace and Athabasca Rivers at the western end of Lake Athabasca, the PAD is a key node in the Mackenzie River Drainage system, the single large freshwater source discharging into the Arctic Ocean from continental Northern America. The delta is one of the world's largest freshwater deltas, has hundreds of shallow lakes and wetlands, and has been regularly monitored for isotopic composition in surface water bodies over a 7-year period. Because of the hydrological significance of the delta, as well as the availability of a wealth of ancillary information collected by previous studies, the PAD serves as a natural laboratory to develop and refine the application of stable isotopes in understanding landscape hydrological conditions in present and past. The outcomes also provide critical information for the development of scientifically informed management strategies for water resources in the delta.

In the study of modern processes, a novel coupled isotope tracer method was developed to characterize the isotopic composition of input water to lakes. The method is based on coupling the well-known Craig-Gordon model, which describes the evaporative enrichment process for both isotopes, with the Local Meteoric Water Line to constrain the isotopic composition of input water to lakes. The application of this method in two sampling campaigns (2000 and 2005) demonstrated significant temporal changes in source water to PAD lakes at landscape scale. The results also revealed the previously underestimated role of snowmelt to the northern part of the delta.

In a laboratory culture experiment, effort was undertaken to understand the constant fractionation between aquatic cellulose and environmental water, which is routinely observed in field studies. This led to the development of a new conceptual characterization of the apparent cellulose-water relation that reconciles discrepancies among previous observations. This new interpretation supports the notion that oxygen in cellulose is fully inherited from CO_2 during photosynthesis, but that aquarium studies may incorporate an unintended artefact from CO_2 that has not undergone complete biochemically mediated exchange with water. The variable slope of the cellulose-water $\delta^{18}O$ relation observed in culture experiments is attributed to varying degree of exchange, related to the residence time of CO_2 in the water. This is in contrast to natural systems where long residence time of CO_2 is

likely to ensure full exchange, thus supporting the application of a constant apparent cellulose-water oxygen isotope fractionation in paleoenvironmental studies.

Insights gained from these studies were applied in a multiproxy paleolimnological investigation of a shallow lake in the central part of the delta near the shoreline of Lake Athabasca. The Craig-Gordon modelling approach was applied to quantitative interpretation of a cellulose $\delta^{18}O$ record from lake sediments. Constraints provided by interpretation of other proxies allowed the development of a semi-quantitative assessment of changes in lake water balance over the past one thousand years. The inferred hydrological history indicated significant shifts in the source of water to the lake, including persistent influence from Lake Athabasca during the Little Ice Age (~ AD 1540-1880), as well as rapid change during the last century that is unprecedented in the last millennium.

Overall, the thesis demonstrates our improved understanding of hydrological conditions based on various isotopic archives such as lake water and aquatic cellulose. New information acquired from these studies concerning the range and rate of hydrological variability in the present and past provides a fundamental baseline for evaluating the potential impacts of future climate change and human disturbance in the Peace-Athabasca Delta.

Acknowledgements

The completion of this thesis is due to the patient advice and kind help of many, many people.

Foremost among them are Drs. Tom W.D. Edwards and Brent B. Wolfe, who tirelessly taught me not only fundamentals, but also the art of scientific research. The depth and breadth of my education under them has been remarkable, and I am deeply grateful for every pint on Friday afternoon and generous support for scientific travel. Sincere thanks also extend to their wives, Marcia and Sheryl, for hosting students parties and narrating anecdotes of the daily life of "superduper" professors.

My advising committee, Drs. Roland I. Hall, James F. Barker deserve a hearty thank-you. They have been encouraging and supportive as I progressed through the Ph.D. program, and never been scared off answering silly questions really beyond their expertise (what is the difference between isotopes and diatoms? Well…). I also would like to express my gratitude to Dr. Jonathan Price for generously providing data from his *Sphagnum* experiment, and Drs. Anthony L. Endres and Joel R. Gat for constructive reviews of the thesis.

I would like to thank all people who helped me adjust to and adopt Canadian culture. In particular, Ken Clogg-Wright, "Mrs. and Mr. Falcone", Dave Porinchu, Joscelyn Bailey, Matt Woo showed me the fun part of daily life in and out of the office. It would be a rare day if I did not use some rules of thumb that they taught me.

The work presented here is collaborative in nature, and I would like to express my thanks to the people who have been involved in this research from various aspects. A big thank-you to Johan Wiklund, Nilo Sinnatamby and Robert Grandjambe for great team work in the field; thank to Trish Stadnyk-Falcone and Dörte Köster for taking over the responsibility of sampling when I could not be present in the field; thanks to Bill Mark for teaching me the nuts and bolts of mass spectrometers; thanks to every MBDer for the friendly research atmosphere every day; thanks to Bob Drimmie and the helpful staff of the Environmental Isotope Laboratory for conducting isotope analyses. Thanks also go to Corina McDonald and Lynn Hoyles for help in the aquarium experiments. I also would like to acknowledge Mike Morin of Wood Buffalo Helicopters for helicopter services. That was fun!!!

Many other folks have helped me in countless ways. Fu Dejian for his help in the matlab coding, John Johnston and Liu Zhifeng for their enthusiasm and guidance, Katherine LaHay for help in mineralogy, Lu Baohong for help in surface water hydrology, Jason Venkiteswaran, Miao Ziheng and many others for stimulating discussions on science. I also would like to express my thanks to Bronwyn Brock, Chen Pengfei, Dong Yan, Maija Heikkilä, Liu Zhanhong, Marlin Rempel, Jen Park, Randy Stotler for friendship and companionship.

Last and most importantly, my parents deserve a great deal of credit for the accomplishment of the thesis. I would not have made such a long journey without support and encouragement from them. On the other hand, as a "fresh PhD", I would also bear in my mind all the people encountered in scientific conferences and post-conference travelling, and the excitement of entering, in a large sense, the family of Isotope Hydrology.

Financial support for this Ph.D. program has been provided by University of Waterloo, NSERC Northern Research Chair and Discovery Grant programs, NSERC CRD grant, BC Hydro, Polar Continental Shelf Project and Environmental Isotope Laboratory at UW.

Table of Contents

List of Figures

List of Tables

Chapter 1
Introduction

1.1 Peace-Athabasca Delta (PAD)

The Peace-Athabasca Delta (PAD) in northern Alberta, Canada, is one of the largest freshwater deltaic landscapes (~3900 cm^2) in the world, located at the convergence of the Peace and Athabasca Rivers at the western end of Lake Athabasca (Figure 1-1). It is recognized by the international Ramsar Convention on Wetlands (Wetlands International, 2005) and the United Nations Educational, Scientific and Cultural Organization (UNESCO) for its hydrological, ecological, and cultural significance. The delta is an undulating hydrological complex, marked by intricate patterns of active and inactive channels, meander scrolls, and hundreds of shallow lakes and wetlands. Ecologically, the delta is home to large populations of muskrat, beaver and free-ranging woodland bison and provides essential feeding, staging and breeding habitat for a variety of waterfowl. Culturally, the delta hosted First Nations and Metis communities for ~200 years and played a crucial role in the success of the fur trade in Canada since the 1700s. From a historical point of view, the cultural prosperity of the region is believed to be strongly associated with the biological productivity, ecological diversity and hydrological variability in the delta.

1.2 Drivers of Change

As indicated by the name, a delta is an extremely dynamic system that is in a state of perpetual change. In general, there are two distinct factors driving changes in such a biologically productive but environmentally sensitive system. The foremost is natural forcing. Obviously, there is natural variation of hydroecology arising from atmosphere-hydrosphere-biosphere interactions. For example, the variation in climate will lead to increased or reduced flows in the river, and subsequently change the fluxes of water, sediments and nutrients brought into the delta, which are essential to biological activity and ecological structure and function. In other words, the intensity and frequency of flooding, which is believed to play an important role in building and shaping the deltaic landscape, change naturally because of climate-hydrology dynamics. The subsequent geomorphologic and hydrologic changes will eventually affect the biology and ecology in the delta.

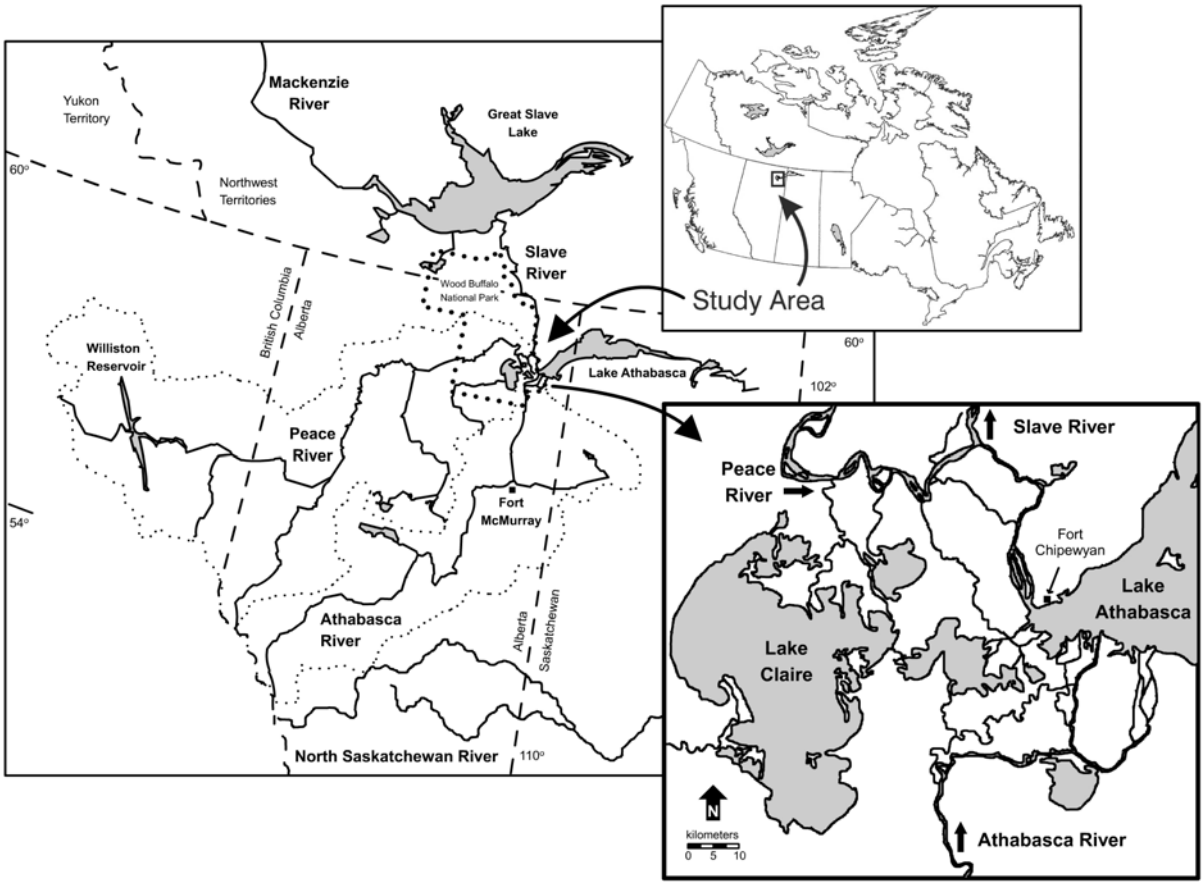

Figure 1-1 The map of study area including Peace River watershed, Athabasca River watershed, WAC Bennett Dam and Peace Athabasca Delta. The Peace and Athabasca rivers drainage basins are outlined. The detailed map of Peace Athabasca Delta showing major hydrological feature is expanded in the lower right panel.

Anthropogenic activity is another driver of change. More than half of the world's large river systems have been subjected to regulation and fragmentation of river flow (Nilsson et al., 2005). These mega-constructions have been proved to change hydrologic characteristics of rivers in many ways, such as discharge hydrograph, nutrient and sediment loading, and river water temperature. Unfortunately, human-induced disturbance on river systems, imposed on the aforementioned natural variability, often results in negative impacts on downstream wetlands and deltas (Junk, 2005). For example, flow regulation in the headwaters of the Peace River since 1968 for the hydroelectric power

generation, has been identified as a potentially important anthropogenic stressor for the PAD (PAD-PG, 1973).

1.3 Issues, Concerns and Previous Studies in the PAD

It is generally accepted among the scientific community that climate change is likely to be amplified in arctic and subarctic regions (Overpeck et al., 1997), and it is already apparent that climate-driven decline in glacier volumes in the Rocky Mountains has reduced late-summer flows of the Athabasca River during the past 40 years (Schindler and Donahue, 2006). On the other hand, instrumental precipitation records document a significant increase over the last 50 years in general across northern North America (Groisman and Easterling, 1994). The hydroclimatic consequences of these natural variations for the PAD are poorly understood.

Significant anthropogenic influence on the PAD is believed to have started in the 1960s with the construction of WAC Bennett Dam in the headwaters of the Peace River (Figure 1-1). The filling of the reservoir during 1968-1971, which coincided with a period of drought in western Canada, temporarily resulted in very low flows in the Peace River (Townsend, 1975). Although extensive ice-jam flooding occurred in 1972 and 1974, an extended period without major flooding between 1975 and 1995 led to concerns about the effects of on-going flow regulation on the ecological integrity of the delta (PAD-TS, 1996). Could these observed changes in the hydrological behaviour of the delta be solely caused by human activities? Or, was this an integrated consequence of natural variability and human disturbance? If so, did both drivers have negative effects? Or, was one negative, and the other positive? How could we separate changes induced by natural variability from anthropogenic impacts?

Over the past few decades, a series of studies were carried out to address these concerns and issues (PAD-PG, 1973; PAD-IC, 1987; PAD-TS, 1996; Gummer et al., 2000). Most of these studies focused on modeling flow regime and hydrological processes in the Peace River and its major distributary channels. An important outcome of these studies was the identification of ice-jam flooding as a critical factor in recharging the PAD, because ice-jams may provide the only mechanism that can bring water, sediments and nutrients to maintain hydroecological conditions in many perched basins and elevated regions (Prowse and Lalonde, 1996). Accordingly, the damped hydrograph of the Peace River (i.e. enhanced winter flow, but decreased spring and summer peak flow) due to river regulation appeared to be a primary factor responsible for the decline in ice-jam events and associated changes in the delta. However, under a scenario of changing climate, watershed snowpacks and peak spring

water levels are expected to decline and the snowmelt period is expected to initiate earlier and become less protracted as the increase of temperature progresses (Pietroniro et al., 2006). The decline in flood frequency may also be attributed to the natural forcing of climate (Prowse and Conly, 1998). Currently, regulation of Peace River and climate variability represent two competing hypotheses to interpret changes, although the perceived unusually dry conditions in the PAD over the last 40 years are more likely due to a combination of both.

1.4 PAD Stratigraphy Research Project

The existing instrumental records (since 1959) in the PAD are too short to objectively evaluate these two hypotheses. Although monitoring and modelling of contemporary conditions are important, retrieving information about the past from paleo-archives, such as lake sediments, is also critical to understand true natural variability, validate hydrological models and test both hypotheses. In an effort to enhance our understanding of the relative role of human disturbance and climate variability on hydroecological change in the PAD, an extensive multiproxy paleoenvironmental research project was initiated in 2000 (Wolfe et al., 2002; Hall et al., 2004). The so-called PAD Stratigraphy Project included spatial and temporal surveying of water, plants and surface sediments from lakes, wetlands and rivers; coring sediments from lake basins; and analyzing water and sediment for chemistry, biota and stable isotopes.

In the studies of modern processes, water isotope data and water chemistry data were combined to assess interactions between hydrology and limnology in targeted lakes that represent a broad hydrological gradient within the delta. An isotope-mass balance model was integrated with systematic water chemistry analysis to classify lakes along the hydrological gradient into four categories: open-, restricted-, closed- and rainfall-dominated basins (Wolfe et al., 2007). Open-drainage basins were identified as those with similar Evaporation/Inflow (i.e., E/I) ratios to major rivers, reflecting a permanent connection to distributary channels. Closed-drainage basins were defined by the high E/I ratios due to strong influence of evaporation. Restricted-drainage basins were lakes characterized by intermediate E/I ratios, high concentration of major ions (e.g., Na^+, K^+), high concentration of nutrients (e.g. dissolved nitrogen and dissolved phosphorus) and high concentration of chlorophyll. A fourth drainage type – rainfall dominated lakes – which are mainly located in the central portion of the delta, was identified because of the particular combination of E/I ratios and water chemistry. These lakes had similar water balance estimates to closed- or restricted-drainage basins, but had low

concentrations of silica and chlorophyll. The strong relationships identified between water balances and limnological conditions further suggests that past and future changes in hydrology are likely to be coupled with changes in water chemistry and, hence, the ecology of the aquatic environments in the PAD. Although these findings set up a useful framework for understanding hydrology over the landscape, the study also provoked more challenging questions such as the relative importance of various hydrological processes from regional (i.e., delta-wide) to local (i.e., lake-specific) scales. Recent advances in the understanding of hydroecological changes in the PAD have even begun to reveal spatial variability of responses to river influence. For example, the northern part of the PAD is relatively resilient to changing flow conditions of the Peace River, while the southern part of the delta is likely more sensitive to flooding from the Athabasca River (Wolfe et al., 2008).

In the paleoenvironmental studies, 11 lakes were cored and a wide variety of proxy indicators were investigated (Hall et al., 2004). For each individual lake, the multiproxy investigations led to a comprehensive interpretation of the hydroecological conditions within the lake and its surrounding area. For example, PAD5, currently classified as a closed-drainage basin, was used to represent the most elevated and the least flood-susceptible basin in the PAD. Interesting discoveries from the PAD5 lake sediments were the remarkable drying trend in the past 30 years and a severe dry period in the mid 1700s (Wolfe et al., 2005). The earlier dry period was believed to have been marked by a near-desiccation condition (even periodic desiccation), indicating an episode of very restricted water supply to upland basins. The paleolimnological interpretations were mainly drawn from diatom community composition and oxygen isotope signals preserved in sedimentary cellulose. The findings in PAD5 were also supported by magnetic susceptibility measurements in oxbow lake sediments, which was a key technique to reconstruct flood frequency (Wolfe et al., 2006). According to results from two oxbow lakes (PAD15 and PAD54) near the Peace River, flood frequency declined during the late 20th century and was relatively low during the 1700s. Overall, results from these lakes were consistent with an independent climate reconstruction that depicts cold and dry atmospheric conditions in the headwater region of Peace and Athabasca rivers during the 1700s, at the peak of the so-called Little Ice Age (LIA; Edwards et al., 2008).

Similar to the upland lake (PAD5) and oxbow lakes (PAD15 and PAD54), paleolimnological records from the southern part of the delta, such as PAD31 and PAD39, showed a drying trend during the 20th century, although it was more likely caused by geomorphological changes (Wolfe et al., 2008). However, back in the LIA, low-lying lakes, especially those in the southern part of the delta,

demonstrated a very different picture of hydroecological conditions. PAD31 was characterized as an open-drainage basin, suggesting pronounced river influence during the 1700s (Hall et al., 2004). Strong supporting evidence was provided by another low-lying lake near the shoreline of Lake Athabasca, which was believed to be periodically connected with Lake Athabasca during the LIA (Sinnatamby, 2006). There appeared to be disparate responses between low-lying lakes and upland lakes to a common climatic driver during the LIA. Nonetheless, a wealth of information on the past has been gleaned in the PAD Stratigraphy Project. Among stratigraphic profiles retrieved from numerous target lakes, there are similarities; more intriguingly there are also discrepancies that are challenging to reconcile.

In addition to intensive investigations of lake sediments, isotope analyses of a composite tree-ring chronology were also conducted in the headwater region and more recently within the PAD (Edwards et al., 2008; Bailey, 2008). Studies of the $\delta^{18}O$ and $\delta^{13}C$ signals preserved in tree-ring cellulose were aimed to provide independent climatic records, which will eventually facilitate the interpretation of lake sediments. Currently, a complete 1000-year reconstruction is available for the headwater region (Edwards et al., 2008), while the tree-ring chronology derived within the delta only extends back ~300 years (Bailey, 2008). In general, climatic conditions in the headwater region were consistent with the well-known pattern of Medieval Warm Period (MWP), Little Ice Age (LIA) and post-LIA climatic amelioration in the Northern Hemisphere extratropics (Jones et al., 2001). The reconstructed millennium temperature and relative humidity records indicated relatively warm and moist conditions between ~950 and 1530 (MWP) and in particular highlighted the Medieval Climate Anomaly between ~1100 and 1250. The MWP was followed by a shift toward cold and dry atmospheric conditions between ~1530 and the late-1880s (LIA). From ~1900 to the present, the reconstructed climate history suggested a return to relatively moist and warm conditions, similar to that of the late MWP.

Overall, a wealth of information was available for the delta after five years of the project and our understanding of on-going change has been significantly improved by placing current conditions in the context of a long-term perspective.

1.5 Literature Review on Other Studies in Isotope Hydrology and Paleohydrology

Similar to the PAD Stratigraphy Project, there are a number of investigations applying the same research strategy (i.e. inform paloehydrological interpretations by studying modern processes), but in different geographical regions. Following the seminal work by Gibson and Edwards (2002) in northern Canada, Leng and Anderson (2003) provided the first isotopic database of lake water from western Greenland; Diefendorf and Patterson (2005) conducted the first regional survey of surface water isotope composition in Ireland; Mayr et al. (2007) reported the first Local Meteoric Water Line and Local Evaporation Line representative for the semi-arid southern Patagonia by regionally sampling groundwater, surface waters and precipitation; more recently, Henderson and Shuman (in review) undertaken an intensive sampling campaign in the western United States. All these studies demonstrate the importance of characterizing local hydrological settings by using lake water isotope compositions, which are essential for understanding lacustrine isotope records as paleoclimate and paleohydrology proxies. Meanwhile, most of these studies proposed that comparison among lakes with different evaporative sensitivities within a region can be useful to provide regional context for the interpretation of sedimentary records. However, the in-depth analysis and discussion of modern lake water isotope values in these papers were largely limited to the spatial correlation with contemporary climatic conditions such as air temperature, precipitation amount and wind direction, with limited consideration of hydrological processes such as runoff generation and recharge.

There is a wide range of isotopic proxies suitable for paleohydrological studies in terrestrial environments, which include tree-ring cellulose, bone phosphate, minerals preserved in lake sediments, lacustrine organics (e.g. sedimentary cellulose) and speleothems. One important goal of investigating isotopic proxies is to infer isotopic compositions of the environmental water during the formation of the archives. Because environmental water in terrestrial environments typically undergoes evaporation, the interpretation of stratigraphic variation of these isotopic signals is far from easy and straightforward. Is the stratigraphic variation caused by change in precipitation conditions, which can be directly related to climatic parameters (e.g., temperature)? or caused by evaporative enrichment, which can be partially attributed to hydrological changes? The question remains a big challenge in the understanding of oxygen isotope profile from lacustrine archives. Edwards et al. (2004) demonstrated two comparable case studies to separate the primary effect of source water from

secondary effects of evaporation based on detailed knowledge of processes affecting the lake hydrology. It is possible to have a precise interpretation of oxygen isotopic variation in lacustrine sediments. On the other hand, some studies have suggested that lake isotope system may be so complex that it is almost impossible to translate the measured isotopic profile in lake sediments into absolute or even relative temperature variations without making significant assumptions (Leng and Marshall, 2004; Jones and Roberts, 2008).

Given different perspective on the interpretation of isotopic profiles, there was an emerging need to improve and refine the application of isotope techniques in hydrology and paleohydrology studies. As another contribution to the PAD Stratigraphy Project, this thesis will primarily focus on analysis and interpretation of contemporary and past hydrological conditions from an isotopic point of view.

1.6 Research Objectives

The overarching objectives of this thesis are to refine and improve isotope techniques and their application in a well-monitored natural laboratory – the Peace-Athabasca Delta – and to enhance our understanding of the current status of the delta by placing contemporary monitoring into a long-term context (~1000 years). The results will provide valuable information for sustainable environmental and water resource management. More specifically, the thesis is seeking to address the following research questions:

Ⅰ How can we infer hydrological processes with dual-isotope signals in lake water?

The contemporary hydrologic regime in the sub-arctic PAD is characterized by strong seasonality. The winter is marked by snowfall, accumulation, and redistribution of snow by wind. The subsequent snowmelt interval is brief and dominated by snowmelt runoff. During the summer, loss of water via evaporation and transpiration becomes a major hydrological process, but occasional large rainfall events can generate significant amounts of runoff and partially (or completely) compensate evaporative water loss. All of these can be investigated by stable isotope analysis in a $\delta^{18}O$-$\delta^{2}H$ space if a systematic sampling plan is carefully designed. $\delta^{18}O$ values are frequently used in the literature for qualitative and quantitative evaluation of these processes, while $\delta^{2}H$ values are generally considered as extra information because of the co-variations of $\delta^{18}O$ and $\delta^{2}H$. So, how could we use the extra information? Can we couple $\delta^{18}O$ with $\delta^{2}H$ to obtain more detailed hydrological

information? Can we quantitatively probe hydrological processes under some conditions by using dual-isotope tracers? These major questions are addressed in Chapter 2.

Ⅱ How does aquatic cellulose isotopically record environmental water?

Isotopic analyses of water in modern environments have proven to be a powerful technique to monitor hydrological variations. Unfortunately, paleo-water is seldom directly preserved; therefore for the purpose of paleohydrology reconstruction it is frequently necessary to infer past water isotopic composition from isotopic proxies. Aquatic cellulose in sediments has been broadly used as an oxygen isotope archive of lake water in paleoenvironmental investigations. Although there is no doubt that environmental water imparts signals during the isotopic labelling of aquatic cellulose, there are inconsistent views regarding how to retrieve information from the isotopic composition of cellulose. Is there a constant oxygen isotope fractionation between cellulose and environmental water? Is environmental water the only factor affecting the isotopic composition of cellulose? Ultimately, how does environmental water label cellulose isotopically? These questions drive the investigations in Chapter 3.

Ⅲ How can the knowledge and insight gained from modern process studies be applied to inform interpretation of a 1000-year stratigraphic record from the PAD?

Results of previous diatom-based investigations of a short sediment core form PAD9 revealed the possible existence of high water levels in Lake Athabasca during the 18th century, which is supported by historical maps and other evidence (Sinnatamby, 2006). However, this time was also marked by severe drought in perched basins like PAD5 (Wolfe et al., 2005). To reconcile this apparent discrepancy, a multiproxy investigation of lake sediment from PAD9 was carried out, with particular emphasis on the oxygen and carbon isotope analysis of sedimentary cellulose to reconstruct paleohydrology and nutrient cycling. Chapter 4 is aimed, in particular, at improving our understanding of past fluctuations in the level of Lake Athabasca and consequent effects on the hydrological behaviour of the delta.

Although individual chapters address separate questions in this order, answers to these questions collectively improve our understanding of hydrology and hydroecology in the PAD and contribute to

our understanding of the impacts of climate change and river water regulation and usage on water resources.

1.7 Thesis Organization

The remainder of this dissertation is composed of three main chapters each being self-contained manuscript for publication, followed by a synthesis chapter and appendices. Manuscripts that have been published (or are in submission) have been subjected to varying degrees of modification for the overall structure and context of the thesis. The appendix includes another manuscript, to which I contribute significantly, although it is independent of the PAD Stratigraphy Project. Chapters 2-4 logically progress from studies of modern processes to investigation in paleo-archives. The following briefs are provided to assist the reader in quickly grasping each chapter individually and building an overall connection among them.

Chapter 2: A Coupled Isotope Tracer Method to Characterize Input Water to Lakes

This chapter develops a new method to characterize isotope composition of input water to lakes by coupling measurements of lake water $\delta^{18}O$ with $\delta^{2}H$. Application of this method in two sampling campaign (2000 and 2005) in PAD demonstrates drastic temporal change in sources water to PAD lakes, and reveals the underestimated role of snowmelt to the northern part of the delta. This method is readily transferable to other environments where regional-scale understanding of recharge processes is desired but conventional hydrometric monitoring networks are absent.

Chapter 3: Evidence that unequilibrated CO_2 influences the $\delta^{18}O$ of cellulose in aquarium experiments

This chapter presents an empirical isotopic relation between oxygen isotope composition in cellulose and environmental water via autotrophically culturing *Ceratophyllum demersum* in aquaria. Comparison of this relation with previously reported results leads to a new mechanistic interpretation that reconciles differences among similar culture experiments, by invoking unequilibrated CO_2 as a source of oxygen. Importantly, it provides support for the use of a constant isotopic fractionation between cellulose and water in paleo-reconstructions, but also raise the possibility of unrecognized influence from atmospheric CO_2 in rapid aeration conditions.

Chapter 4: A multiproxy millennium reconstruction of hydroecology in a shallow delta lake, northern Canada: with an emphasis on stable isotopes

This chapter presents a multiproxy paleolimnological investigation of a shallow basin near the shoreline of Lake Athabasca. Results provide unprecedented insight into the range, variability and evolution of hydroecological conditions over the past 1000 years. Building on a rich source of quantitative understanding of the climatic conditions in the region provided by previous studies, the chapter attempts to model the changing water balance of the lake. This work showcases the recent advancement in our ability to interpret sedimentary cellulose $\delta^{18}O$ stratigraphy in the context of a multiproxy investigation. According to this reconstruction, conditions over the past several decades in this lake are analogous to those at the end of the Medieval Warm Period, but the rate of change in modern time appears to be unprecedented in the last millennium.

Chapter 2

A coupled isotope tracer method to characterize input water to lakes*

Summary We develop a new coupled isotope tracer method for characterizing the isotopic composition of input water to lakes, and apply it in the context of ongoing hydrological process studies in the Peace-Athabasca Delta, a large, remote, riparian ecosystem in the boreal region of western Canada. The region has a highly seasonal climate, with floodplain lakes typically receiving input only during the 4-6 month open-water season from varying proportions of spring snowmelt, summer rains and river flooding. These possible input sources have distinct ranges of isotopic compositions that are strongly constrained to a well-defined Local Meteoric Water Line, thus affording the opportunity to derive lake-specific estimates of the integrated isotopic composition of input waters after accounting for the effects of secondary evaporative isotopic enrichment. As shown by comparison of the results of isotopic surveys of delta lakes prior to freeze-up in 2000 and 2005, this isotopic characterization of input waters can be combined with other data and field observations to provide new insight into spatial and temporal variability in delta lake recharge processes. This includes evidence that summer rainfall in 2000 played an important role in replenishing shallow basins delta-wide, especially in the central low-lying region, compensating for below-average snow accumulation during the previous winter. In contrast, 2005 was marked by greater relative contributions from both snowmelt and river flooding because of high winter snow accumulation and a spring ice-jam that caused river floodwaters to enter some basins in the southern part of the delta. The method is readily transferable to investigations in other remote regions that are sparsely monitored by conventional hydrometric networks.

* Published as : Yi Y., Brock B.B., Falcone M.D., Wolfe B.B., Edwards T.W.D., 2008. A coupled isotope tracer method to characterize input water to lakes. *Journal of Hydrology* 350: 1-13.

2.1 Introduction

Understanding the relative roles of hydrological processes on lake water balances in large and remote freshwater ecosystems is important for their management but is challenging because approaches that depend upon conventional instrumentation may be impractical. Installation of hydrometric devices in ecosystems with numerous aquatic basins requires substantial investment and assumptions are frequently required to, for instance, close lake water balances. For basins located in deltas and river floodplains that receive multiple sources of water, lake level recorders may provide useful knowledge of water level increases but other independent hydroclimatic information is needed to identify the cause of the observed change. Furthermore, results derived from only a few instrumented sites may be difficult or inappropriate to extrapolate over complex landscapes where the relative importance of hydrological processes is expected to vary spatially.

In recent years, water isotope tracers have become increasingly utilized as an alternative approach for providing assessments of lake water balances in remote regions. For example, Gibson and Edwards (2002) conducted a systematic survey of lake water isotope compositions to understand regional variations in evaporation losses and water budgets associated with the climate gradient across the northern boreal treeline in Canada. More recently, Mayr et al. (2007) used water isotope tracers in the southern Patagonia of Argentina to characterize contemporary lake water balances with the purpose of informing paleolimnological investigations. In these and other studies, quantitative estimates of lake water balances are derived using variations of the Craig and Gordon (1965) linear resistance model that describes isotopic evaporative enrichment. Applications commonly utilize lake water oxygen and hydrogen isotope compositions separately, which frequently generates small differences in water balance estimates using the individual tracers. Although these differences are often attributed to analytical or model uncertainties, mass conservation dictates that lake water balances calculated from lake water oxygen and hydrogen isotope compositions must agree.

Here we develop a new approach to the application of water isotope tracers that preserves the fundamental assumption of mass conservation allowing additional hydrological information to be derived regarding the nature of source waters to lakes in the Peace-Athabasca Delta (PAD), Canada. This large freshwater ecosystem contains hundreds of shallow (most are <2 m) basins where rainfall, snowmelt and river water are important to sustain aquatic habitat but their relative roles over space and time are not well characterized. These investigations build upon quantitative assessment of lake water balances across the PAD, which identified distinct landscape sectors of hydrolimnological

conditions based on integration of isotope and chemistry analyses of lake water samples collected in October 2000 (Wolfe et al., 2007). In this previous study, as elsewhere, comparison of oxygen- and hydrogen-isotope estimated evaporation-to-inflow ratios revealed a small but systematic departure from the 1:1 line that was thought to emanate from uncertainties in model input values. We re-visit this dataset and utilize another from September 2005 to evaluate input water isotope compositions during two years characterized by very different hydrological and meteorological conditions. Results show marked spatial and temporal variability in input waters to lakes using our new coupled isotope tracer method, one that is readily transferable to other large, freshwater ecosystems.

2.2 Study Area

The Peace-Athabasca Delta (PAD) is a large (~3900 km^2) wetland complex located at the convergence of the Peace, Athabasca and Birch rivers at the western end of Lake Athabasca, northern Alberta, Canada (Fig. 2-1). The PAD can be subdivided into three deltaic sectors: the Athabasca sector to the south (~1970 km^2), the Peace sector to the north (~1680 km^2) and the much smaller Birch sector to the west (~170 km^2) (PADPG, 1973). Several large shallow lakes (Claire, Baril and Mamawi lakes) are located in the center of the PAD, where the three sectors coalesce (Fig. 2-1). The Peace sector lies to the north of these lakes and is a relict fluviodeltaic landscape that is covered by mature forests with bedrock inliers in the northeast. This sector is flooded only during major ice-jams that periodically develop on the Peace River. The southern Athabasca sector is an active delta of extremely low relief that frequently receives river floodwaters during both the spring thaw and open-water seasons. Ice-jam flooding of portions of the Athabasca sector occurred in the spring of 2005, preceding one of our lake water sample collections (September 2005).

There are numerous shallow lakes in the PAD, which span a broad hydrological spectrum. Based on previous studies incorporating water isotope tracers and limnological characteristics, basins have been categorized into four drainage types (Wolfe et al., 2007). Open-drainage basins are located mainly in the low-lying central portion of the delta where they frequently receive discharge from many of the rivers and creeks that constitute the complex channel network of the PAD. Closed-drainage basins are generally found in the Peace sector and receive widespread river water only during periodic ice-jam flood events on the Peace River, and thus, input from precipitation is an important source of water to these lakes. Restricted-drainage basins are located mainly in the Athabasca sector, where the input of river water is the primary hydrological process that controls lake

water balances. Rainfall-influenced basins are found mainly in the central portion of the delta adjacent to the large open-drainage basins and occupy shallow depressions in the landscape (depth <50 cm). Their water balances are similar to those of restricted-drainage basins but their source waters are dominated by summer precipitation.

Climate in the PAD is strongly seasonal. According to 1971-2000 climate normals at Fort Chipewyan, Alberta, (Weather Station ID 3072658; Environment Canada, 2004), mean annual air temperature is -1.9°C, mean January air temperature is -23.3°C and mean July air temperature is 16.7°C. Precipitation averages 391.7 mm annually, with about 59% falling as rain during the May-September period. Meteorological conditions preceding the two sample collections (October 2000 and September 2005) were different (Fig. 2-2). The winter of 1999/2000 was warm and dry (especially from January to April); rainfall was evenly distributed throughout the following summer. In contrast, the winter of 2004/2005 had much greater snowfall throughout the latter months of the season and greater rainfall in August.

2.3 Sampling and Analysis

Water samples for oxygen and hydrogen isotope analysis were collected from 62 lakes on 25 October 2000 and most of these same lakes (n = 54) were re-sampled on 14 September 2005 (Fig. 2-1). Samples were collected from approximately 10 cm below the surface at the center of each lake with the aid of a helicopter. All samples were sealed in 30 ml high-density polyethylene bottles and were analyzed at the University of Waterloo - Environmental Isotope Laboratory, where $^{18}O/^{16}O$ and $^{2}H/^{1}H$ ratios were measured using standard methods (Coleman et al., 1982; Drimmie and Heemskerk, 1993; Epstein and Mayeda, 1953). Results are reported in δ values, representing deviations in per mil (‰) from VSMOW on a scale normalized to values of Standard Light Antarctic Precipitation (-55.5‰ for $\delta^{18}O$; -428‰ for $\delta^{2}H$; Coplen, 1996). Analytical uncertainties are ±0.2 ‰ for $\delta^{18}O$ and ±2.0 ‰ for $\delta^{2}H$. To demonstrate the potential variability in input water isotope composition to lakes in the PAD, results from water samples collected over six years from two basins located in different hydrological settings (PAD 37 and PAD 54; Fig. 2-1) are also reported.

2.4 Theory

2.4.1 Isotopic labelling in the hydrological cycle

The distribution of water isotopes on the earth's surface (i.e., in precipitation and surface waters) is characterized by the existence of strong linear relations between δ^2H and $\delta^{18}O$ over a broad range of spatial and temporal scales, reflecting systematic mass-dependent isotope fractionation in the hydrological cycle (Rozanski et al., 1993; Gat, 1996; Gibson and Edwards, 2002). The most salient feature of the covariant behaviour between hydrogen and oxygen isotopes in the global water cycle is the Global Meteoric Water Line (GMWL), which is expressed by the linear function $\delta^2H = 8\delta^{18}O + 10$ (Craig, 1961). The slope reflects the dominant influence of temperature-dependent equilibrium fractionation of heavy isotope species between atmospheric vapour and condensing precipitation, while the linearity is consistent with the notion that, at the global scale, atmospheric moisture primarily arises from one large water source (i.e., the subtropic ocean surface) and undergoes progressive distillation during poleward atmospheric transport. The GMWL has proven to be an especially useful reference line for understanding spatial patterns in the variability of the isotopic composition of mean annual precipitation (Rozanski et al., 1993). Analogous labelling of precipitation occurs at local scale in the form of Local Meteoric Water Lines (LMWLs), reflecting temporal variability in the isotopic composition of local precipitation. LMWLs commonly lie close to the GMWL, usually with a lower slope because of raindrop re-evaporation and kinetic effects during snow formation (Rozanski et al., 1993).

The isotopic composition of water that has undergone evaporation diverges from the GMWL (or LMWL) and the variation of hydrogen- and oxygen-isotope signals in surface waters is systematic because of mass-dependent fractionation that occurs during isotopic enrichment. Typically, the isotopic compositions of neighbouring water bodies receiving input water similar in isotopic composition cluster along a well-defined linear trajectory termed a Local Evaporation Line (LEL). In $\delta^{18}O$-δ^2H space, the slope of the LEL usually ranges between 4 and 6 and is primarily controlled by local atmospheric conditions including relative humidity (h), temperature (T) and the isotopic composition of atmospheric moisture (δ_A) (Gibson et al., in press). Moreover, the relative position of a given lake along the LEL is strongly associated with the water balance of the lake (Gonfiantini, 1986; Gat, 1996; Gibson and Edwards, 2002). Overall, the existence of two linear trends in $\delta^{18}O$ - δ^2H space allows differentiation of meteoric water from surface water that has undergone secondary isotopic enrichment due to evaporation.

2.4.2 Isotope-mass balance modelling

Quantitative investigations of lake water balances using water isotope tracers have been based on a conceptual framework incorporating individual water budget components in $\delta^{18}O$-$\delta^{2}H$ space (Fig. 2-3). For any given lake, δ_L, δ_E and δ_I represent the isotopic composition of the lake water, evaporative flux from the lake and the input water to the lake, respectively. δ_I is commonly estimated by the intersection of the LMWL with the best-fit line through a time-series of lake water isotope compositions or a spatial distribution of lake water isotope compositions in a watershed (e.g., Gibson et al., 1993). According to mass conservation, δ_E should lie on the extension of the LEL to the left of the LMWL. Also shown in Figure 2-3 is the isotopic composition of atmospheric moisture δ_A and the limiting isotope composition δ^*, which is the maximum isotopic enrichment attainable under local atmospheric conditions when a water body approaches desiccation. δ^* is independent of hydrological conditions (i.e., δ_L and δ_I) but related to atmospheric conditions (i.e., h, T and δ_A; Welhan and Fritz, 1977; Allison and Leaney, 1982). Theoretically, regardless of the hydrological complexity of a landscape, the isotopic composition of all lakes in an area with similar atmospheric conditions will converge towards δ^*.

2.4.3 Isotopic composition of evaporated vapour (δ_E)

Evaporated flux is a critical component for isotope mass-balance calculations but it is difficult to obtain samples directly for isotopic measurements. Studies have conventionally quantified δ_E using the Craig and Gordon (1965) linear resistance model, which includes a molecular diffusion layer bounded below by a "virtually saturated" layer and above by a turbulent transportation layer. The fluxes through the molecular diffusion layer are linearly proportional to the vapour concentration difference between the upper and lower boundaries. As such, the vapour flux of $^{1}H_2{}^{16}O$ (i.e., the common "light" water isotopologue) across the liquid-vapour interface is given by:

$$E = (C_s - C_a)/\rho = C_s(1-h)/\rho \qquad (2\text{-}1)$$

where C_s is the vapour concentration in the "virtually saturated" layer, C_a is the vapour concentration in the turbulent transportation layer, h is the relative humidity of the turbulent layer normalized to the water surface temperature and ρ is a resistance coefficient (Gonfiantini, 1986; Gat, 1996). Similarly, the vapour flux of heavy water isotopologues (i.e., $^{1}H^{2}H^{16}O$ or $^{1}H_2{}^{18}O$) across the same molecular diffusion layer is given by:

$$E_i = (C_s R_s - C_a R_a)/\rho_i = C_s (R_s - hR_a)/\rho_i \qquad (2\text{-}2)$$

Here, the subscript *i* designates water molecules bearing the heavy isotope species. R_s and R_a are the isotopic ratios of the water vapour in the saturated and turbulent layers, respectively. Since water vapour in the saturated layer should be in equilibrium with surface water at the saturated condition, R_s can be quantitatively related to the isotopic ratio of lake water (R_L) by the definition of equilibrium fractionation:

$$R_L / R_s = \alpha^* \qquad (2\text{-}3)$$

where α^* is the liquid-vapour equilibrium fractionation factor (i.e., $\alpha^*>1$). Isotopic fractionation is also commonly expressed by a separation term (ε^*), where $\varepsilon^* = \alpha^* - 1$ (for ε^* in decimal notation). The ε^* and α^* parameters are dependent on temperature and can be calculated using empirical equations (Horita and Wesolowski, 1994).

According to the definition of the isotopic ratio, R_E can be expressed as $R_E = E_i/E$. By combining Equations (2-1), (2-2) and (2-3), R_E can be expressed as:

$$R_E = \frac{\rho}{\rho_i} \cdot \frac{R_L/\alpha^* - hR_a}{1-h} \qquad (2\text{-}4)$$

Introducing ε_k, the kinetic separation term according to Craig and Gordon (1965) and Gonfiantini (1986):

$$\varepsilon_k = (1-h)\left(\frac{\rho_i}{\rho} - 1\right) \qquad (2\text{-}5)$$

Equation (2-4) can then be rewritten in δ-notation:

$$\delta_E = \frac{(\delta_L - \varepsilon^*)/\alpha^* - h\delta_A - \varepsilon_k}{1-h+\varepsilon_k} \qquad (2\text{-}6)$$

where δ_L and δ_A are the isotopic compositions of lake water and atmospheric moisture, and ε^* and ε_k are equilibrium and kinetic separation terms, as defined above. ε_k is estimated as a function of the relative humidity deficit, described elsewhere (Gonfiantini, 1986; Gibson and Edwards, 2002; Edwards et al., 2004). Note that Equation (2-6) is formulated for δ, ε and *h* values in decimal notation. Equation (2-6) can be further simplified on the basis of various assumptions (Welhan and

Fritz, 1977; Allison and Leaney, 1982; Ferhi et al., 1983; Gat, 1996; Yakir and Sternberg, 2000; Gibson and Edwards, 2002; Vallet-Coulomb et al., 2006) but we apply Equation (2-6) as it was presented by Gonfiantini (1986) and as shown here.

The quantitative evaluation of δ_E, as expressed in Equation (2-6), requires values for the isotopic composition of atmospheric moisture (δ_A), the isotopic composition of lake water (δ_L), relative humidity (h) and temperature (T). Of these parameters, δ_L, h and T can be measured routinely. Direct measurement of δ_A, on the other hand, is difficult because sample collection is logistically challenging and can introduce unintended isotopic fractionation. Given the dynamic nature of the atmosphere, single sample of atmospheric moisture may not accurately represent an integrated isotopic mean value, especially in regions with strong seasonality (e.g., Jacob and Sonntag, 1991). Alternatively, several indirect methods have been used to estimate δ_A. The most straightforward and frequently applied method is to assume isotopic equilibrium between evaporation-flux-weighted local precipitation and atmospheric moisture (Gibson, 2002). Although this method has been applied extensively in hydrological studies (Zuber, 1983; Gibson et al., 1993; Edwards et al., 2004), the assumption of equilibrium between precipitation and atmospheric moisture may not be valid if terrestrial recycling of evapotranspirative vapour is significant, as is the case in the Great Lakes region (Gat et al., 1994) and the Amazon basin (Gat and Matsui, 1991). A constant-volume pan can be used to derive δ_A (Welhan and Fritz, 1977; Allison and Leaney, 1982; Gibson et al., 1999) but this requires careful maintenance of the pan over the investigation period, which may not be practical in remote regions. Where available, studies have used an index lake (e.g., Dinçer, 1968) as a natural analogue of a constant-volume pan to generate a time-integrated estimate of δ_A.

Fortunately, our studies have identified a deep (>8m) closed-drainage lake (PAD 18; see Fig. 2-1) that is an excellent index lake for the PAD region. The lake is perched well beyond the possible influence of river flooding, and hence is fed solely by precipitation. Several years (2000 to 2006) of field observation have revealed minimal interannual variation in water level (±0.2m) and near-constant isotopic composition (-9.1 ± 0.5‰ for $\delta^{18}O$; -104 ± 2‰ for $\delta^{2}H$), as expected if input is closely compensated by evaporation (i.e., $E/I \approx 1$) (Hall et al., 2004; Falcone, 2007; Wolfe et al., 2007). Based on catchment area and meteorological records, the lake water has an estimated mean residence time on the order of 10 years, which suggests that the system integrates precipitation inputs over multi-annual time-scales. The mean annual isotopic composition of precipitation based on the nearest monitoring station (Fort Smith, Northwest Territories, 60°N 112°W; -18.8‰ for $\delta^{18}O$; -147‰

for δ^2H, Birks et al., 2004) agrees very closely with shallow groundwaters sampled directly in the catchment of PAD 18 in 2003 (-18.5‰ for $\delta^{18}O$; -146‰ for δ^2H). By solving Equation (2-6) for both isotopes on the basis that the isotopic composition and mass of annual liquid input and thaw-season vapour output from PAD 18 are identical ($\delta_E = \delta_I$), we obtain an estimate of δ_A (-26.6‰; -205‰). Notably, this is very close to δ_A (-25.4‰; -211‰) estimated previously by Wolfe et al. (2007) assuming equilibrium with thaw-season precipitation (Gibson and Edwards, 2002), and in good agreement with various "snapshot" estimates of δ_A that we have obtained from field experiments using constant-volume pans (Falcone, 2007). As a result, we apply the index lake method to infer δ_A in this paper.

2.4.4 General lake water balance

The water-mass and isotope-mass balances of a well-mixed lake at hydrological and isotopic steady-state are (Gonfiantini, 1986; Gibson and Edwards, 2002):

$$I = Q + E \tag{2-7}$$

$$I\delta_I = Q\delta_Q + E\delta_E \tag{2-8}$$

where I is the inflow rate ($m^3\ s^{-1}$), Q is the outflow rate ($m^3\ s^{-1}$) and E is the evaporation rate ($m^3 s^{-1}$). δ_I, δ_Q and δ_E represent the isotopic compositions of their corresponding hydrological components. Physical outflow does not cause isotopic fractionation, therefore outflow is isotopically equal to lake water (i.e., $\delta_Q = \delta_L$). By combining Equations (2-7) and (2-8), the evaporation-to-inflow (E/I) ratio can be expressed using the isotopic compositions of each water budget component:

$$E/I = \frac{\delta_I - \delta_L}{\delta_E - \delta_L} \tag{2-9}$$

Equation (2-9) has been used extensively to assess lake water balances (e.g., Dinçer, 1968; Gat and Levy, 1978; Gonfiantini, 1986; Gibson and Edwards, 2002; Vallet-Coulomb et al., 2006; Mayr et al., 2007).

2.5 Results and Discussion

2.5.1 Developing a coupled isotope tracer method to characterize lake-specific input water

Isotopic composition of water samples collected from two lakes, PAD 37 and PAD 54, over a six-year period (2000-2005) show characteristic linear patterns when plotted in $\delta^{18}O$-$\delta^{2}H$ space (Fig. 2-4a). Although all samples plot below the LMWL ($\delta^{2}H=6.7\delta^{18}O-19.2$; Birks et al., 2004), indicating varying degrees of the importance of evaporation to the lake water balances, their respective trajectories are subtly offset, suggesting these two lakes are fed by input waters with slightly different time-integrated isotopic compositions (δ_I). For PAD 54, the estimated δ_I (-22.9‰ for $\delta^{18}O$ and -173‰ for $\delta^{2}H$) is more depleted than that for PAD 37 ($\delta^{18}O$ = -19.2‰; $\delta^{2}H$ = -148‰), which is consistent with their different hydrological settings. PAD 54 is a deep (~4m) oxbow lake near the Peace River, which is known to receive isotopically-depleted input from both occasional river floodwater and snowmelt runoff generated from its large contributing area. On the other hand, PAD 37 is a shallow basin (<1m deep) in the central part of the PAD having minimal contributing catchment, and is thus more dependent on the input from rainfall, which is typically isotopically-enriched relative to snowmelt and river water. Indeed, at least one sampling episode appears to have captured almost complete replenishment of the lake by recent rainfall, judging by the sample point lying on the LMWL (Fig. 2-4a).

Variability in δ_I can also affect the accuracy of isotope-based water balance assessments (see Equation 2-9). In this environment, individual lakes (such as PAD 37 and PAD 54) possess their own evaporation lines anchored by lake-specific input water isotope compositions. Moreover, in a region with similar, well-mixed atmospheric conditions (i.e., h, T and δ_A), the limiting isotope compositions (δ^*) for different lakes, regardless of lake water balance status (including δ_I), are predicted to be the same. As a result, all lake-specific LELs of varying δ_I and slope will converge towards a common δ^* (Fig. 2-4b).

In previous isotope-mass balance studies of lakes in the PAD (Wolfe et al., 2007), variability in δ_I was recognized and estimated from the intersection of lake-specific LELs, drawn parallel to a regional predicted LEL, and the LMWL. This resulted in conservative estimates of δ_I with respect to variability about the mean annual isotope composition of precipitation and generated reasonable water balance estimates largely supported by limnological parameters. However, this approach is

obviously not consistent with the notion that all lakes in a region should tend towards the same δ^*. Below, we present a more rigorous mathematical solution for δ_I by assuming equivalent *E/I* ratios derived from both $\delta^{18}O$ and δ^2H signatures, thereby conserving both mass and isotopes.

As illustrated in Figure 2-4b, δ_I is expected to lie on the line between δ_L and δ_E. δ_I can be further constrained to the LMWL, since the input water is primarily meteoric water that has not undergone evaporation. Rain and snow samples collected during 2000-2005 showed good agreement with this LMWL (Falcone, 2007). This leads to the expression below that directly couples oxygen and hydrogen isotope signatures from Equation (2-9):

$$\frac{\delta^2H_I - \delta^2H_L}{\delta^2H_E - \delta^2H_L} = \frac{\delta^{18}O_I - \delta^{18}O_L}{\delta^{18}O_E - \delta^{18}O_L} \qquad (2\text{-}10)$$

With calculation of δ_E from Equation (2-6) and measurement of δ_L, Equation (2-10) can be used to solve for a unique pair of $\delta^{18}O_I$ and δ^2H_I values by incorporating the LMWL. Herein, we refer to this approach as a coupled isotope tracer method for estimating input water isotope composition to lakes. In the following section, we test this approach by characterizing input waters to lakes in the PAD sampled at the end of two thaw seasons having contrasting hydrological and meteorological conditions.

2.5.2 Lake water input composition in the Peace-Athabasca Delta for 2000 and 2005

Isotopic compositions of lake water sampled in October 2000 and September 2005 show similar linear trends offset from the LMWL in $\delta^{18}O$-δ^2H space but different distribution patterns (Fig. 2-5 a,b). For lake waters sampled in 2000 (Fig. 2-5a), the isotopic compositions range from -13.9‰ to -6.7‰ in $\delta^{18}O$ (-124‰ to -89‰ in δ^2H) with the exception of PAD 45, which has a low isotopic composition (-17.3‰ and -139‰ for $\delta^{18}O$ and δ^2H, respectively) and lies close to the LMWL. For 2005 (Fig. 2-5b), lake water isotope compositions range from -16.9‰ to -9.6‰ in $\delta^{18}O$ (-137‰ to -105‰ in δ^2H). In general, lake water isotope compositions in 2005 are more depleted than for 2000 and exhibit less scatter (R^2 is 0.88 for 2000 and 0.96 for 2005).

Applying the coupled isotope tracer method (Equation 2-10) to the 2000 and 2005 lake water isotope composition datasets yields lake-specific δ_I values, integrated over the thaw season, for each corresponding δ_L (Fig. 2-5a,b). Calculations revealed that δ_I values for the two years span discrete (though overlapping) spectra along the LMWL. In 2000, δ_I values vary from -22.7‰ to -12.0‰ in

$\delta^{18}O$ (-171‰ to -100‰ in $\delta^{2}H$), while δ_I values in 2005 range from -26.2‰ to -16.1‰ in $\delta^{18}O$ (-195‰ to -127‰ in $\delta^{2}H$).

Snowmelt, rainfall and river water are the three main sources of water to lakes in the PAD (Peters, 2003; Peters et al., 2006). It is expected that snowmelt and rainfall will affect all delta lakes to some extent, while influence from river water occurs perennially for lakes in direct connection with the channel network (i.e., open-drainage basins) and only during flood events for other lakes. These different types of source waters also bear distinct isotopic signatures based on extensive sampling of snow, rain and river water from 2000-2005. The isotopic composition of rain ranges from -20.5‰ to -13.9‰ for $\delta^{18}O$ (-168‰ to -112‰ for $\delta^{2}H$), whereas the isotopic composition of snow ranges from -30.6‰ to -19.4‰ for $\delta^{18}O$ (-233‰ to -141‰ for $\delta^{2}H$). While a wide range of isotopic compositions have been obtained for rain and snow, the isotopic composition of river water spans a much narrower range. The isotopic composition of the Athabasca River ranges from -19.3‰ to -17.5‰ for $\delta^{18}O$ (-154‰ to -142‰ for $\delta^{2}H$). The Peace River is isotopically depleted compared to the Athabasca River but also brackets a narrow range of values (-20.1‰ to -19.0‰ for $\delta^{18}O$; -159‰ to -150‰ for $\delta^{2}H$). For the convenience of illustration and discussion, we present the isotopic ranges of potential source waters to lakes (i.e., rain, snow and river water) as gray lines in Figure 2-5.

The relative influence of the three main source waters to lakes can be evaluated by the position of δ_I along the defined segments of the LMWL. Based on mixing, input water with a high proportion of snowmelt will tend to be more isotopically depleted than input water composed of a high proportion of rainfall. Therefore, lakes with low δ_I values, within the isotopic range of snow, would suggest that snowmelt plays an important role in the lake's water budget for that particular year, while higher δ_I values would suggest a greater proportion of rainfall contributing to these lake basins. Because of the narrow isotopic variability of river water, δ_I values for flooded lakes are expected to be similar to that of river water. This concept is readily demonstrated in the δ_I results for lakes with well-understood and relatively simple water budgets. For instance, a group of lakes (n=10) have previously been identified as rainfall-influenced basins based on their hydrolimnological characteristics and others, such as PAD 45 (Mamawi Lake; Fig. 2-1), are open-drainage basins that have permanent channel connections with major rivers (see Appendix D in Wolfe et al., 2007). The input to these basins is dominated by a single source of water (i.e., summer rainfall for the rainfall-influenced lakes and river water for PAD 45) and they have straightforward water budgets. δ_I results

for rainfall-influenced basins are positioned at the enriched end of the isotopic spectrum of input waters for both 2000 and 2005, whereas δ_I for PAD 45 averages -18.7‰ in $\delta^{18}O$ (-144‰ in δ^2H) over the two sample collection years, which is well within the range of its primary source of water, the Athabasca River (-19.3‰ to -17.5‰ for $\delta^{18}O$; -154‰ to -142‰ for δ^2H) (Fig. 2-5a,b).

At the other end of the input water isotope spectrum, some lakes are primarily influenced by snowmelt runoff during the spring thaw. Based on the δ_I results, PAD 15 and PAD 49 appear to be strongly influenced by snowmelt in 2000 and 2005, respectively (Fig. 2-5a,b). PAD 15 is a deep (~4m) oxbow lake possessing catchment attributes similar to PAD 54 described above. Its large contributing area likely also provides substantial isotopically-depleted snowmelt runoff to the lake. PAD 49 is a small, shallow (~0.6m), closed-drainage basin. Both of these lakes are surrounded by mature forests, which tend to accumulate snow during the winter, while the forest canopy intercepts direct rainfall during the thaw season. As a result, locally accumulated winter snowpack recharges these lakes rapidly during spring snowmelt and more gradually by sustained shallow groundwater flow over the thaw season. Examination of the spatial distribution pattern of δ_I reveals that lakes with the lowest δ_I values for the two sample collection years are all located in the northern Peace sector where closed-drainage basins are dominant and mature forest covers the landscape (Fig. 2-5c,d). Topographic relief from outcropping bedrock knolls in the northeast likely also captures snowdrifts. In comparison, δ_I results indicate that no basins from the southern Athabasca sector were strongly influenced by snowmelt in either 2000 or 2005 (Fig. 2-5e,f), consistent with the wetland-covered, active floodplain landscape containing mainly restricted-drainage basins in this portion of the PAD. Instead, a small number of lakes in the Athabasca sector may have received river floodwaters from an ice-jam on the Athabasca River during the spring of 2005, which likely also accounts for the narrower range of δ_I for these basins (of composition similar to the Athabasca River) compared to 2000 (Fig. 2-5e,f).

There are also notable differences in the distribution patterns of δ_I for Peace sector basins between collection years 2000 and 2005 (Fig. 2-5c,d). The average isotopic composition of the three main sources of water (i.e., rain, snow and river water) is -19.7‰ for $\delta^{18}O$ and -155‰ for δ^2H (Falcone, 2007; also shown in Fig. 2-5). For lakes sampled in 2000, 30 of 31 (97%) have δ_I values isotopically-enriched relative to this reference point (Fig. 2-5c). In contrast, only 9 of 30 (30%) lakes in 2005 have δ_I values that are higher compared to this reference point (Fig. 2-5d). As shown in Figure 2-2, the winter of 1999-2000 was relatively warm with less-than-average snowfall (especially from

January to April) and summer 2000 rainfall was near-normal. In contrast, snowfall in 2004-2005 was much higher than 1999-2000, although subsequent total summer rainfall was similar. Consistent with these meteorological conditions, our δ_I results indicate far greater relative importance of snowmelt to Peace sector lake water budgets in 2005 compared to 2000 (Fig. 2-5c,d).

2.6 Conclusions

A coupled isotope tracer method is described to characterize the dual-isotope composition of input water (δ_I) to individual lake basins. Estimation of δ_I is based on the assumption that input waters fall along a definable LMWL in $\delta^{18}O$-$\delta^{2}H$ space and that mass and isotopes are conserved during evaporation, which is described by the linear resistance model of Craig and Gordon (1965). We demonstrate the viability of this technique by applying it in the Peace-Athabasca Delta to show that lakes receive input derived from varying proportions of rainfall, snowmelt and river water, which can be systematically related to lake catchment characteristics and hydrological settings, as well as antecedent meteorological conditions.

Our case study is drawn from late thaw-season lake water sample collections during two years of contrasting hydrological and meteorological conditions. Lakes at this time are likely to closely approach hydrologic and isotopic steady-state, although a similar approach could be applied under non-steady-state conditions. The method has the added advantage of potentially combining the identification of δ_I with basin evaporation-to-inflow ratio assessments over large, hydrologically complex landscapes like deltas and floodplains from single point-in-time measurements, where widespread time-series isotopic sampling of individual basins is not feasible.

Acknowledgements

We would like to thank the staff of Wood Buffalo National Park for logistical support and Dorte Koester, Trish Stadnyk, Niloshini Sinnatamby and Johan Wiklund for field assistance. We are also grateful to Natalie St. Amour for compiling meteorological data for the PAD and the Environmental Isotope Laboratory - University of Waterloo for conducting stable isotope analysis of water samples. Funding for this research was provided by the British Columbia Hydro and Power Authority, the Polar Continental Shelf Project, the Northern Scientific Training Program of Indian and Northern Affairs Canada, the Canada Foundation for Innovation and Ontario Innovation Trust, and the

Northern Research Chair Program of the Natural Sciences and Engineering Research Council of Canada. We especially thank the reviewers and the editor for their helpful comments.

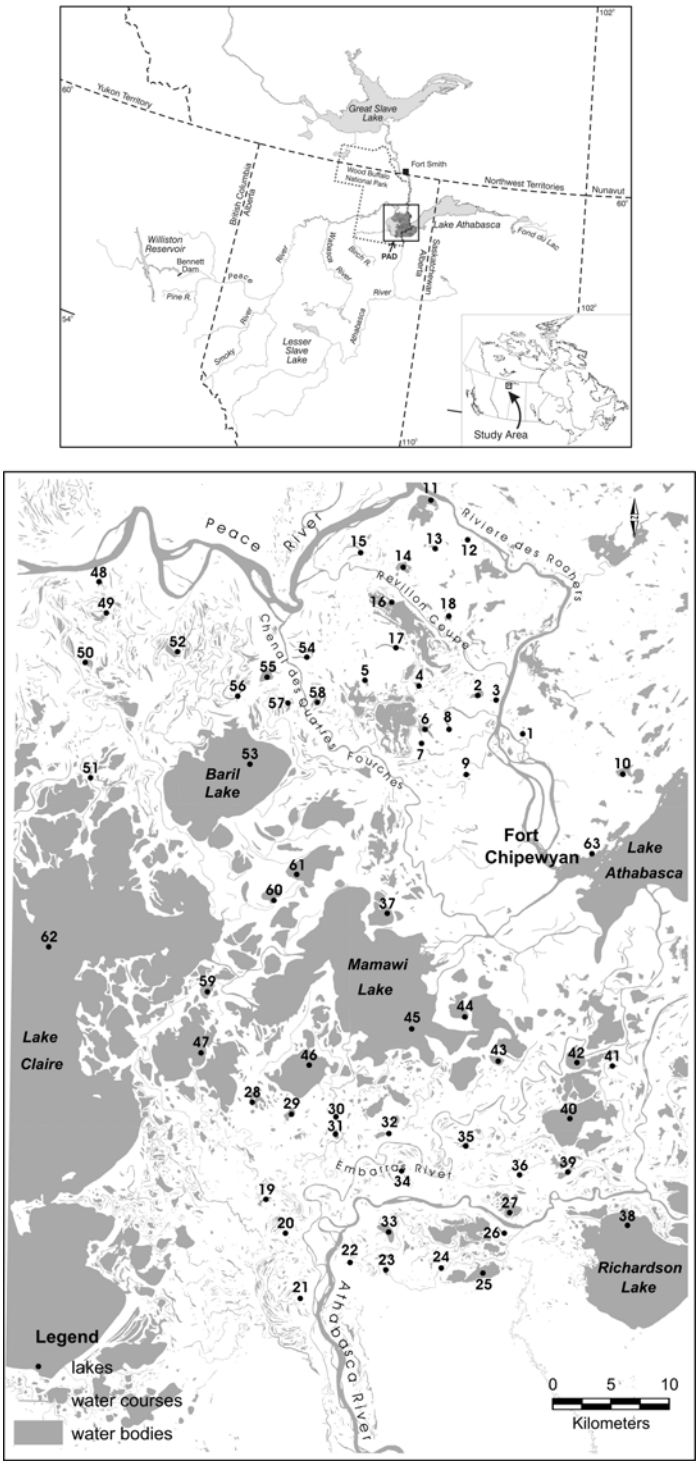

Figure 2-1 Location of the Peace-Athabasca Delta, Alberta, Canada and lake water sampling sites.

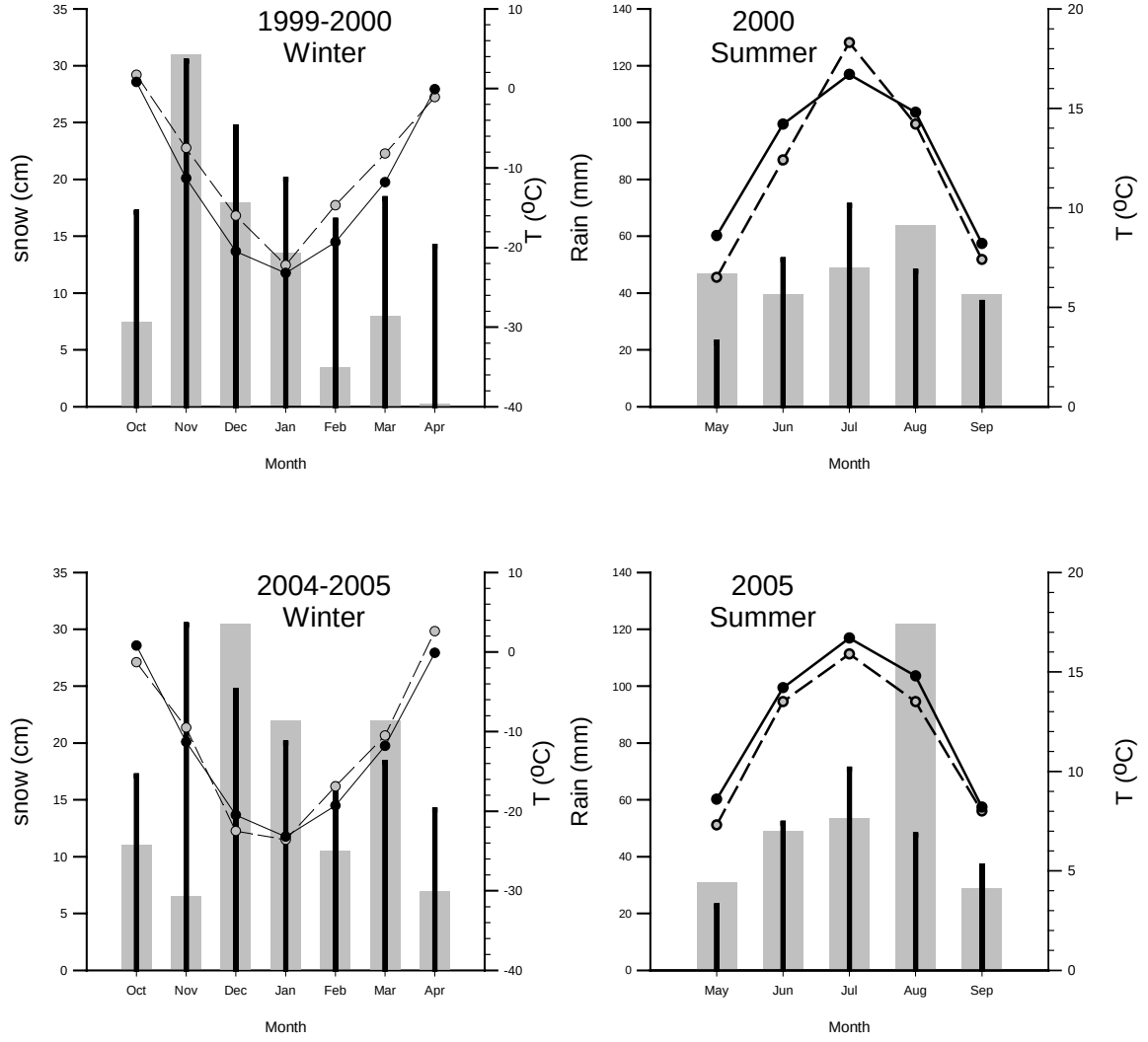

Figure 2-2 Winter and summer monthly mean temperature and accumulated precipitation for 1999/2000 and 2004/2005 compared to 1971-2000 climate normals. Climate normals are shown as solid circles (temperature) and bars (precipitation).

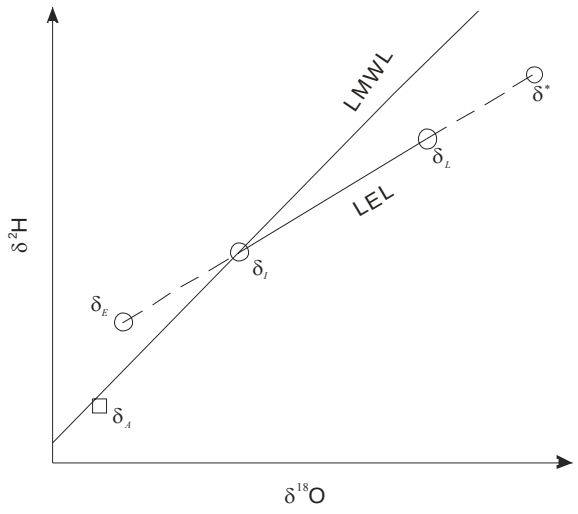

Figure 2-3 Schematic $\delta^{18}O$ - $\delta^{2}H$ diagram identifying key isotopic parameters used in isotope-mass balance studies. These include lake water isotope composition (δ_L), input water isotope composition (δ_I), isotopic composition of evaporated vapour from the lake (δ_E) and the limiting isotopic composition (δ^*). The atmospheric moisture isotope composition (δ_A) is also shown.

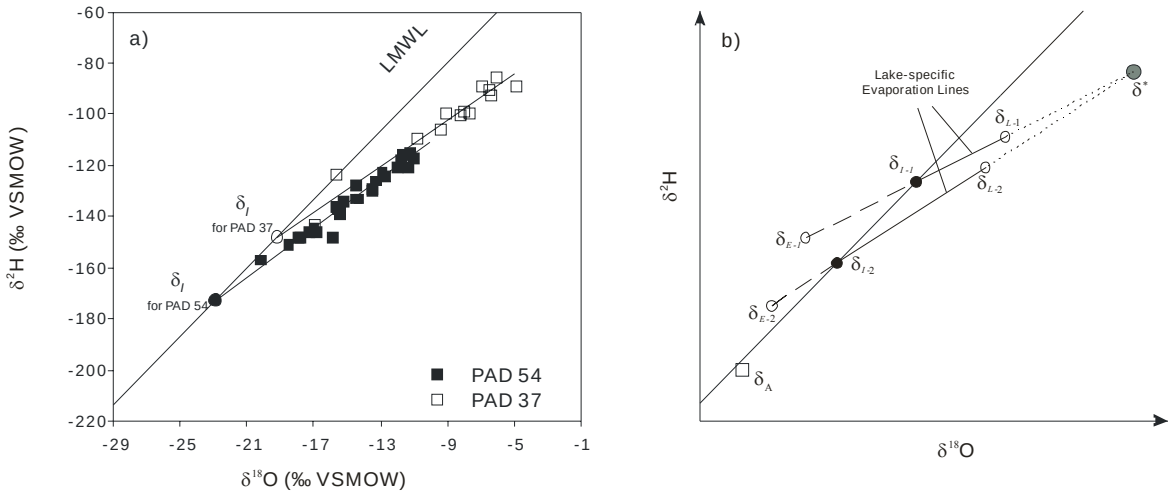

Figure 2-4 a) Lake water isotope compositions (2000 to 2005) for PAD 54 and PAD 37. Best-fit lines through these datasets intersect the LMWL at different points, suggesting that the lakes are fed by water of differing isotopic compositions. b) Schematic $\delta^{18}O$ - δ^2H diagram illustrating that the isotopic composition in a region that experiences similar atmospheric conditions will converge to the limiting isotopic composition (δ^*) with increasing evaporation, independent of δ_I.

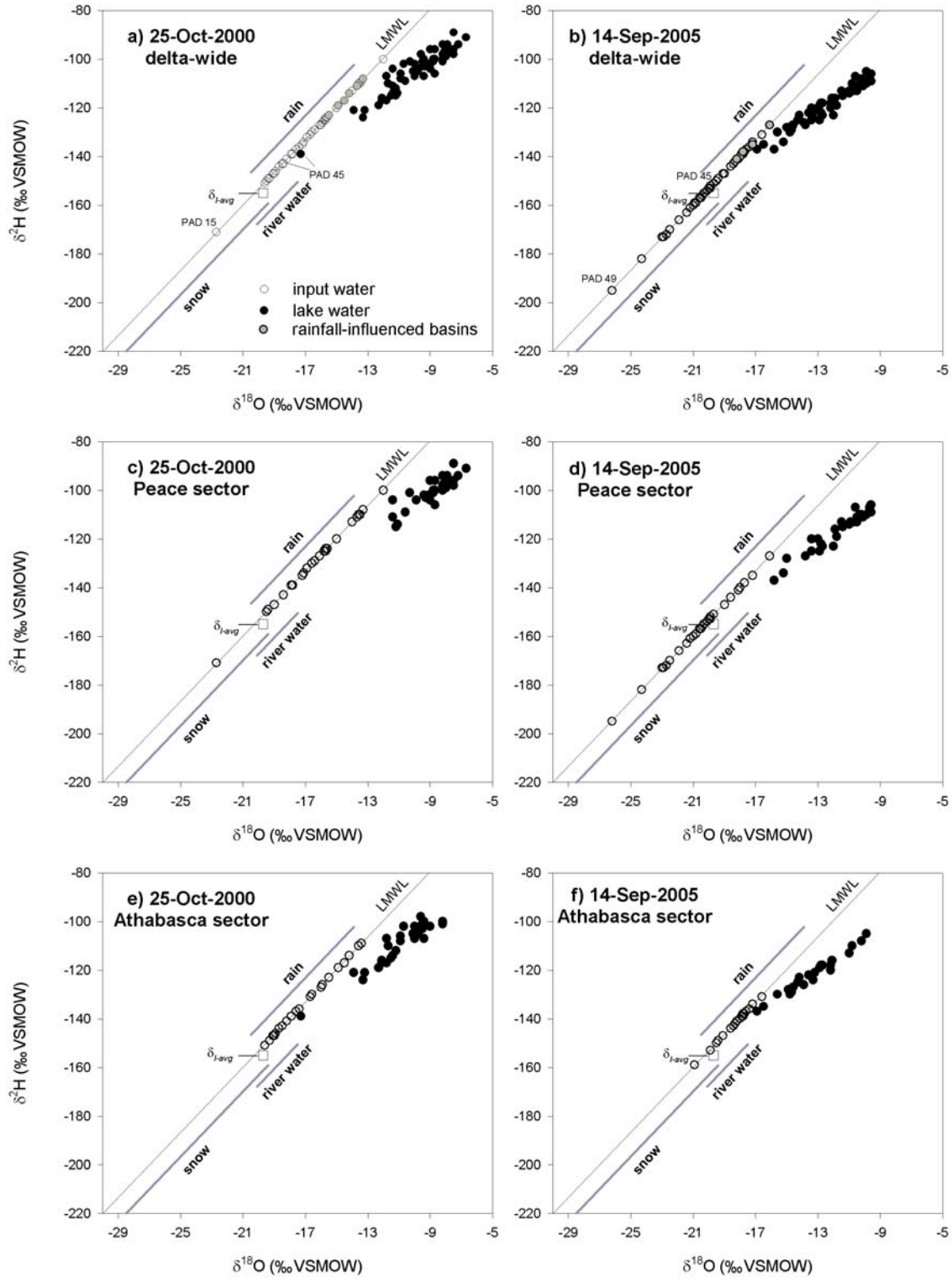
a) 25-Oct-2000
delta-wide
b) 14-Sep-2005
delta-wide
c) 25-Oct-2000
Peace sector
d) 14-Sep-2005
Peace sector
e) 25-Oct-2000
Athabasca sector
f) 14-Sep-2005
Athabasca sector
LMWL
rain
river water
snow
PAD 45
PAD 15
PAD 49
δI-avg
input water
lake water
rainfall-influenced basins
δ2H (‰ VSMOW)
δ18O (‰ VSMOW)
-80
-100
-120
-140
-160
-180
-200
-220
-29
-25
-21
-17
-13
-9
-5

Figure 2-5 $\delta^{18}O$-$\delta^{2}H$ diagrams with measured lake water isotope compositions and calculated lake-specific input water isotope compositions using Equations (2-6) and (2-10) (see Table 2-1 for input parameters). a) and b) Delta-wide results for 25-Oct-2000 and 14-Sep-2005. The gray circles are for previously identified rainfall-influenced basins (Wolfe et al., 2007). Labelled sites are mentioned in the text. c) and d) Peace sector results for 25-Oct-2000 and 14-Sep-2005. e) and f) Athabasca sector results for 25-Oct-2000 and 14-Sep-2005. Note that drier and more variable conditions in 2000 led to greater overall enrichment and scatter in isotopic composition of lake waters. Isotopic ranges for snow, rain and river water are also shown (gray lines), as well as the average isotope composition ($\delta_{I\text{-}avg}$) for the three water sources (Falcone, 2007). Note that these ranges lie on or are close to the LMWL, but are offset for graphic purposes only.

Table 2-1 Input parameters used in Equations (2-6) and (2-10) to calculate lake-specific input water isotope composition. Thaw season temperature (T) and relative humidity (*h*) are based on evaporation flux-weighted mean daily values measured at Fort Chipewyan, Alberta . Note, all parameters are in decimal expression when applied in Equation (2-6). For example, 60%=0.6 for *h* values; -18‰ = -0.018 for δ values and 10‰ = 0.01 for ε values.

	2000	2005	Reference
h(%)	65.7	69.7	Environment Canada (2004)
T (^{o}C)	12.0	11.4	
α^{*} (^{18}O, ^{2}H)	1.0105, 1.0943	1.0106,1.0951	Horita and Wesolowski (1994)
ε^{*} (^{18}O, ^{2}H) ‰	10.5 , 94.3	10.6, 95.1	
ε_k (^{18}O, ^{2}H) ‰	4.9, 4.3	4.3, 3.7	Gonfiantini (1986)
δ_A (^{18}O, ^{2}H) ‰	-26.6, -205	-26.6, -205	Index lake method (based on average *h* and T of 67.7% and 11.7 °C)

Chapter 3

Evidence that non-exchanged CO_2 influences the $\delta^{18}O$ of aquatic plant cellulose in culture experiments*

Summary We re-examined the oxygen isotope relation between aquatic plant cellulose and environmental water by growing *Ceratophyllum demersum* in an autotrophic culture experiment. Despite the exceptional linearity in these results, this relation does not describe constant fractionation between cellulose and water, which indicates environmental water was not the only factor affecting the isotopic labelling of cellulose in our experiment. We estimate the isotopic composition of unknown cellulose oxygen that is not controlled by environmental water, and the results indicate that CO_2 is the most likely source. Accordingly, we propose a new unifying conceptual characterization of the cellulose-water oxygen isotope relation, which partitions the cellulose oxygen into two components: one is from CO_2 that is re-labelled by biochemically mediated exchange with environmental water and the other is from CO_2 that has not undergone bio-exchange with the water. The observation of non-constant-fractionation relations in this and previous aquarium experiments can be quantitatively explained by unintentional introduction of non-exchanged CO_2 induced by forced aeration. However, the likelihood of full exchange between CO_2 and H_2O in natural waters supports the use of a constant cellulose-water oxygen isotope fractionation factor in field studies.

* Submitted to *Geochimica et Cosmochimica Acta* as: Yi Y., Wiklund J., Wolfe B.B., Edwards T.W.D., Evidence that non-exchanged CO_2 influences the $\delta^{18}O$ of aquatic plant cellulose in culture experiments.

3.1 Introduction

Oxygen isotope analysis of aquatic cellulose is a widely used technique for reconstructing lake water isotope composition from sediment records (Edwards and McAndrews, 1989; Edwards, 1993; MacDonald et al., 1993; Beuning et al., 1997, 2002; Buhay and Betcher, 1998; Anderson et al., 2001; Sauer et al., 2001; Abbott et al., 2003; Birks et al., 2007; see review of Wolfe et al., 2001). A fundamental basis for this technique is the assumption of a constant cellulose-water fractionation factor, yet laboratory investigations by culturing aquatic plants in aquarium experiments have typically yielded results that do not seem to support this notion (Cooper and DeNiro, 1989; Yakir and DeNiro, 1990; Sauer et al., 2001). Therefore, questions remain on mechanisms that lead to oxygen isotope labelling of aquatic cellulose.

Two mechanisms have been developed over the past 30 years to explain the oxygen isotope labelling of cellulose from environmental water. Epstein et al. (1977) first proposed that the typically observed cellulose-water isotope separation of ~27‰ is caused by quantitative incorporation of oxygen from two sources in isotopic equilibrium (1/3 from H_2O and 2/3 from CO_2) during photosynthate production. Given ~41‰ for the equilibrium isotopic separation between carbon dioxide and water at 25 ^oC, the $\delta^{18}O$ value in cellulose is expected to be ~27.3 ‰ (27.3 ‰ ≈ 2/3 x 41‰) higher than that of the environmental water, which is in good agreement with isotopic measurements on aquatic plants collected in the field. However, this model implies that the cellulose-water oxygen isotope separation should be sensitive to temperature, but no clear temperature dependency has been reported (Sternberg, 1989; Wolfe et al., 2001). The model would also require quantitative conversion of oxygen from CO_2 and H_2O to cellulose without any isotopic discrimination, which is unlikely. Moreover, the same cellulose-water isotope separation occurs in heterotrophic organisms such as tunicates (marine animals that produce cellulose in their body wall) (DeNiro and Epstein 1981) indicating the occurrence of isotopic fractionations mediated by biochemical processes. Alternatively, DeNiro and Epstein (1981) proposed that hydration of the carbonyl group during cellulose synthesis defines the overall isotopic fractionation between water and cellulose. This “Carbonyl Hydration Model” is supported by the observation that the carbonyl-water fractionation factor for oxygen in an *in vitro* acetone-water system is 1.027 on average (from 1.026 to 1.028) and is not subject to temperature effects (Sternberg and DeNiro, 1983). The model has become a widely accepted mechanism to justify the use of a constant cellulose-water oxygen isotope fractionation factor.

However, numerous culture experiments have failed to demonstrate the expected constant fractionation relation between cellulose and water (Sternberg et al., 1986; Cooper and DeNiro, 1989; Yakir and DeNiro, 1990; Sauer et al., 2001), which has potential implications for the use of aquatic cellulose as a water isotope archive in paleo-environrnental studies. These findings have fueled speculation that an additional source of oxygen, aside from water, may contribute to the isotopic labelling of aquatic cellulose. This has been demonstrated in heterotrophic experiments, where the additional source of oxygen, such as sucrose, glycerol and dextrose, can be well-constrained isotopically (Sternberg et al., 1986; Yakir and DeNiro, 1990), but the question remains unresolved under autotrophic conditions. Besides water, what might contribute oxygen to the formation of cellulose during photosynthesis? DeNiro and Epstein (1979) postulated that the isotopic composition of CO_2 may affect the isotopic composition of cellulose and tested the hypothesis by varying the $\delta^{18}O$ of CO_2 over a very large range (> 900‰) in a controlled growth experiment using wheat plants. Although minor $\delta^{18}O$ variations in cellulose did occur (8.5‰), they concluded that CO_2 undergoes complete equilibration with leaf water during CO_2 uptake and therefore no isotopic signal of CO_2 should be preserved in cellulose. Subsequent experiments conclusively demonstrated that oxygen gas (O_2) does not influence the isotopic labelling of cellulose (Cooper and DeNiro, 1989; Yakir and DeNiro, 1990), but Cooper and DeNiro (1989) and Yakir (1992) suggested that the role of ambient CO_2 in the synthesis of aquatic cellulose should be re-examined.

Here we present oxygen isotope results of another aquatic culturing experiment under autotrophic conditions. As in previously conducted experiments, the cellulose-water oxygen isotope correlation is remarkably linear, but deviates systematically from a constant-fractionation line. We argue that this deviation does indeed reflect constant fractionation between cellulose and CO_2, but is confounded by CO_2 that has not completely exchanged with environmental water because of rapid aeration in the aquaria. This mechanism reconciles results of previous autotrophic experiments, as well as supporting the existence of a constant fractionation between cellulose and water in natural settings where CO_2 is more likely to be fully exchanged with environmental water.

3.2 Experiment

Submergent aquatic macrophytes (Ceratophyllum demersum L.) were cultured under controlled conditions in the greenhouse at the University of Waterloo. The experiment began on 26 April and ended on 11 May 2005. Four aquaria (40L each) were filled with isotopically different water (Table

3-1). Five C. demersum individuals in each aquarium were anchored by Plant Plug® (Aquarium Products Company), with blue threads marking the tip of each individual. The length and weight of plants were measured before they were transferred into the aquaria. Plants were mainly grown under natural lighting, though a high intensity discharge light was turned on during cloudy days. A standard aquarium air pump was used to aerate the system with a flow rate of 300 mL/min. A commercial filter system (AquaClear® Rolf C. Hagen Inc., flow rate 6.3L/min) was utilized to maintain the cleanliness and the circulation of the water in each aquarium. To ensure minimal isotopic variation of water due to evaporation, aquaria were covered by plexiglass and the water levels were maintained with the same water source. Total water loss during the experiment was <4%. Plants were measured for length and mass at the end of the experiment and individuals with more than 12cm new growth were harvested. The top 10cm (to preclude any potential bias introduced by pre-existing tissue) was processed for cellulose extraction and subsequent oxygen isotope analysis.

3.3 Cellulose extraction and isotope analysis

Cellulose extraction from plant materials was a simplified version of Wolfe et al. (2001). Samples were rinsed with de-ionized water and then oven-dried at 60°C. Dry samples (0.19g to 0.73g) were ground to powder and weighed before transfer into test tubes for de-lipidification. Samples were treated with benzene/ethanol (2/1, volume/volume) and acetone to dissolve lipid, resins and tannin. Lignins were removed by applying a sodium chlorite ($NaClO_3$) / acetic acid (CH_3COOH) bleach at 70°C, followed by an alkaline hydrolysis with 17% sodium hydroxide (NaOH) to remove hemicellulose. The final products were freeze-dried and sub-sampled (0.1mg) for oxygen isotope analysis.

Oxygen isotope analysis of cellulose was conducted on a continuous flow isotope ratio mass spectrometer (CF-IRMS) at the Environmental Isotope Laboratory, University of Waterloo (UW-EIL). Cellulose samples were pyrolyzed to CO at high temperature (1300°C) (Werner et al., 1996). The CO gas was separated from other pyrolysis products in a EuroVector elemental analyzer (GV Instruments, U.K.) and introduced into an IsoPrime mass spectrometer (GV Instruments, U.K.) for isotopic measurement. Oxygen isotope composition of aquarium water collected during the experiment was determined on a dual-inlet VG-Micromass903 mass spectrometer using the CO_2 equilibration method (Epstein and Mayeda, 1953). Results are reported in δ notation, such that, $\delta = 10^3 \cdot \left[\left(R_{sample}^{18/16} \Big/ R_{s\tan dard}^{18/16}\right) - 1\right]$ where R is the $^{18}O/^{16}O$ ratio in samples or the VSMOW (Vienna

Standard Mean Ocean Water) standard. The results were corrected to VSMOW (0‰) and Standard Light Antarctic Precipitation (–55.5‰) in $\delta^{18}O$ (Coplen, 1996). The analytical uncertainty is ±0.4‰ for cellulose $\delta^{18}O$ and ±0.2 ‰ for water $\delta^{18}O$.

3.4 Results

The results from the culture experiments, including the oxygen isotope composition of aquarium water and aquatic cellulose, are summarized in Table 3-1. During the course of the experiment, minimal isotopic change occurred in the water ($\delta^{18}O_{water}$) of four aquaria set up to collectively span ~9‰. $\delta^{18}O$ values in aquatic cellulose ($\delta^{18}O_{cellulose}$) from each aquarium are identical within analytical uncertainty, but the differences among aquaria are significant. $\delta^{18}O_{cellulose}$ values span a range of ~7‰. As shown in Figure 3-1, mean $\delta^{18}O_{cellulose}$ values are related in a strongly linear fashion to mean $\delta^{18}O_{water}$ values, described by:

$$\delta^{18}O_{cellulose} = 0.738 \cdot \delta^{18}O_{water} + 29.8 \quad (R^2=0.9985) \qquad (3\text{-}1)$$

3.5 Interpretation and Discussion

The strong linearity in Figure 3-1 (also Equation 3-1) indicates that variation in the oxygen isotope composition of environmental water ($\delta^{18}O_{water}$) controls variation in the isotopic composition of aquatic cellulose ($\delta^{18}O_{cellulose}$). However, Equation 3-1 clearly does not reflect constant isotopic fractionation between water and cellulose, which would be of the form $\delta^{18}O_{cellulose} = \alpha \cdot \delta^{18}O_{water} + \varepsilon$, where $\varepsilon = (\alpha - 1)1000$.

Moreover, previous aquarium experiments that examined cellulose-water $\delta^{18}O$ relations under autotrophic growth, including Cooper and DeNiro (1989), Yakir and DeNiro (1990) and Sauer et al. (2001), have produced similar results (Table 3-2), also with strong linearity (R^2 >0.98) in all cases. The simplest explanation to account for these systematic results is the existence of another oxygen pool, besides water, that influences the oxygen-isotope labelling of cellulose in autotrophic experiments.

As proposed by Sternberg et al. (1986), if there is an additional pool of oxygen influencing cellulose oxygen isotope composition, then the isotopic labelling of cellulose can be expressed as the following:

$$\begin{aligned}\delta^{18}O_{cellulose} &= f\cdot(\alpha_{c-w}\cdot\delta^{18}O_{water}+\varepsilon_{c-w})+(1-f)\cdot\delta^{18}O_x \\ &= f\cdot\alpha_{c-w}\cdot\delta^{18}O_{water}+\ [f\cdot\varepsilon_{c-w}+(1-f)\cdot\delta^{18}O_x]\end{aligned} \tag{3-2}$$

where $\delta^{18}O_x$ is the isotopic composition of "mystery" cellulose oxygen that is not influenced by water; f is the proportion of oxygen in cellulose that is influenced by water; $\alpha_{c\text{-}w}$ is the apparent cellulose-water fractionation factor; and $\varepsilon_{c\text{-}w}$ is the corresponding isotopic separation. According to Equation (3-2), the oxygen isotope composition of cellulose is a linear mixing of two oxygen pools, one associated with water and the other unknown.

Rearrangement of Equation (3-2) (second line) emphasizes that the slope of the observed cellulose-water oxygen isotope relation is determined by the proportional contribution of water-influenced oxygen (*f*) and the apparent cellulose-water isotope fractionation factor ($\alpha_{c\text{-}w}$). Because $\alpha_{c\text{-}w}$ is close to 1, the observed empirical slope is a good first-order approximation of the proportion of oxygen influenced by water. The intercept is controlled by more parameters, including *f*, the apparent cellulose-water isotope separation ($\varepsilon_{c\text{-}w}$) and the composition of cellulose oxygen influenced by the "mystery" source ($\delta^{18}O_x$), and hence is more complex. Alternatively, Equation (3-2) can be expressed more simply in R notation, which eliminates the ε term:

$$R^{18/16}_{cellulose} = f\cdot\alpha_{c-w}\cdot R^{18/16}_{water}+(1-f)\cdot R^{18/16}_{x} \tag{3-3}$$

where $R^{18/16}_{cellulose}$, $R^{18/16}_{water}$ and $R^{18/16}_{x}$ refer to the isotopic ratios of $^{18}O/^{16}O$ in the bulk cellulose, water and the "mystery" cellulose oxygen. The relation between $R^{18/16}_{cellulose}$ and $R^{18/16}_{water}$ is linear, since δ is a linear derivation from *R*. Expressed in this manner, the slope is a function of *f* and $\alpha_{c\text{-}w}$, while the intercept is related to *f* and $R^{18/16}_{x}$ only, thus:

$$S = f\cdot\alpha_{c-w} \tag{3-4}$$

$$\mathrm{I} = (1-f)\cdot R^{18/16}_{x} \tag{3-5}$$

The slope (S) and intercept (I) are both proportionally related to *f*. If two sets of S and I from two independent experiments are statistically different, and we assume that $R^{18/16}_{x}$ and $\alpha_{c\text{-}w}$ remain the same, it is possible to infer individual *f* values from the following:

$$\frac{S_1}{S_2} = \frac{f_1 \cdot \alpha_{c-w}}{f_2 \cdot \alpha_{c-w}} = \frac{f_1}{f_2}$$
$$\frac{I_1}{I_2} = \frac{(1-f_1) \cdot R_x^{18/16}}{(1-f_2) \cdot R_x^{18/16}} = \frac{1-f_1}{1-f_2} \qquad (3\text{-}6)$$

where subscripts 1 and 2 are used to distinguish results from the two experiments. The unknown variables f_1 and f_2 can be determined first in this two-equation system. Subsequently, $\alpha_{c\text{-}w}$ and $R_x^{18/16}$ can be inferred according to the corresponding S and I values.

To demonstrate, we chose results from Sauer et al. (2001) and our experiment to determine $\alpha_{c\text{-}w}$ and $R_x^{18/16}$.

$$\delta^{18}O_{cellulose} = 0.738 \cdot \delta^{18}O_{water} + 29.8 \qquad \text{(present study)} \qquad (3\text{-}7)$$

$$\delta^{18}O_{cellulose} = 0.882 \cdot \delta^{18}O_{water} + 28.3 \qquad \text{(Sauer et al., 2001)} \qquad (3\text{-}8)$$

A statistical test of the equality of slope and intercept (Draper and Smith, 1998) confirms that the slopes are significantly different ($F=160.74$, $p \leq 0.0001$), as are the intercepts ($F=46398.4$, $p \leq 0.0001$), between the two sets of experimental results (Figure 3-1). We converted Equations (3-7) and (3-8) into R notation by applying $R_{VSMOW}^{18/16} = (2005.20 \pm 0.45) \times 10^{-6}$ (Baertschi, 1976):

$$R_{cellulose}^{18/16} = 0.738 \cdot R_{water}^{18/16} + 585.12 \times 10^{-6} \qquad (3\text{-}9)$$

$$R_{cellulose}^{18/16} = 0.882 \cdot R_{water}^{18/16} + 293.36 \times 10^{-6} \qquad (3\text{-}10)$$

Substituting the coefficients in (9) and (10) for S_1, S_2, I_1 and I_2 in equation system (3-6), generates $f_1 = 0.7187$ for (9) and $f_2 = 0.8590$ for (10). Then we determined that $\alpha_{c\text{-}w} = 1.0268$ and $R_x^{18/16} = 2080.39 \times 10^{-6}$ for the system; the latter converted to δ notation yields 37.5‰ for $\delta^{18}O_x$.

Unfortunately, since no data exist to verify that the $\delta^{18}O_x$ was identical in both experiments, this set of parameters constitutes a non-unique solution. On the other hand, the fact that the calculated $\alpha_{c\text{-}w}$ value lies within the reported range (1.026 – 1.028; Sternberg and DeNiro, 1983) is consistent with the notion of a common fractionation factor, which does suggest that the actual $\delta^{18}O_x$ values are similar and ^{18}O-enriched. For example, an assumed $\alpha_{c\text{-}w}$ value of 1.028, corresponding to an "operational best-fit" value obtained from field studies over more than 20 years (Edwards and Fritz,

1986; Edwards and McAndrews, 1989; Edwards, 1993; MacDonald et al., 1993; Wolfe et al., 1997, 2000, 2007; Birks et al., 2007), yields respective estimates of $\delta^{18}O_x$ in the two experiments of 34.4‰ and 30.1‰. Similarly, using the lower reported value (1.026) for $\alpha_{c\text{-}w}$ yields respective estimates of 39.5‰ and 42.4‰. Although these estimates are sensitive to $\alpha_{c\text{-}w}$, all three potential solutions are in harmony with the influence of relatively ^{18}O-rich oxygen from another source. Because the influence of O_2 during the oxygen-isotope labelling of cellulose can be discounted (Yakir, 1992), CO_2 is the most likely source of this ^{18}O-rich oxygen.

Indeed, plant physiologists have long argued that CO_2 is the sole source of oxygen in plant tissues (e.g. Ruben et al., 1941; Guy et al., 1993). If this is the case, then we can describe the isotopic labelling of cellulose oxygen by the following expression, which partitions the oxygen conceptually into two components:

$$\delta^{18}O_{cellulose} = f \cdot (\alpha_b \cdot \delta^{18}O^{*}_{CO_2} + \varepsilon_b) + (1-f) \cdot (\alpha_b \cdot \delta^{18}O^{non}_{CO_2} + \varepsilon_b) \qquad (3\text{-}11)$$

where $\delta^{18}O^{*}_{CO_2}$ represents oxygen in carbon dioxide that has been re-labelled through biochemically-mediated exchange with environmental water (i.e., aquarium water in this case); $\delta^{18}O^{non}_{CO_2}$ represents oxygen from carbon dioxide that has not undergone bio-exchange with water and hence retains its original isotopic signature; f indicates the percentage of CO_2 that has undergone biochemically-mediated exchange with environmental water; α_b and ε_b account for the oxygen-isotope fractionation between cellulose and carbon dioxide in biological processes, which is common to both components. This fractionation, which reflects the overall discrimination against ^{18}O in carbon dioxide during photosynthesis can be estimated from the combination of the equilibrium fractionation between carbon dioxide and water (α^{*}~1.041 at 25ºC; Brenninkmeijer et al., 1983) and our operational cellulose-water fractionation ($\alpha_{c\text{-}w}$ ~1.028), yielding an α_b value of 1.028/1.041 = 0.9875 and associated ε_b value of -12.5‰.

According to Equation (3-11), $\delta^{18}O_{cellulose}$ would seem to be independent of $\delta^{18}O_{water}$. However, bio-exchange between CO_2 and water links $\delta^{18}O_{cellulose}$ with $\delta^{18}O_{water}$. Thus, Equation (3-11) can be rewritten as follows:

$$\delta^{18}O_{cellulose} = f \cdot (\alpha_{c-w} \cdot \delta^{18}O_{water} + \varepsilon_{c-w}) + (1-f) \cdot (\alpha_b \cdot \delta^{18}O^{non}_{CO_2} + \varepsilon_b) \qquad (3\text{-}12)$$

where $(\alpha_{c-w} \cdot \delta^{18}O_{water} + \varepsilon_{c-w})$ is equivalent to $(\alpha_b \cdot \delta^{18}O^*_{CO_2} + \varepsilon_b)$ in Equations (3-11) and (3-12), respectively.

According to Equation (3-12), the isotopic composition of non-exchanged CO_2 ($\delta^{18}O^{non}_{CO_2}$) in culture experiments can be derived based on the slope and intercept of individual experiments. In our experiment ($\delta^{18}O_{cellulose} = 0.783\delta^{18}O_{water} + 29.8$), $\delta^{18}O^{non}_{CO_2}$ would be 47.5‰; in the Sauer et al. (2001) experiment ($\delta^{18}O_{cellulose} = 0.882\delta^{18}O_{water} + 28.3$), $\delta^{18}O^{non}_{CO_2}$ would be 43.2‰; while in the Yakir and DeNiro (1990) experiment ($\delta^{18}O_{cellulose} = 0.77\delta^{18}O_{water} + 29.3$), $\delta^{18}O^{non}_{CO_2}$ would be 46.3‰. These inferred isotopic values of non-exchanged CO_2 are similar to each other and lie within the feasible range for non-oceanic atmospheric CO_2 (e.g., Yakir and Wang, 1996), especially in the presence of transpiring greenhouse plants (see Cernusak et al., 2004), as in our experiment. This is consistent with the fact that all of these aquarium experiments were aerated with ambient air. In contrast, Cooper and DeNiro (1989) used carbon dioxide of known composition ranging between 30.4‰ and 33.1‰. Our inferred $\delta^{18}O^{non}_{CO_2}$ value (33.6‰) from their experimental cellulose-water relation ($\delta^{18}O_{cellulose} = 0.48\delta^{18}O_{water} + 24.1$) agrees with these measurements, providing further support for our unifying characterization of cellulose-water oxygen isotope relations in laboratory experiments.

Moreover, Equations (3-11) and (3-12) indicate that a constant fractionation line can be achieved only if CO_2 is fully exchanged with water, which requires some minimum residence time of CO_2 to ensure full exchange. A common feature of autotrophic experiments is the continuous aeration to ensure abundant carbon for the success of growth (refer to the "Experiment" section in this paper, as well as Cooper and DeNiro, 1989; Yakir and DeNiro, 1990; Sauer et al., 2001). The continuous bubbling of air certainly reduces the residence time of CO_2 and hampers exchange between water and CO_2. This mechanism is also supported by the reduction in slope from 0.77 to 0.71 induced by Yakir and DeNiro (1990) (see Table 3-2) when they increased the concentration of CO_2 being bubbled through the aquaria. On the other hand, a longer residence time should lead to a greater degree of exchange, hence steepening the slope of the cellulose-water relation towards $\alpha_{c\text{-}w}$. Importantly, the isotopic composition of CO_2 will only have an effect on the intercept.

We note that, in contrast to these very specific experimental conditions in the laboratory, lakes or ponds in natural settings have more complicated CO_2 cycling and much longer residence time.

Collectively, CO_2 is more likely to be fully exchanged with environmental water in natural systems. As reflected in Equation (3-12), under these conditions, *f* becomes unity; the CO_2-associated term disappears; and water fully influences the isotopic composition of cellulose. This is consistent with a constant separation between cellulose and water routinely reported from field studies (DeNiro and Epstein, 1981; Edwards and McAndrews, 1989; Wolfe et al., 2001; Zanazzi and More, 2005).

3.6 Conclusions

An aquarium experiment culturing *C. demersum* in waters having a range of oxygen isotope compositions was conducted between 26 April and 11 May 2005. The $\delta^{18}O$ of cellulose in new tissues from *C. demersum* exhibits a strong linear correlation to the $\delta^{18}O$ in culturing water, but the linear regression is different from that obtained from a previous study on *P. denticulatum* (Sauer et al., 2001). The strong linearity plus the non-constant-fractionation slope strongly indicates that an isotopically distinct source of oxygen other than water influences the isotopic composition of cellulose. We propose a new conceptual characterization of the cellulose-water relation, supporting the notion that oxygen in plant cellulose is actually inherited from CO_2 during photosynthesis. However, biochemically mediated isotopic exchange between CO_2 and H_2O leads to an apparent linear relation between cellulose and water $\delta^{18}O$ values. The varying slope of this relation reflects the degree of exchange, while the intercept is influenced by the isotopic composition of non-exchanged CO_2 ($\delta^{18}O_{CO_2}^{non}$). We conclude that the existence of non-constant-fractionation slopes in multiple culture studies is an artifact of the experimental procedure, in which atmospheric or tank CO_2 is supplied by forced aeration. The constant apparent fractionation between cellulose and environmental water often observed in field studies (DeNiro and Epstein, 1981; Edwards and McAndrews, 1989; Wolfe et al., 2001; Zanazzi and More, 2005) probably reflects full CO_2-H_2O exchange because of longer residence time of CO_2 in natural waters.

Acknowledgements

We would like to thank Lynn Hoyles from Department of Biology, University of Waterloo for accessing the greenhouse facilities; M. Falcone and C. McDonald for laboratory assistance; R.J. O'Hara Hines, E. Harvey and J. Park for help with statistics; and the UW-EIL for conducting stable isotope analysis. Funding was provided by the British Columbia Hydro and Power Authority and the

Natural Sciences and Engineering Research Council of Canada (Northern Research Chair, Collaborative Research and Development Grant and Discovery Grant programs).

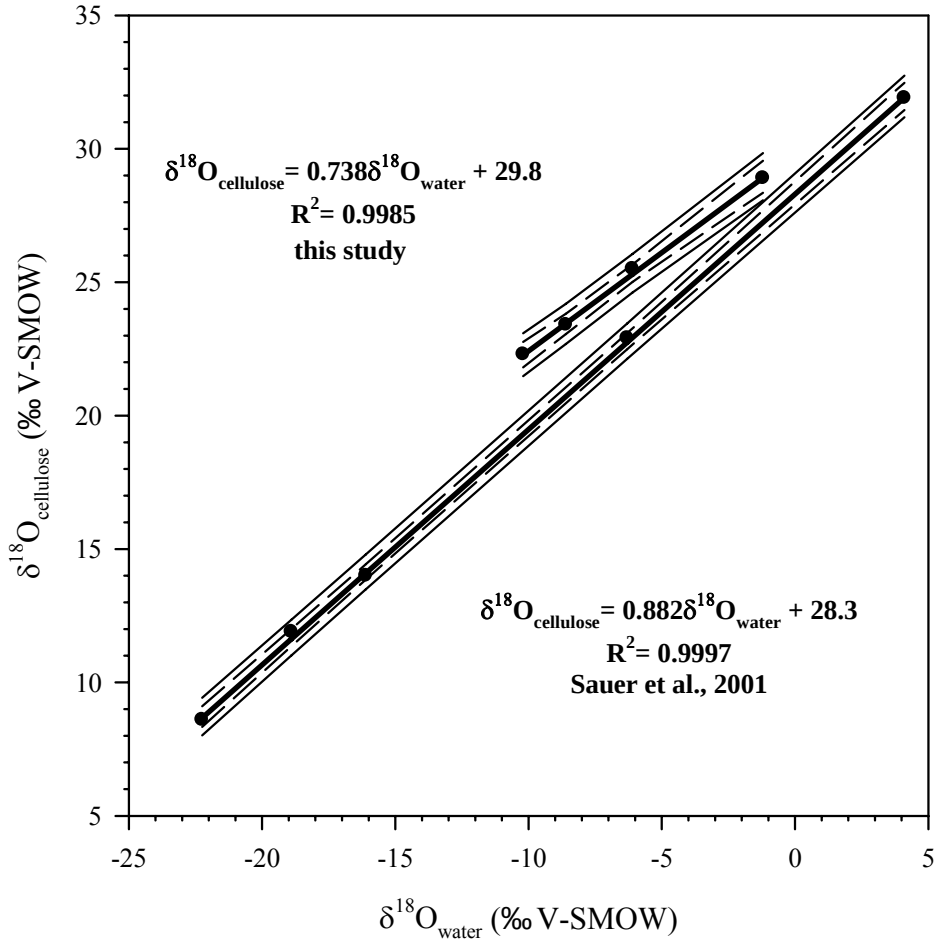

Figure 3-1: Comparison of results from Sauer et al. (2001) and current experiment reported in this paper. Both experiments demonstrate a strong linear relationship between cellulose and the environmental water from which the cellulose is produced.

Table 3-1: Isotopic compositions of environmental water and aquatic cellulose in the culture experiment.

	$\delta^{18}O_{water}$ (‰ V-SMOW)			$\delta^{18}O_{cellulose}$ (‰ V-SMOW)			
Aquarium #	Begin	End	Average	Plant #1	Plant #2	Plant #3	Average
1	-10.3	-10.0	-10.2	22.2	22.3	N/A	22.3
2	-8.6	-8.5	-8.6	23.4	23.3	N/A	23.4
3	-6.2	-5.9	-6.1	25.8	25.4	25.3	25.5
4	-1.4	-1.0	-1.2	29.1	29.1	28.5	28.9

Table 3-2: Correlation obtained between $\delta^{18}O$ values of cellulose and source water in autotrophic growth experiments. Note that the lower slope of the two reported by Yakir and DeNiro (1990) was obtained under conditions of elevated CO_2 concentration, whereas all other results were obtained with CO_2 at normal atmospheric concentration.

Species	Relationship	Statistics	Source	T (^{o}C)
Egeria densa Planch	Y=0.48X+24.1	R^2=0.98	Cooper and DeNiro (1989)	22 ± 2
Lemna gibba L.	Y=0.77X+29.3	not reported	Yakir and DeNiro (1990)	27
	Y=0.71X+24.8	R^2=0.995		
Plagiothecium denticulatum Hedwig	Y=0.882X+28.3	R^2=0.9997	Sauer et al. (2001)	4
Ceratophyllum demersum L.	Y=0.738X+29.8	R^2=0.9985	This Study	23 ± 3

Chapter 4

A multiproxy millennium reconstruction of hydroecology in a shallow delta lake, northern Canada: with an emphasis on stable isotopes*

Summary Multiproxy paleolimnological analyses of a lake sediment core from a shallow closed-drainage basin in the Peace-Athabasca Delta (PAD), northern Alberta, document marked hydroecological variability over the past millennium. Utilizing an array of proxy indicators, including the oxygen isotope composition of lake water inferred from sedimentary cellulose, organic carbon content, organic carbon isotope composition, composition of diatom assemblage and abundance of macrofossils, the 1000-year history of the basin can be divided into 5 hydroecological zones. Of particular interests are zone 3 and 4. Zone-3 time span (~ AD 1540 to ~1880) is characterized by periodic inundation from Lake Athabasca, whereas zone-4 time span (~ AD 1880 to 1930) appears to be a through-flow-lake phase. Both zones emphasize the important role of Lake Athabasca on the hydrological conditions in the surrounding lowland area. Further quantitative reconstruction of the water balance is made using an isotope-mass balance model. Reconstruction of Evaporation to Inflow ratios (E/I) reveals interesting patterns that can be related to regional climate. For example, low E/I values correspond to the Little Ice Age (LIA, ~ AD 1540 to ~1880) whereas high E/I values are associated with the Medieval Warm Period (MWP, ~ AD 1140 to ~1540). Results also suggest that post-LIA (after 1880) hydroecological conditions, which reflect a shift to a rainfall-dominated runoff regime, may be analogous to conditions that prevailed during the Medieval Warm Period. However, E/I values in the most recent decades increase very rapidly and are in striking contrast to the step-wise increase in E/I during the MWP, which raised concern over the unprecedented rate of hydrological changes during the last century and potential consequences for the future integrity of this northern freshwater ecosystem.

---

* In preparation for submission to *Journal of Paleolimnology* as: Yi Y., Sinnatmaby R.N., Hall R.I., Asada T., Wolfe B.B., Edwards T.W.D., A multiproxy millennium reconstruction of hydroecology in a shallow delta lake, northern Canada: with an emphasis on stable isotopes.

4.1 Introduction

Lake sediments are very important terrestrial archives of environmental change, which can continuously record temporal information at variable spatial scales, ranging from the local catchment to the contributing watershed (Cohen, 2003). Study of lake deposits has traditionally focused on sedimentology and biological remains, which has provided evidence of geological and ecological change within and around lakes (Reeves, 1968; Frey, 1974; Smol, 1990). More recently, process-based studies have begun to recognize a lake and its watershed as a complex system and the analysis of isotopic records preserved in sediments has become an increasingly common approach (Bradbury and Dean, 1993; Roberts and Jones, 2002). For example, oxygen contained in inorganic or organic components of lake sediments such as carbonate, diatom frustules and cellulose is completely or partially derived from oxygen atoms in lake water. According to studies of contemporary isotope hydrology, isotopic composition of lake water is strongly associated with hydrological and climatic conditions of a lake (Gonfiantini, 1986; Gat, 1996; Gibson and Edwards, 2002). Thus, the oxygen isotopic composition in lake sediments primarily bears information about changes of climate and hydrology that a lake has experienced. In addition, the isotopic fractionation between minerals (for example calcite) and lake water is dependent on lake water temperature. Sometimes, vital (i.e. biological) effects also have to be taken into account (von Grafenstein et al., 1999). Overall, isotopic signals preserved in lake sediments are controlled by multiple factors related to physical, chemical and biological properties of a lake. Therefore, thorough understanding of isotopic composition of lacustrine sedimentary materials can yield a wide range of useful information for paleoclimate, paleohydrology, paleolimnology and paleoenvironment studies.

The multiple factors that potentially control the isotopic signatures of lacustrine archives make precise and quantitative interpretation of isotope stratigraphy intriguing and challenging (Leng and Marshall, 2004; Jones and Roberts, 2008). Among the challenges is to separate primary effects of source water from secondary effects of evaporation in stratigraphic $\delta^{18}O$ profiles (Edwards et al., 2004). In general, alteration in isotopic composition of lake water can be caused either by changes in precipitation (i.e. the primary effect) or by variations in evaporation (i.e. the secondary effect). Many previous studies have carefully considered the primary and secondary effects, and utilized inferred $\delta^{18}O$ in lake water to reconstruct hydroclimatological conditions, but inevitably some assumptions have to be made. For example, the isotopic composition of source water or evaporation is presumed to have remained constant while the other variable is considered to change (Jones et al., 2005; Leng et

al., 2006). Such studies are often limited by lack of supporting data to effectively constrain quantitative paleohydrological reconstructions.

In this paper, we present a multi-proxy study of lake sediments, which includes diatom analysis, plant macrofossil analysis, and elemental and stable isotope analyses. Use of multiple proxies provides constraints on changes in source water to the lake. With the aid of a quantitative reconstruction of climatic conditions (i.e., relative humidity and temperature) from isotopes in tree-rings (Edwards et al., 2008), a quantitative reconstruction of the lake water balance is derived from an isotope-mass balance model. The paper demonstrates that a multi-proxy approach can effectively constrain quantitative interpretation of $\delta^{18}O$ values in lake sediments. An important outcome of the study is the estimated rates of recent rapid hydrological change in a northern freshwater ecosystem, with implications for water resource management.

4.2 Study Site

4.2.1 The Peace-Athabasca Delta (PAD)

The Peace-Athabasca Delta (PAD) is a large (~3900 km^2) floodplain landscape formed by the convergence of the Peace, Athabasca and Birch rivers at the western end of Lake Athabasca, northern Alberta, Canada (Figure 4-1). The delta has been designated as a Ramsar Wetland of International Importance and a UNESCO (United National Educational, Scientific and Cultural Organization) World Heritage Site because of its ecological and cultural significance. It is home to large populations of muskrat, beaver and free-ranging wood bison, lies along several important North American migratory bird flyways, and serves as the breeding ground for a variety of unique waterfowl. Moreover, the delta's biological productivity and ecological diversity are important natural resources to the local First Nations community in Fort Chipewyan, Alberta.

Hydrological and ecological changes observed over the last 40 years have raised concerns on the potential impact of climate variation and river flow regulation on the delta (PADPG, 1973; PADIC, 1987; PADTS, 1996; Gummer et al., 2000; Prowse et al., 2002). However, lack of long-term understanding of delta evolution has limited the ability to objectively assess contemporary observations of hydrological and ecological changes. As such, a multidisciplinary research program was launched aiming to provide a long-term hydroecological baseline beyond instrumental records

(Wolfe et al., 2002; Hall et al., 2004). Several shallow delta lakes are targeted, and lake sediments are analyzed as archives to retrieve environmental information on century to millennium timescales.

4.2.2 Hydrological and climatic setting of the delta

The PAD can be subdivided into three (mainly two) deltaic sectors: the Athabasca sector to the south (~1970 km^2), the Peace sector to the north (~1680 km^2) and the much smaller Birch sector to the west (~170 km^2) (PADPG, 1973). The Peace sector is an elevated relict fluviodeltaic landscape that is covered by mature forests with bedrock inliers in the northeast. This sector is flooded only during major ice-jams that periodically develop on the Peace River. The southern Athabasca sector is an active delta with extremely low relief that frequently receives floodwaters from the Athabasca River during the spring thaw and the open-water season. In general, the landscape of the PAD is marked by a complex pattern of active and inactive channels and meander scrolls, superimposed by hundreds of shallow lakes and wetlands.

Shallow lakes in the PAD span a wide hydrological spectrum ranging from basins that are influenced by river waters only at times of extensive flooding, to basins that are directly connected to rivers. Among numerous factors that may affect the hydrology of lakes, the nature and frequency of river connection and catchment runoff have often been considered to be the most important basis for hydrological classifications. These classification schemes typically employ terminologies that include open-, restricted-, and closed-drainage basins (PADPG, 1973). For open-drainage basins, contribution from river water dominates water budgets, while rivers play a minor role in sustaining closed-drainage basins. Precipitation and catchment runoff are considered to be important components in maintaining the water balance of closed-drainage basins. Between the two end members lies a continuum of restricted-drainage basins having highly variable water budgets. A new category, referred as rainfall-influenced basins, was identified in a recent study (Wolfe et al., 2007a). These lakes are similar to closed-drainage basins with high conductivity and high concentration of calcium and sodium, but are also somewhat different from closed-drainage basins because of low concentration of silica and chlorophyll. This is primarily due to the overriding influence of summer rainfall on their water balance.

Climate in the PAD is strongly seasonal. According to 1971-2000 climate normals at Fort Chipewyan, Alberta, (Weather Station ID 3072658; Environment Canada, 2004), mean annual air temperature is -1.9°C, mean January air temperature is -23.3°C and mean July air temperature is

16.7°C. Precipitation averages 391.7 mm annually, with about 59% falling as rain during the May-September period.

4.2.3 Lake description – PAD9

PAD9 (58°46.46′ N, 111°19.48′ W, 208.8 m asl) is a small, shallow (ca. 12 ha, Z_{max} = 0.8 m) lake located between Chenal des Quatre Fourches and Rivière des Rochers in the southern portion of the Peace sector. It is currently classified as closed-drainage lake (Wolfe et al., 2007a), and separated from Lake Athabasca to the northwest by an extensive lowland sedge meadow (ca. 70 km^2). With the exception of a bedrock outcrop on the southern shore, the lake is mainly bordered by willow-shrub-dominated lowland. The shoreline is marked by a double fringe of dead willow shrubs, with prominent adventitious rooting well above current lake levels, indicating previous higher water levels. Currently, the lake is nutrient-rich and highly productive, with abundant *Ceratophyllum* and extensive coverage of filamentous algae (Table 4-1; Hall et al., 2004). Historical maps and paleolimnological analyses of a short sediment sequence (Sinnatamby, 2006) suggest that the basin of PAD9 was likely heavily influenced by Lake Athabasca during the 18th and 19th century. Because of its location and evidence of water level fluctuations, PAD9 is expected to be a sensitive indicator of hydrological change in Lake Athabasca and the surrounding area.

4.3 Methods

4.3.1 Lake water sampling and water isotope tracer analyses

Lake water samples were collected ~10 cm below the surface at the centre of PAD9 several times between October 2000 and September 2006 to examine seasonal and inter-annual variability in lake water isotope composition. Samples were sealed in 30 ml high-density polyethylene bottles and were analyzed at the University of Waterloo - Environmental Isotope Laboratory (UW-EIL) for $\delta^{18}O$ and $\delta^{2}H$. $\delta^{18}O$ in water was measured on a dual-inlet VG-Micromass903 mass spectrometer by applying the CO_2 equilibration method (Epstein and Mayeda, 1953). $\delta^{2}H$ in water was determined on a Continuous-Flow Isotope Ratio Mass Spectrometer (CF-IRMS) system, by reduction of water to H_2 gas using chromium metal as active reducing agent (Morrison et al., 2001). Results were reported in δ values, representing deviations in per mil (‰) from VSMOW on a scale normalized to values of

Standard Light Antarctic Precipitation (-55.5‰ for $\delta^{18}O$; -428‰ for $\delta^{2}H$; Coplen, 1996). Analytical uncertainties are ±0.2‰ for $\delta^{18}O$ and ±2‰ for $\delta^{2}H$.

4.3.2 Paleolimnological analyses of lake sediments

An 80 cm sediment core was collected near the center of PAD9 on June 3, 2001 using a 10cm-diameter Russian peat corer. The recovered sediment was wrapped in plastic sheets and labelled in the field, then sectioned into 0.5 cm intervals in the laboratory. Each interval was subsampled for diatom analyses, plant macrofossil analyses and elemental and isotope analyses.

Dating: Seeds of emergent shoreline plants from the base of the core were sampled for radiocarbon dating. The radiocarbon analysis was performed by an accelerator mass spectrometry (AMS) at Beta Analytic Radiocarbon Dating Laboratory (Miami, Florida). Radiocarbon years were calibrated to calendar years (cal. yr. AD) by the probability distribution method using the Intcal98 calibration curve (Stuiver et al., 1998).

Diatom analyses: Subsamples for diatom analyses were pretreated following standard techniques (Hall and Smol, 1996). Every second pretreated sediment samples were counted by N. Sinnatmaby at 1000× magnification, and counting results were reported in relative abundance (%). A Zeiss Axioskop Ⅱ plus light microscope fitted with differential interference optics (numerical aperture = 1.3) was used for diatom identification and count. Krammer and Lange-Bertalot (1986-1991) was the main reference for taxonomic identification. Counts aimed for 350 diatom valves per sample. Due to decreasing diatom abundance with increasing depth, a minimum of 150 valves were counted for the deep part of the core. Stability curves were used to demonstrate that the 350 and 150 minima were likely to estimate similar percent abundance of the diatom taxa (Sinnatamby, 2006).

Plant macrofossil analyses: Subsamples for macrofossil analyses (5 cm^3) were washed through a 125-μm mesh screen with warm tap water. Materials retained on the sieve were sorted in water using a binocular dissecting microscope at 8-40× magnification. All identifiable macrofossil remains were counted by T. Asada and counting results were presented in absolute abundance (speciments/5cm^3 sediment). References for specimens and keys include Bertsch (1941), Martin and Barkley (1961), Berggren (1969, 1981), Montgomery (1977), and Artjuschenko (1990).

Elemental and stable isotope analyses: Subsamples for elemental and stable isotope analyses were processed following 7 steps detailed in Wolfe et al. (2001a; 2007b).

1. Wash with 10% (by volume) HCl at 60°C to remove carbonate.
2. Rinse with de-ionized water, freeze-dry and sieve to <500μm to remove coarse terrestrial debris including macrofossils. ~8mg materials from fine fraction are analyzed for carbon stable isotope ($\delta^{13}C_{bulk}$) and organic carbon content (C%) in bulk.
3. Fine fraction is treated with benzene/ethanol (2/1, v/v) and acetone to dissolve lipid, resins and tannin.
4. Bleach with sodium chlorite ($NaClO_3$)/acetic acid solution at 70°C to remove lignin.
5. Alkaline hydrolysis with 17% sodium hydroxide (NaOH) to remove hemicellulose.
6. Leach with sodium dithionite ($Na_2S_2O_4$), ammonium citrate ($(NH_4)_3C_6H_5O_7$) and hydroxylamine hydrochloride ($NH_2OH{\cdot}HCl$) to remove Fe- and Mn- oxyhydroxides.
7. Heavy-liquid density separation with sodium polytungstate to separate cellulose from most minerogenic constituents.

After rinse with de-ionized water and freeze-dry, concentrated cellulose samples from sediments are ready for oxygen and carbon stable isotope analyses.

Organic carbon content and carbon isotope analyses in bulk samples were conducted on a CF-IRMS system at UW-EIL. Bulk samples (~8mg) were combusted with the presence of an oxidant such as chromium oxide at 1020°C. Organic carbon was completely converted to CO_2 and measured for content and isotopic composition. Carbon isotope analysis of sedimentary cellulose was conducted on the same CF-IRMS system, with smaller sample amount (~0.7mg) but the same instrumental configuration and analytical procedure. Oxygen isotope analysis of sedimentary cellulose was conducted on a different CF-IRMS system at UW-EIL. Cellulose samples (~1mg) were pyrolyzed to CO at high temperature (1300°C) (Werner et al., 1996). The CO gas was separated from other pyrolysis products in an EuroVector elemental analyzer (GV Instruments, U.K.) and then led into an IsoPrime mass spectrometer (GV Instruments, U.K.) for oxygen isotope measurements.

As mentioned before, all isotope measurements are reported in δ notation. Carbon isotope results are reported in relative to standard VPDB, while oxygen isotope results are reported in relative to VSMOW. Carbon content is reported in relative abundance (by weight). The analytical uncertainty is ±0.5‰ and ±0.3‰ for $\delta^{18}O$ and $\delta^{13}C$ in sedimentary cellulose; ±0.3‰ for bulk organic $\delta^{13}C$; and ±1.0% for organic carbon content.

4.4 Results and Interpretation

4.4.1 Modern isotope hydrology

The distribution of water isotopes on the earth's surface (i.e., in precipitation and surface water) is characterized by the existence of strong linear relations between $\delta^{18}O$ and $\delta^{2}H$, reflecting systematic mass-dependent isotope fractionation in the hydrological cycle (Rozanski et al., 1993; Gibson and Edwards, 2002). In general, the covariant behaviour between oxygen and hydrogen composition in precipitation at a global scale defines a global meteoric water line (GMWL), which is expressed by the linear function ($\delta^{2}H = 8\delta^{18}O + 10$) (Craig, 1961). Analogous to GMWL, a local meteoric water line (LMWL), which is usually similar to the GMWL but with a lower slope, is commonly applied in regional scale studies. The LMWL for the PAD is defined as $\delta^{2}H = 6.7\delta^{18}O - 19.2$ based on precipitation collected at Fort Smith, Northwest Territories between 1960 and 1969 (Wolfe et al., 2007a). The isotopic composition of water that has undergone evaporation diverges from the GMWL (or LMWL) and typically plots on another well-defined linear trend termed a local evaporation line (LEL). In $\delta^{18}O$-$\delta^{2}H$ space, the slope of the LEL usually range between 4 and 6 and is primarily controlled by local atmospheric conditions including relative humidity (h), temperature (T) and the isotopic composition of atmospheric moisture (δ_A). The relative position of a given lake along the LEL is strongly associated with the water balance of the lake (Gonfiantini, 1986; Gat, 1996; Gibson and Edwards, 2002). Therefore, the investigation of isotopic composition in lake waters has become an important tool to characterize the hydrological conditions of a lake. As a part of a multidisciplinary project on studying past and present hydroecology in the PAD, lake water was collected from PAD9 on multiple occasions between October 2000 and September 2006. The multiple-sampling strategy aims to capture seasonal and inter-annual variability in lake water isotope composition.

As shown in Figure 4-2a, an isotope framework, based on available isotopic and climatic data has been established (Wolfe et al., 2007a). Key features include the predicted LEL, LMWL (or GMWL), the mean isotopic composition of amount-weighted annual precipitation (δ_p), the isotopic composition of a terminal lake fed by δ_p in hydrologic and isotopic steady state (δ_{ss}), the limiting isotopic composition of a desiccating lake (δ^*), the mean isotopic composition of amount-weighted summer precipitation (δ_{ps}), and the mean isotopic composition of amount-weighted winter precipitation (δ_{pw}).

Superimposed on the independently defined LMWL and LEL trajectories, isotopic compositions of PAD9 lake water over 7 years (October 2000 to September 2006) are shown to span a broad range of

values (~12.2‰ in $\delta^{18}O$; ~57‰ in $\delta^{2}H$), reflecting strong sensitivity to seasonal hydrological variations (Figure 4-2b). In $\delta^{18}O$-$\delta^{2}H$ space, the temporal changes of lake water isotope composition distributed along the predicted LEL indicate that the isotope-hydroclimatic regime of the PAD did not change significantly over the 7-year monitoring period and the pre-existing isotope framework can be used to semi-quantitatively assess instantaneous water balance at the timing of sampling. Lake water can be very depleted early in the thaw season (Figure 4-2c). In $\delta^{18}O$-$\delta^{2}H$ space, these water samples are generally below the LEL, indicating the influence of relatively depleted source water (i.e. winter snow). Substantial snowmelt input to PAD9 can have a prolonged effect on lake water composition (Figure 4-2c). For example, the lake water composition is depleted in general in a snow-abundant-year (e.g. 2003 with 93.3 cm accumulated snowfall) compared to a snow-deficit-year (e.g. 2001 with 47.4 cm accumulated snowfall). As thaw-season progresses, lake water isotope signatures evolved beyond δ_{ss} suggesting the lake has undergone pronounced evaporation at times, such as August 2001 and July 2002 (Figure 4-2c). These isotopically enriched samples generally plot above the LEL, also indicating the influence of late summer rain, which is consistent with the observation that slight shifts in lake water isotope composition usually occurred in late summer (Figure 4-2c).

Overall, water isotope results suggest that PAD9 receives sufficient input water to maintain standing water in the basin. Multiple sources of water (such as rainfall, snowmelt and catchment runoff) play variable roles in maintaining water balance. In the modern time frame, precipitation probably is the most important component. Furthermore, time series of isotope signals in lake water reflects varying roles of multiple sources in different time periods of a year. Therefore, reconstruction of lake water isotope composition via sediment archives will allow us to understand hydrological changes, especially changes in dominant input water over a longer term perspective.

4.4.2 Sediment core chronology

The sediment core chronology is based on a combination of ^{210}Pb dates in the surficial sediment sequence collected in a gravity corer, and calibrated AMS radiocarbon dates in deep sediments collected by a Russian peat corer (Table 4-2, and Sinnatamby, 2006). As illustrated in Figure 4-3, the Constant Rate of Supply (CRS) model of the 210Pb activity provides age estimates for depths between 0 and 21.25 cm. The age-depth profile between 21.25 cm and 78.75 cm is established by linear interpolation between the oldest CRS-modeled age (21.25 cm, AD 1886) and the two calibrated 14C ages at 74.50 cm (cal. yr. AD 540) and 78.75 cm (cal. yr. AD 220). Although sedimentation rates

likely varied over this multi-centennial time interval, linear interpolation between dated stratigraphic horizons provides the best estimate of the sediment chronology using the information available. Additional dates between 21.25 cm and 74.50 cm would help refine the age-depth profile between AD 1886 and 540, but are not available due to an absence of adequate plant macrofossil remains or other organic material suitable for radiocarbon dating.

4.4.3 Hydroecological reconstruction

Below, we integrate an array of paleolimnological proxies, including cellulose-inferred lake water oxygen isotope composition ($\delta^{18}O_L$), organic carbon content in bulk sediments (C%), stable carbon isotope composition in bulk organic matter and cellulose ($\delta^{13}C_{org}$ and $\delta^{13}C_{cell}$), diatom community composition, and abundance of macrofossil remains such as *Chara* oospores and ostracod shells, to reconstruct the evolution of the PAD9 during the past 1000 years. Allowing for minor chronological discrepancies among individual proxies, which is probably caused by different sensitivities of proxies to environmental changes, the PAD9 sediment sequence can be divided into five zones, as illustrated in Figure 4-4, reflecting a broad range and variability of hydroecological conditions.

AD 1000 to ~ 1140 (Zone 1)

The early time interval is characterized by the most depleted lake water isotope composition (ca. -20‰) in the profile, moderate organic content in the bulk sediments (~11%), low carbon isotope composition in both the bulk organic sediment ($\delta^{13}C_{org}$; ~ -26.8‰) and sedimentary cellulose ($\delta^{13}C_{cell}$; ~ -25.5‰), dominance of closed-drainage indicator diatoms, and high abundance of *Chara* oospores and ostracod shells. Diatom assemblages suggest the lake was a closed-drainage basin and the high abundance of *Chara* oospores and ostracod shells suggests the existence of a shallow aquatic environment. Lake water (~ -19.7‰) was isotopically depleted compared to modern lake water values (-4.9‰ to -17.1‰), possibly because of greater contributions from snowmelt or lower isotopic values of precipitation. Moderate organic content (C%) accompanied by low $\delta^{13}C_{org}$ and $\delta^{13}C_{cell}$ values suggest that the primary productivity in the lake was moderate and the carbon pool was not a limiting factor for the aquatic ecosystem.

~ AD 1140 to ~1540 (Zone 2)

Although the diatom community composition is not significantly different from Zone 1, the lake water oxygen isotope composition is enriched by about 3‰. These results indicate that the lake was still a closed-drainage basin but may have been fed by more isotopically-enriched precipitation. Organic C% increases during this time period and peaks (13.7%) at ~AD 1450. Corresponding to the increase in C% is enrichment in both $\delta^{13}C_{org}$ and $\delta^{13}C_{cell}$, suggesting diminished ability of isotopic discrimination in aquatic biota as the lake productivity increased. The abundance of *Chara* oospores and ostracod shells decrease during this time period, although the latter is highly variable. The compositional change in macrophytes and aquatic invertebrates may indicate an aquatic environment that suppressed the growth of macrophytes such as *Chara*.

~ AD 1540 to ~ 1880 (Zone 3)

This time period was marked by pronounced hydroecological change from the previous two zones. Open-drainage indicator diatoms increased from <5% to >35% in relative abundance, while closed-drainage indicator diatoms remained constant (~40%) for most of Zone 3. The marked increase of open-drainage diatom indicates that the hydrological status of the lake began to change from closed-drainage to open-drainage at ~AD 1540. According to multi-proxy paleolimnological records in gravity cores from the same lake and historic maps, Sinnatamby (2006) suggested that the westward expansion of Lake Athabasca influenced PAD9 until AD 1880, but the initial rise of Lake Athabasca was unclear. The longer sediment record presented here not only confirms the end of this phase at ~ AD 1880, but also captures the initiation of the influence from Lake Athabasca (~AD 1540). Reconstructed lake water oxygen isotope composition values (-17.8‰ to -13.8‰) are similar to the isotopic range of contemporary water from Lake Athabasca (-16.8 to -14.8‰) supporting the notion that Lake Athabasca waters began to enter the PAD9 basin at this time. The apparent increase in variability of lake water oxygen isotope composition compared to Zone 2 suggests that the influence of Lake Athabasca water may have been episodic rather than an extended period of inundation. An overall trend towards isotopically-enriched values during this 320-year period may indicate the receding trend of Lake Athabasca toward the ending of this period.

Additional insights into this Lake Athabasca phase are provided by the organic C%, carbon isotope records and macrofossil profiles. Organic C% declines to ~9% (the lowest value in the profile) by ~AD 1650, then rapidly increases to 13% around AD 1800. Similarly, $\delta^{13}C_{org}$ and $\delta^{13}C_{cell}$ decrease to -26.9‰ and -25.5‰ respectively at the beginning of this zone, and then increases to -26.4‰ and -

23.9‰ by the mid-1800s. The co-variance of organic carbon content (C%) and carbon isotope records suggest that PAD9 experienced a significant reduction in productivity between ~1540 and 1700 AD. The reduction in lake productivity appears to be associated with initial phases of the expansion of Lake Athabasca. The influence of Lake Athabasca evidently had a profound impact on the aquatic ecology at the PAD9 basin. Open-drainage basins are generally more turbid and have less light penetration than closed-drainage basins, which may be the major reason this interval was unfavorable to aquatic macrophytes and phytoplankton and ultimately led to a reduction in lake productivity. *Chara* oospores and ostracod shells are at their lowest abundance during this interval, which is consistent with reduced lake productivity. Combining evidence of frequent influence of lake Athabasca on PAD9 (e.g., high variability of inferred $\delta^{18}O_L$ values) with ecological changes characterized by carbon geochemistry and macrofossil abundance, we postulate that ~ AD 1540 to ~1700 was the maximum highstand of Lake Athabasca.

~ AD 1880 to ~1930 (Zone 4)

In Zone 4, open-drainage indicator diatoms become even more dominant, approaching 90% in relative abundance. In contrast, closed-drainage indicator diatoms decline from ~40% to <5%. Archival maps suggest that PAD9 may have been very close to a river channel connecting the receding Lake Athabasca with a major water conduit (the Rivière des Rochers) during this period (Sinnatamby, 2006). The through-flow-lake phase is also supported by reconstructed lake water oxygen isotope values (-18.4 to -16.7‰), which are similar to the modern isotopic composition of the Athabasca River (-19.7 to -16.5‰). Accompanying the marked hydrological change at PAD9 are marked changes in C%, $\delta^{13}C_{org}$ and $\delta^{13}C_{cell}$. These proxies increase initially, then rapidly decline toward the end of this zone, suggesting a transient ecological status in the lake system. Similar to Zone 3, turbid water may be the major reason for the sharp decline in productivity. The low productivity condition is also supported by low abundance of *Chara* oospores and ostracod shells during this period.

~ AD 1930 to present (Zone 5)

After 1930, closed-drainage indicator diatoms rapidly regain dominance in the diatom community. Open-drainage indicator diatoms, on the other hand, almost disappear completely (<5%). Lake water oxygen isotope composition inferred from sedimentary cellulose increases significantly to values (-15.1‰) similar to those measured during the early thaw season over the 7-year monitoring period.

These results indicate the lake rapidly returned to closed-drainage basin conditions after AD 1930. The marked hydrological changes may have profound consequence on the aquatic ecology. Increasing organic C% and carbon isotope records suggest the recovery of productivity within the lake. Macrofossil and aquatic invertebrate are slightly more abundant than in the previous two zones, also indicating the re-establishment of an aquatic macrophyte community during this period. Judging by the overall similarity between Zone 5 and Zone 2, which is shown by multiple proxies, the interval of AD 1140 to 1540 may be an analogue of the most recent period (after 1930).

4.4.4 Quantitative water balance reconstruction

Changes in lake water isotope composition ($\delta^{18}O_L$) are frequently interpreted as variations in isotopic composition of source water to lakes, or changes in lake water balance alone. The combined effects of two factors, however, can enhance or suppress the isotopic variability in lake water, which may lead to ambiguous interpretation. Given the multiproxy-constrained understanding of changes in source water to the PAD9, and the availability of millennium temperature (e.g. T) and relative humidity (e.g. RH) estimates from isotope dendroclimatology studies in the headwater region of Athabasca River (Edwards et al., 2008), we attempted to separate changes in these two factors (Figure 4-5a). Warm winter temperatures and humid growth season conditions prevailed in the headwaters region between AD 1000 and 1500. Cold winter and dry summer conditions developed in the late 1500s through to the early 1900s, which was followed by the return to intermediate conditions by ~1930. The reconstruction is consistent with the well-known pattern of MWP and LIA, followed by post-LIA climatic amelioration (Jones et al., 2001). As discussed below, quantitative estimates of T and RH are critical starting points to estimate the oxygen isotope composition in evaporation flux ($\delta^{18}O_E$), which is an essential parameter in isotope-mass balance calculations.

At isotopic steady-state, the relative ratio of lake water lost by evaporation to that gained by inflow can be quantified by the following equation (Gibson and Edwards, 2002):

$$E/I = \frac{\delta^{18}O_L - \delta^{18}O_I}{\delta^{18}O_L - \delta^{18}O_E} \qquad (4\text{-}1)$$

where E/I is the evaporation to inflow ratio. $\delta^{18}O_L$, $\delta^{18}O_I$ and $\delta^{18}O_E$ represent the isotopic composition of lake water, inflow flux and evaporation flux, respectively. Since $\delta^{18}O_L$ is readily reconstructed from the oxygen isotope composition of aquatic cellulose (Figure 4-4, Figure 4-5b), the evaluation of

the lake water balance of PAD9 in the past depends upon estimation of $\delta^{18}O_I$ and $\delta^{18}O_E$. Also note that the tree-ring based estimation of T and RH was presented in decadal resolution (Edwards et al., 2008), while the sediment-based $\delta^{18}O_L$ profile had varying temporal resolution because of changing sedimentation rate along the core (Figure 4-4). To prepare the incorporation of $\delta^{18}O_L$ into final water balance assessment, the original $\delta^{18}O_L$ was converted to decadal resolution by simple averaging of samples dated within each decade. The converted $\delta^{18}O_L$ profile is presented in Figure 4-5; the absence of noticeable differences in major features suggests the conversion in time scale is reasonable.

Based on the multi-proxy hydroecological reconstruction, PAD9 clearly experienced changes in drainage type, from closed-drainage conditions to open-drainage conditions at ~ AD1540, and from open-drainage back to closed-drainage conditions at ~ AD 1930. These changes were probably accompanied by changes in source water for the lake. When the lake was hydrologically closed, input waters to the lake likely were weighted precipitation through the year. If we assume that the pattern of change in the isotopic composition of local precipitation was parallel to that in the headwaters, then we can use the headwater record as a proxy for changes in δ_I. When the lake was hydrologically open, it was strongly influenced by Lake Athabasca (and hence Athabasca River) as discussed above. Given the average isotopic composition in contemporary water samples from the Athabasca River (-18.1‰), the temporal isotopic variation of input water under open-drainage conditions can be approximated by adjusting to temperature variation (again assuming the headwater temperature record is a reasonable first-order proxy) with 0.695 ‰/°C (Dansgaard, 1964). Merging these two records yields a composite "best-guess" of input water ($\delta^{18}O_I$) for PAD9 (Figure 4-5c). This semi-quantitative profile indicates the pattern of changes in source water that is consistent with our multiproxy hydroecological reconstruction.

As for the isotopic composition of evaporated flux ($\delta^{18}O_E$), this parameter can be estimated based on Craig-Gordon model (Craig and Gordon, 1965; Gonfiantini, 1986; Yi et al., 2008)

$$\delta^{18}O_E = \frac{(\delta^{18}O_L - \varepsilon^*)/\alpha^* - h\delta^{18}O_A - \varepsilon_k}{1 - h + \varepsilon_k} \qquad (4\text{-}2)$$

where $\delta^{18}O_L$ and $\delta^{18}O_A$ are the isotopic composition of lake water and atmospheric moisture. ε^* and ε_k are equilibrium and kinetic separation terms as defined elsewhere (Gonfiantini, 1986; Edwards et al., 2004). ε^* is dependent on temperature, while ε_k is estimated as a function of relative humidity deficit.

α^* is the equilibrium fractionation factor, which is related to ε^* simply by $\varepsilon^* = (\alpha^*-1)$. Note that the equation is formulated for δ, ε and h in decimal notation.

The estimation of $\delta^{18}O_E$, as expressed in the Equation (4-2), requires values for the isotopic composition of atmospheric moisture ($\delta^{18}O_A$). The most frequently applied method is to assume isotopic equilibrium between evaporation-flux-weighted local precipitation and atmospheric moisture (Zuber, 1983; Gibson et al., 1993; Edwards et al., 2004). Other solutions have relied upon the constant-volume pan method (Welhan and Fritz, 1977; Allison and Leaney, 1982; Gibson et al., 1999), the index lake method (Dinçer, 1968; Yi et al, 2008), and real-time sampling and isotopic analysis (Jacob and Sonntag, 1991). Here, we apply the most straightforward method (i.e. equilibrium between precipitation and atmospheric moisture) to generate a millennium profile of variation of $\delta^{18}O_A$. The estimated $\delta^{18}O_A$ ranges between –32.0‰ and –22.0‰, averaging around –27.0‰, which is consistent with the estimation of contemporary atmospheric moisture (–26.6‰) in the PAD (Yi et al., 2008). This estimation of $\delta^{18}O_A$ will be further used in Equation (4-2) for $\delta^{18}O_E$ calculation, and eventually incorporated in the assessment of lake water balance by Equation (4-1).

By applying $\delta^{18}O_L$, $\delta^{18}O_A$, RH and T in Equation (4-2), we estimate the isotopic variation of evaporated flux ($\delta^{18}O_E$) from PAD9 for the past millennium (Figure 4-5d). The results show a wide range of variation (from -34.1‰ to -62.1‰) in $\delta^{18}O_E$. In general, the variation of oxygen isotope composition in evaporated flux resembles the stratigraphic change of $\delta^{18}O_L$ to some extent. The long-term enrichment trend between AD 1000 and 1540 in Figure 4-5d probably partially reflects the enrichment of lake water isotope composition ($\delta^{18}O_L$). The short period of depletion in $\delta^{18}O_E$ between AD 1900 and 1930 is also largely attributable to the depleted $\delta^{18}O_L$ during the flow-through-lake phase.

Estimations of $\delta^{18}O_L$, $\delta^{18}O_I$ and $\delta^{18}O_E$ now allow assessment of the water balance for PAD9 by using Equation (4-1). The results are presented in Figure 4-5e. In general, the E/I values varied between 0 and 0.4 in the past millennium. For the purpose of crosscheck, we compared the estimated E/I value in the topmost sediments with an independent estimation of E/I for PAD9 based on lake water oxygen composition. Wolfe et al., (2007a) estimated 1.53 for PAD9 in 2000, while the sediments based E/I estimation indicated 0.33 during 1960s. The sediments inferred E/I values seem to underestimate the water balance given the apparent discrepancy in the comparison. Although this discrepancy can be partially attributed to the mismatch in time scale (e.g., sediment-based estimation

suggests decadal average in 1960s versus lake water based estimation suggests annual condition in 2000) and remarkably dry meteorological conditions in 2000 (Wolfe et al., 2007a), which probably significantly enhanced the effect of evaporation in a single year, we believe the relatively low E/I estimations from sediments are largely caused by the $\delta^{18}O_L$ reconstruction. Aquatic plants typically flourish during the middle of growth season, monthly before the end of the open-water season. Since the $\delta^{18}O_L$ was inferred from isotope signatures preserved in aquatic cellulose, the values must be representative of the lake water composition in the early part of the open-water season. Therefore, the reconstructed $\delta^{18}O_L$ should be more depleted than the isotopic composition at the end of the open-water season and this can be well supported by our knowledge of the modern isotope hydrology in the PAD. For example, the inferred $\delta^{18}O_L$ in the topmost sediments is -15.1‰, which is well within the range of modern variability, but more importantly significantly lower than the expected values (~-9‰) for the end of the open-water season as shown in Figure 4-2. As a consequence, the E/I estimates based on reconstructed $\delta^{18}O_L$ are expected to lower than those for the entire open-water season because it incompletely accounts for the effect of open-water evaporation and only reflects conditions in the early part of the open-water season. Nonetheless, the E/I profile presented in Figure 4-5 underestimates water balance conditions in the open-water season and the following discussion on E/I will emphasize the pattern of change rather than the exact values.

Between AD 1000 and 1540, the water balance reconstruction demonstrates a pattern of step-wise increase from <0.1 to >0.3 (Figure 4-5e), which is different from the pattern of change in $\delta^{18}O_L$ (note the sharp and rapid enrichment around AD 1100 Figure 4-5b). The comparison suggests that the change in $\delta^{18}O_L$ around AD 1100 is not only attributed to changes in water balance. In fact, the significant enrichment (>3‰) in $\delta^{18}O_L$ was probably caused by a combination of enhanced E/I (Figure 4-5e) and enriched isotopic composition in input water (Figure 4-5c). During the time period of AD 1140 to 1540, the general trend of depletion in $\delta^{18}O_I$ and the step-wise increase in E/I values suppressed each other, and led to ~-17‰ in $\delta^{18}O_L$ values with small variations. When the lake switched to open-drainage, E/I values decreased significantly. Although $\delta^{18}O_L$ did not show a clear difference between the open-drainage period (AD 1540 to 1880) and the closed-drainage period (AD 1140 to 1540) (Figure 4-5b), the water balance (E/I) reconstruction shows expected trends. Low E/I values correspond to the open-drainage time period, whereas high E/I values represent the closed-drainage time period (Figure 4-5e). Furthermore, the period of through-flow conditions (AD 1880 to 1930) is also striking in the E/I reconstruction. Low E/I values (approaching zero) suggest that minor

evaporation occurred in the lake water, consistent with reconstructed hydrological conditions at this time. After the through-flow lake phase, the E/I increased quickly, and became similar to the reconstructed values prior AD 1540.

4.5 Discussion

An isotope-mass balance method is used to reconstruct water balance conditions in the past, with the aid of a high-resolution climatic reconstruction and multi-proxy paleolimnological records. Changes in the oxygen isotope composition of lake water ($\delta^{18}O_L$) are integrated results from the primary change in input water ($\delta^{18}O_I$) and secondary variation in evaporative ^{18}O-enrichment (E/I). Deconvolution of $\delta^{18}O_L$ into $\delta^{18}O_I$ and E/I provides an opportunity to better understand the relevant hydrological processes influencing the basin over the past 1000 years.

As presented in Figure 4-5, the patterns in $\delta^{18}O_L$, $\delta^{18}O_I$ and E/I are different from each other, but share some similarities during certain time periods. For example, $\delta^{18}O_I$ value increased while the E/I value decreased around AD 1540. The opposite trends in E/I and $\delta^{18}O_I$ offset each other, resulting in only minor variation in $\delta^{18}O_L$. This is probably the main reason that the lake water oxygen isotope composition does not clearly show the transition from open-drainage to closed-drainage conditions, although it is clearly evident in the diatom profile (Figure 4-4). On the other hand, the diatom community composition does not delineate the transition at ~ AD 1100, which is clearly marked by changing $\delta^{18}O_L$. There were minor increases in the $\delta^{18}O_I$ around ~ AD 1100 and gradual increases in E/I value according to the reconstruction. But, as a result of combined effect of enrichment in $\delta^{18}O_I$ and increasing role of evaporation (i.e., increasing E/I values), lake water oxygen isotope composition ($\delta^{18}O_L$) exhibited pronounced change, as large as 3‰, at the transition period from Zone 1 to Zone 2 (Figure 4-5).

The Little Ice Age (LIA, between AD 1540 and 1930) is an intriguing period. The climate during this time interval was characterized by lower-than-mean T and RH (Figure 4-5a). $\delta^{18}O_L$ shows a long-term enrichment, but with a large range of variability (Figure 4-5b) as is the case for Figure 4-5e. When PAD9 was frequently influenced by Lake Athabasca, the E/I was low. When PAD9 was not affected by Lake Athabasca, the role of evaporation would become pronounced and lead to higher E/I values. The flow-through-lake phase (~AD 1880 to 1930) was marked by extremely low values of E/I, although the $\delta^{18}O_I$ values were even slightly enriched compared to the rest of the open-drainage

time period. This feature further supports the dominant role of river during the flow-through-lake phase.

Moreover, the expansion of Lake Athabasca seems to correspond to the LIA, when the region was characterized by dry and cold climate. It is also apparent that the open-drainage conditions only occurred once, lasting for ~300 years, in the last millennium. According to these observations, warm and humid climate was not likely associated with rising water level in lake Athabasca, while cold and dry climate seems to favour the expansion of Lake Athabasca. Therefore, we speculate that low temperature (especially during the summer) will lead to more prolonged snowmelt runoff generation in the eastern Rocky Mountains, and sustain greater summer discharge in the Athabasca and Peace rivers (Edwards et al., 2008). On the other hand, the Medieval Warm Period (MWP) seems to resemble the current hydrological status of PAD9, such as similar $\delta^{18}O_L$, similar E/I, and very similar T and RH, especially the latter part of MWP. As a result, hydroecological response to climate variability during the MWP may be a good analogue for current and future response to on-going climate change. Detailed studies of conditions during the MWP may provide critical insight into future projections of hydroecological change in the delta.

Although there are many similarities between MWP and present, there is also one pronounced difference evident from the quantitative reconstruction of water balance (E/I). Both periods exhibit a trend of increasing E/I, but the increase after 1930 was much more dramatic than anything during the MWP. This unprecedented rate of change may point toward continued drying in such closed-drainage lakes.

4.6 Conclusions and implications

Multi-proxy analysis of sediments from PAD9 indicates that hydroecological conditions varied substantially over the past 1000 years. Based on diatom community composition, oxygen isotope composition of lake water inferred from sedimentary cellulose, organic carbon content, stable carbon isotope composition in organic component and abundance of macrofossils preserved in lake sediments, the stratigraphic sequence of lake sediments can be divided into 5 hydroecological zones including :

1. AD 1000-1140 closed-drainage basin, mainly fed by ^{18}O-depleted annual precipitation
2. AD 1140-1540 closed-drainage basin, mainly fed by ^{18}O-enriched annual precipitation

3. AD 1540-1880 open-drainage, frequently influenced by relatively ^{18}O-rich Lake Athabasca
4. AD 1880-1930 through-flow-lake phase, strong river influence
5. AD 1930 to present, closed-drainage basin, fed by annual precipitation

The paleolimnological record suggests that the open-drainage condition only occurred once (AD 1540 to 1930) in the last millennium, although it lasted for a long period (>300 years). During this time period, high water level of Lake Athabasca probably caused periodic inundation of the PAD9. We hypothesize that the snowmelt-dominated runoff in the eastern Rocky Mountains sustained greater summer discharge in the Athabasca River and raised lake levels in Lake Athabasca during the LIA, although this hypothesis requires further paleolimnological investigations along the lower reaches of the Athabasca River. As the climate regime subsequently shifted around the beginning of the 20th century, the elevated summer discharge could not be maintained, hence leading to the separation of PAD9 from Lake Athabasca.

Because $\delta^{18}O_L$ values can be affected either by changes in primary source or alteration in secondary evaporation, the interpretation of stratigraphic variation in $\delta^{18}O_L$ is rarely straightforward. With the availability of millennium climate records based on isotopic signals in tree-ring cellulose and multi-proxy paleolimnological records, we separate the changing isotopic composition of input water for the lake ($\delta^{18}O_I$) and evaporation over inflow ratios (E/I). The comparison among $\delta^{18}O_I$, $\delta^{18}O_L$, and E/I provides an opportunity to closely examine the interactions among climate, water sources and water balances for PAD9. The E/I reconstruction supports the idea that the lake has maintained substantial aquatic habit for at least one thousand years, with a broad range of variability in water balance. The MWP was characterized by increasing E/I over 600 years, indicating progressively intensified role of evaporation. The LIA was characterized by low E/I values (even extremely low during through-flow lake phase), highlighting the important role of inflow, which can be related to expansion of Lake Athabasca. In the context of this long-term reconstruction, rapid changes over the last ~70 years may be a cause for concern about future drying in the central portion of the delta.

Acknowledgements

We are grateful to the staff of Wood Buffalo National Park for logistical support. We also would like to thank Ken Clogg-Wright, Adam Jeziorski, Andrew Paterson, Jacqueline Pridham, Peter van Driel, Sheila Vardy and Tammy Karst-Riddoch for field and lab assistance; Paul Wilkinson of the Freshwater Institute for radiometric analysis; and the Environmental Isotope Laboratory – University of Waterloo for conducting stable isotope analysis. Funding for this research was provided by the British Columbia Hydro and Power Authority and the Northern Scientific Training Program of Indian and Northern Affairs Canada.

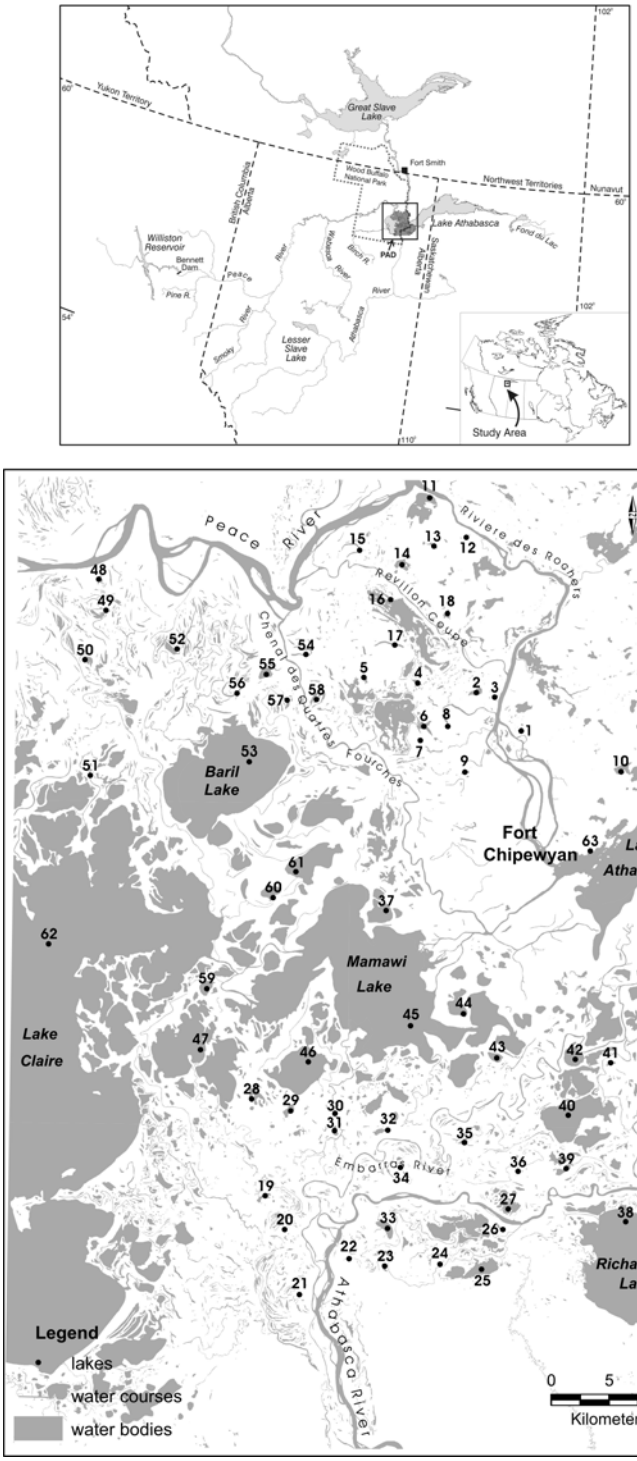

Figure 4-1 Location of the Peace-Athabasca Delta in northeastern Alberta, Canada.

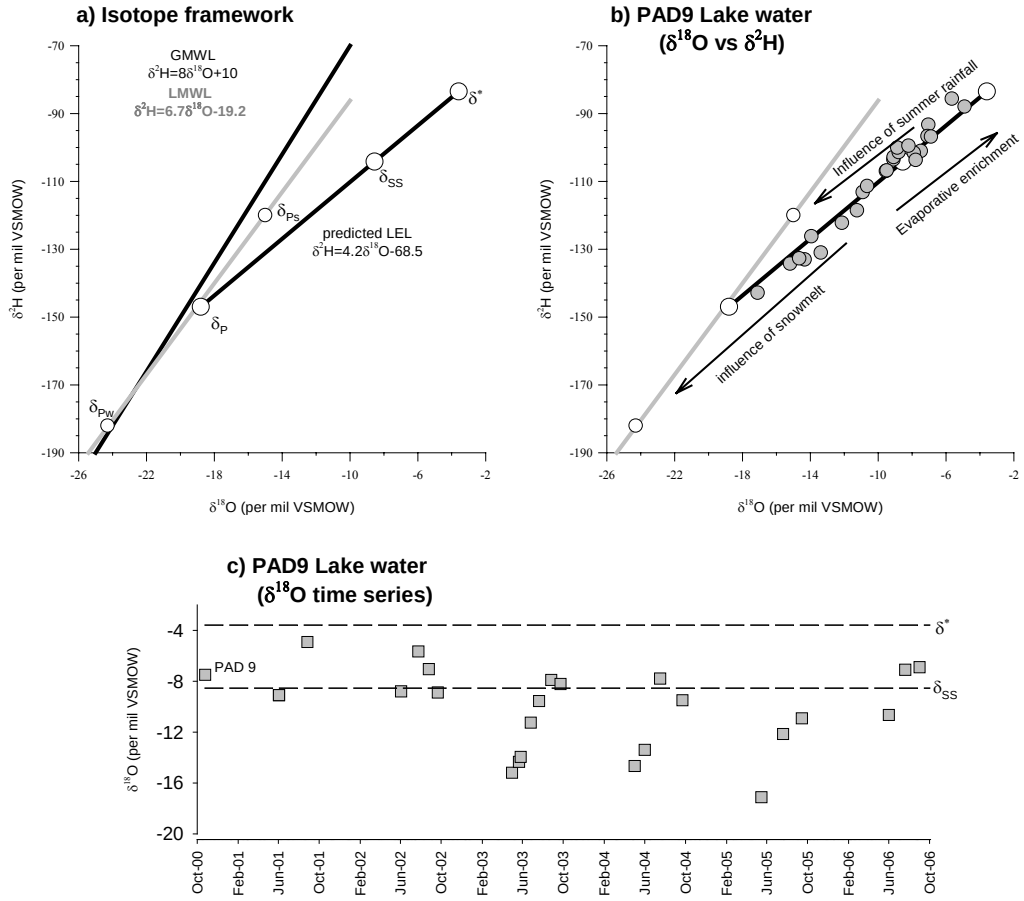

Figure 4-2 The contemporary isotope hydrology framework and lake water isotope compositions in PAD9. a) Water-isotope framework based on local isotopic and climatic means. The Global Meteoric Water Line (GMWL) is defined by $\delta^2H=6.7\delta^{18}O-19.2$ (Craig, 1961). The Local Meteoric Water Line (LMWL; $\delta^2H=8\delta^{18}O+10$) is based on precipitation collected at Fort Smith, Northwest Territories from 1960-1969 (Canadian Network for Isotopes in Precipitation, Birks et al., 2004). The Local Evaporation Line (LEL) was established by Wolfe et al., (2007a). δ_{ss} represents a terminal lake in isotopic and hydrologic steady-state fed by mean annual precipitation (δ_p), while δ^* represents the theoretical limiting isotopic enrichment attainable by a desiccating water body under average thaw-season conditions. In comparison to δ_p, δ_{pw} and δ_{ps} are the isotopic compositions of evaporation-flux-weighted precipitation during winter and summer respectively. b) Stable isotope results for PAD9 lake water (filled circles) collected over a 7-year period shown in relation to δ_p, δ_{ss}, δ^* δ_{pw}, δ_{ps} (open circles). c) Variation of $\delta^{18}O$ in PAD9 lake water with time.

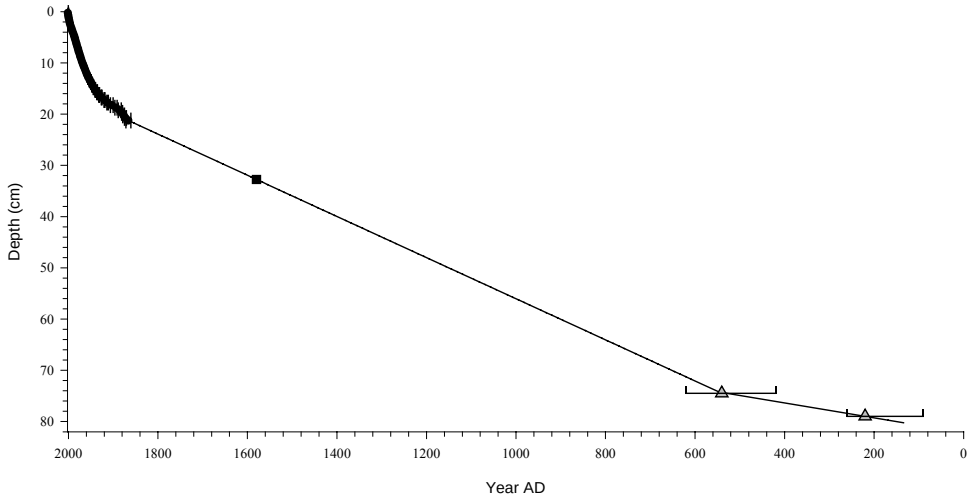

Figure 4-3 Age-depth profile for PAD9 lake sediments. The chronology is based on Constant Rate of Supply (CRS) modelling of the ^{210}Pb activity from the top the sediment sequence to 21.25cm, where supported ^{210}Pb levels are reached. From 21.25 to 74.5cm, the ages for sediments are estimated by linear interpolation between the CRS-modelled age for 21.25cm (AD 1866) and calibrated ^{14}C date for 74.5cm (AD 540).

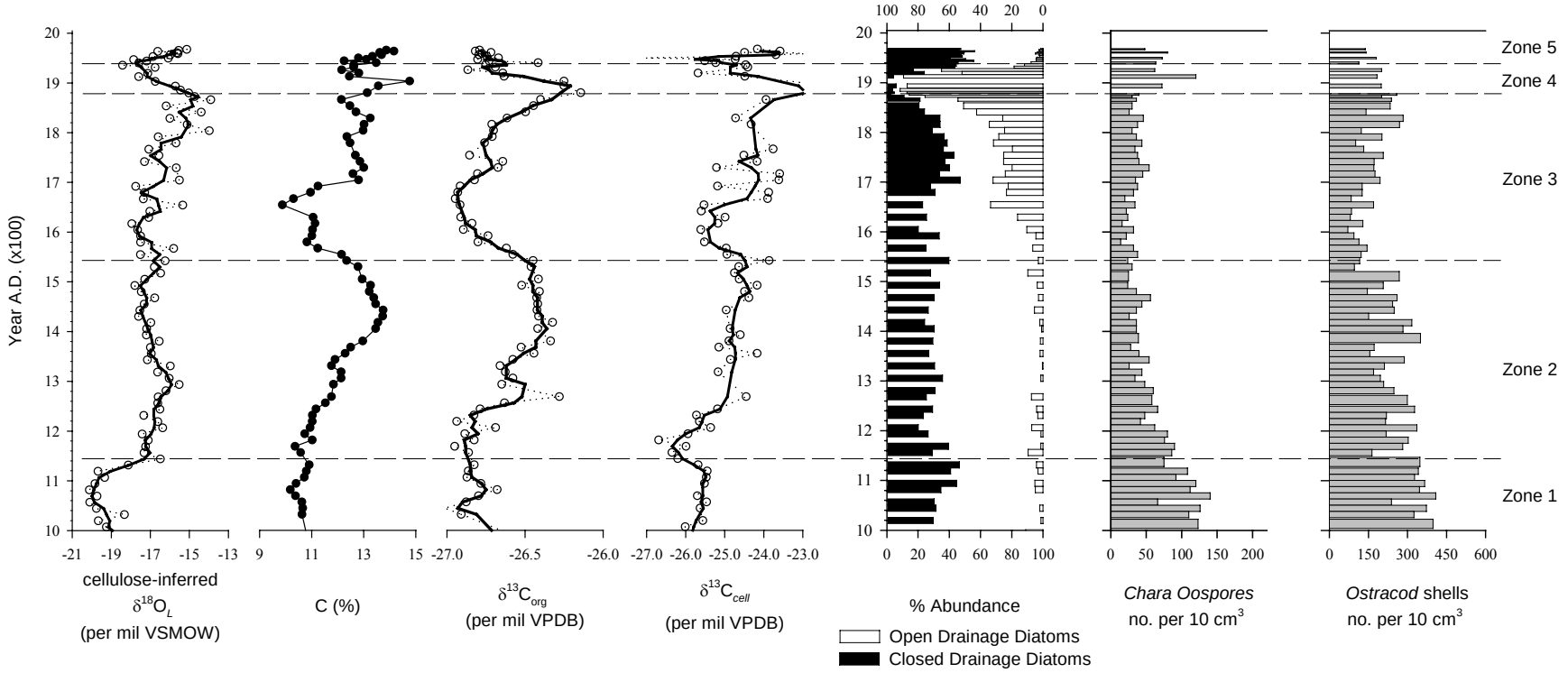

Figure 4-4 Summary diagram of key paleolimnological indicators including $\delta^{18}O_L$ inferred from sedimentary cellulose, organic carbon content (C%), carbon isotope composition in bulk and sedimentary cellulose ($\delta^{13}C_{bulk}$ and $\delta^{13}C_{cell}$), diatom community compositions, and abundance of macrofossils (e.g. *Chara* oospores and Ostracod shells) from PAD9. The dashed lines delineate the five eco-hydrological zones discussed in the paper.

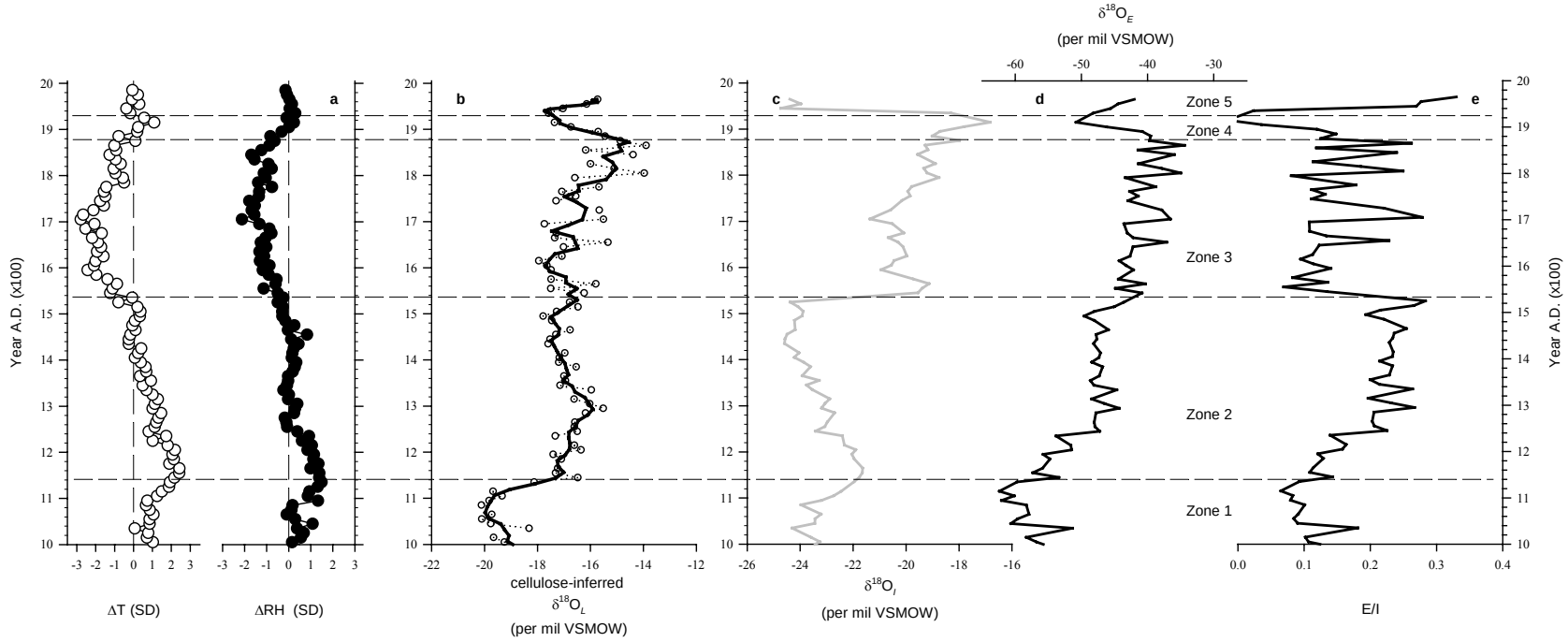

Figure 4-5 Summary diagram of quantitative reconstruction of lake water balance in the past. a) millennium reconstruction of climate in headwater region of the Athabasca River (Edwards et al., 2008); b) lake water oxygen isotope composition ($\delta^{18}O_L$) inferred from sedimentary cellulose; c) calculated oxygen isotope composition of input water ($\delta^{18}O_I$) for PAD9 over the last millennium; d) calculated oxygen isotope composition of evaporated flux ($\delta^{18}O_E$) from PAD9 over the last millennium; e) calculated evaporation to inflow ratios (E/I) for PAD9 over the last millennium.

Table 4-1 Selected physical and chemical limnological characteristics of PAD9 in October 2000 (Hall et al., 2004)

Limnology conditions	Units	Concentration
Total phosphorus	μg/L	42
Dissolved phosphorus	μg/L	32
Total nitrogen	μg/L	1920
Dissolved nitrogen	μg/L	1840
Chlorophyll α	μg/L	2.4
Dissolved organic carbon	μg/L	32
SiO_2	μg/L	430
pH	meq/L	8.3
Alkalinity	ms/L	4.63
Conductivity	mg/L	0.433
Ca	mg/L	43.5
Mg	mg/L	20.5
K	mg/L	12.9
Cl^-	mg/L	7.5

Table 4-2 Radiocarbon data obtained by accelerator mass spectrometry for PAD9 lake sediments

Depth (cm)	Material	Calibrated ^{14}C age (AD)	Calibrated age range (AD)	$\delta^{13}C$ (‰ PDB)
74.50	*Sparganium, Carex, Scirpus* and *Rumex* seeds	540	420-620	-27.0
78.75	*Carex* and *Scirpus* seeds	220	90-260	-26.1

Chapter 5
Synthesis

5.1 Summary and Outlook of Significant Results

This dissertation comprises a series of studies that improve and refine the application of isotope techniques in hydrological and paleohydrological studies. Self-contained manuscripts presented in this thesis (Chapter 2 to 4) are contributions to the multidisciplinary PAD Stratigraphy project led by researchers at University of Waterloo and Wilfrid Laurier University.

In the study of modern isotope hydrology, a new coupled-isotope approach was developed to evaluate input water into individual lakes. Although oxygen and deuterium analyses of water have become routine and the usage of $\delta^{18}O$-$\delta^{2}H$ plot is fundamental in the field of isotope hydrology, the two dimensional (even three dimensional) information in the $\delta^{18}O$-$\delta^{2}H$ space was not fully explored yet. The isotopic composition of input water to multiple lakes in a region is usually inferred from the intersection of Local Meteoric Water Line and Local Evaporation Line, and therefore treated as homogenous over a broad area. As such, the isotopic composition of lake water, which is the result of primary recharge process and secondary evaporative enrichment, is used to provide quantitative information only on water balance in most studies. Recognizing the surface heterogeneity and variable roles of multiple recharging sources, the coupled-isotope approach also provides an opportunity to quantitatively estimate the isotopic composition of input water to individual lakes

The application of the coupled-isotope approach in two regional water-sampling campaigns (2000 and 2005 respectively) in the PAD demonstrates remarkable temporal changes of source waters in the delta (refer to Figure 2-5). Summer rainfall in 2000 played an important role in replenishing shallow basins delta-wide. In contrast, contribution from snowmelt was significantly increased in the northern Peace sector in 2005, while, in the same year, river flooding brought substantial amounts of water to maintain the water balance in the southern Athabasca sector. The changes in recharge processes appeared to be strongly related to catchment characteristics and antecedent meteorological conditions. Moreover, future investigation of the valuable datasets obtained during intensive field campaign in three consecutive years (i.e. 2004, 2005, 2006) holds great potential to uncover intriguing spatio-temporal patterns in the PAD. The modelled δ_I scenario (Figure 5-1) is remarkably consistent with

observation on local meteorological conditions (Figure 5-2), indicating the strong linkage between local climate and runoff generation. For example, δ_I values for 2006 are generally higher compared to results for 2004 and 2005, suggesting a minor role of snowmelt for lake recharge during 2006. This is supported by the fact that the 2005-2006 winter was significantly warmer than climate normal (1971-2000), which is probably partially attributed to less snowfall as presented in Figure 5-2. Further spatially interpolation of results from coupled-isotope analysis can produce illustrations such as color-coded contour map in Figure 5-1, and these maps are useful to identify areas that are likely to receive particular types of source water. According to maps in Figure 5-1, the northwest (centering around PAD 52) and the northeast (east of PAD 13) parts of the delta are probably the areas most susceptible to snowmelt runoff generation, but the intervening area in the northern Peace sector probably receives an even balance between snowmelt and summer rainfall from year to year. In contrast, the central low-lying area including PAD59, 61, 41 and 42 is likely reliant on isotopically enriched water from summer rainfall and occasional summer flooding. On one hand, further geostatistical analysis is needed to quantify and strengthen the simple observation of these mapping products. On the other hand, the integration of lake-specific hydrological information, as presented in Figure 5-1, with well-monitored limnological and ecological records in the PAD may eventually lead to comprehensive understanding of interaction between hydrology and aquatic ecology.

Given the merits of the coupled-isotope approach, it is also important to keep in mind an essential assumption behind the method - the LMWL constraints on the $\delta^{18}O$-$\delta^{2}H$ relation in input waters. It is a good first-order approximation with current knowledge, however, is there any room to improve the coupled-isotope approach with regard to this assumption? To be more realistic, the isotopic composition of input water (δ_I) should be clouded around the LMWL. In other words, a polygon rather than a line (i.e. LMWL) would be a better approach to constrain the δ_I in addition to isotope mass balance. If a triangular polygon is used in lake specific δ_I calculation, it is highly possible to develop an analytical solution for contributing proportions from each isotopically distinct source. If a more complicated polygon than a triangle is used in lake specific δ_I calculation, it is impossible to quantify the proportional contribution from individual sources, because only two tracers (i.e. ^{2}H and ^{18}O) are applied in the investigation. However, it is possible to determine the distribution pattern of source contributions (i.e., frequency and range of feasible solutions for individual sources). Overall, research based on the concept of coupling $\delta^{18}O$ and $\delta^{2}H$ in quantitative analysis should be continued.

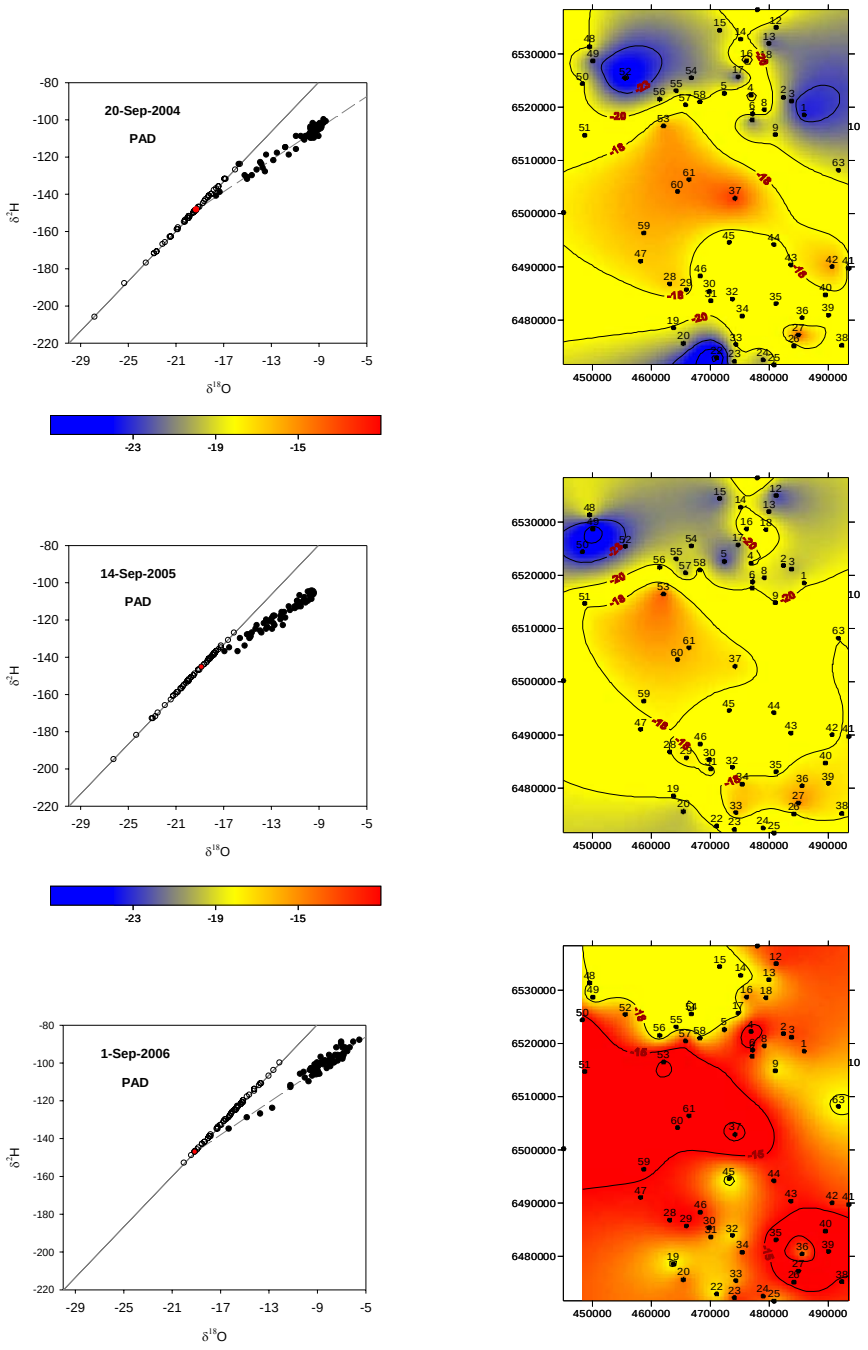

Figure 5-1 Modelled isotopic composition of lake specific input waters in three consecutive years (left column) and their correspondents spatial presentation (right column). The colour scheme for the spatial mapping is: blue represents isotopic values less than -23‰; red indicates isotopic values greater than -15‰; yellow is assigned to isotopic range between -18‰ and -20‰; isotopic values intermediate to these three end members are presented with transitional colours.

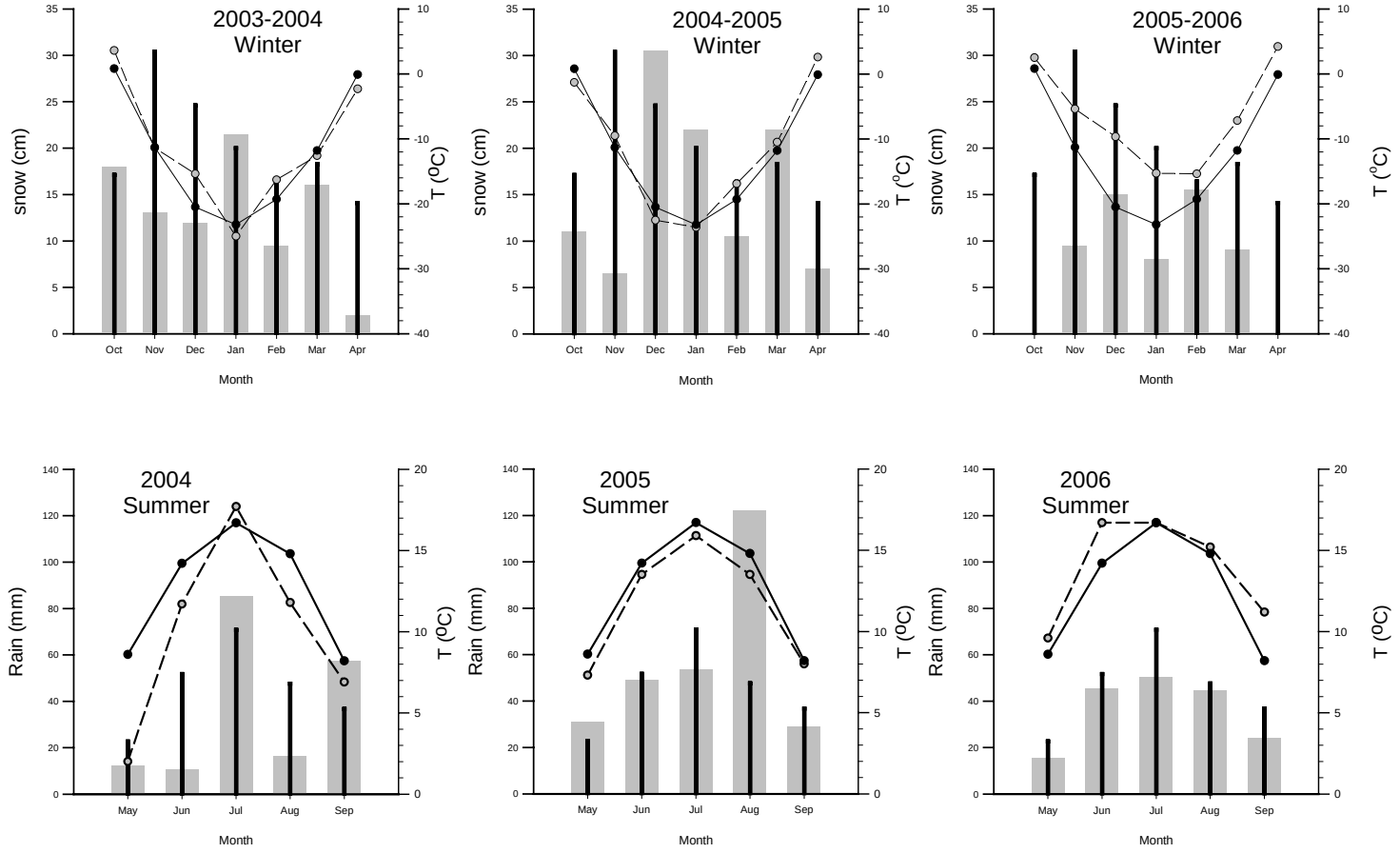

Figure 5-2 Winter and summer monthly mean temperature and accumulated precipitation for 2003/2004, 2004/2005 and 2005/2006 compared to 1971-2000 climate normals. Climate normals are shown as solid circles (temperature) and bars (precipitation).

the preceding discussion is just one possible future direction to improve the results from coupled-isotope analysis, although other methods may allow more sophisticated analysis.

Besides contributing to the understanding of contemporary isotope hydrology in the PAD, this thesis also makes an effort to further our understanding of isotopic labelling of aquatic cellulose from environmental water. Although the isotopic composition of lake water records important information on current hydrology and climate, paleo-water (i.e., water in the past) is seldom preserved in terrestrial environments. Proxy-based reconstruction of water isotope composition, especially $\delta^{18}O$, from natural archives has been an essential technique to infer environmental and climatic conditions in the distant past, given tremendous knowledge gained in contemporary studies as presented in Chapter 2 and numerous other studies. Among many proxies, the isotopic signature in aquatic cellulose is the one broadly used. However, transfer functions to infer the isotopic composition of lake water based on isotopic signals in aquatic cellulose have been questioned, because laboratory calibration from several experiments yielded inconsistent views on the isotopic labeling of aquatic cellulose from water.

Consequently, a *Ceratophyllum demersum* culture experiment (Chapter 3) was conducted as a part of the thesis to make an attempt to reconcile cellulose-water oxygen isotope relations, which eventually contributes to the cellulose-based isotopic reconstruction of hydrology in the PAD. The strong linear correlation between aquatic cellulose and environmental water obtained from the experiment, once again, casts no doubt on the prominent influence of environmental water on isotopic signature (oxygen) in cellulose. It is possible and feasible to achieve fairly accurate and precise lake water history based on isotopic composition of aquatic cellulose preserved in sediments. However, as in other experiments, the linear relation between cellulose $\delta^{18}O$ and water $\delta^{18}O$ is not a constant-fractionation line, which indicates that environmental water is not the only factor affecting the $\delta^{18}O$ of aquatic cellulose in these experiments. There probably is an unknown source of oxygen, which contributes to the $\delta^{18}O$ in aquatic cellulose. Combining current and previous laboratory results, the chapter makes an effort to estimate the isotopic composition of "mystery" cellulose oxygen, which indicates the source is CO_2. Moreover, we propose a new conceptual characterization of the cellulose-water relation. Although biochemically mediated isotope exchange between CO_2 and H_2O leads to an apparent linear relation between cellulose and water $\delta^{18}O$ values, oxygen in cellulose is actually fully inherited from CO_2 during photosynthesis. The new characterization readily reconciles inconsistencies in multiple experimental results, which is caused by varying proportion of non-

exchanged CO_2. More importantly, the new development in understanding cellulose-water relation also suggests that the existence of apparent constant fractionation typically observed in field studies probably reflects the long residence time of CO_2 in natural waters, which ensures full exchange between CO_2 and H_2O.

To rigorously test the new conceptual characterization, a carefully designed field culture experiment is required. Besides water and cellulose sampling for isotopic correlation, dissolved CO_2 samples for oxygen isotope analysis would be desirable. In addition, inevitable natural variation of isotopic composition in lake water can cause difficulty in the interpretation of field data, therefore, a careful choice of lake with minimum isotopic fluctuation during growth season should be considered in order to produce straightforward and convincing field data to test the proposed characterization.

Knowledge gained in studies of contemporary processes (Chapter 2 and Chapter 3) paves the way to reconstruct hydrological conditions in the PAD, with a special emphasis on the isotopic records in lake sediments. Chapter 4 presents an attempt to quantitatively reconstruct lake water balance over the past 1000 years, with the constraint of the variability of climate and change in isotope compositions of input water and atmospheric moisture. The results demonstrate progressively increasing roles in evaporation during the Medieval Warm Period (~AD 1000 to 1540); low evaporation relative to input ratios (i.e., E/I) between 1540 and 1880; minor role of evaporation (i.e., E/I approaching zero) during a short period from 1880 to 1930; and a rapid increase of E/I in the most recent decades (i.e., after 1930 to present). The changes in water balance were consistent with changes in drainage type of the lake, which are indicated by an array of paleolimnological proxies. Relatively high E/I values are associated with closed drainage, while relatively low E/I conditions are related to open-drainage lake conditions. The extremely low E/I (approaching zero) corresponds to an interesting phase of PAD9 when the lake functioned like a river channel connecting Lake Athabasca with the major water conduit passing through the delta.

In summary, this thesis improves our ability to interpret isotopic signals from lake water samples and sedimentary archives in lacustrine environments. It also demonstrates the capacity to integrate contemporary processes studies into the context of millennium reconstruction of lake hydrology and ecology. Clearly, studies at different time scales benefit each other and facilitate a comprehensive understanding of the delta in the past and present.

5.2 Recommendations for Future Research

First of all, regional isotopic sampling of these basins should be continued on a regular basis over the long term. The initial reconnaissance dataset has provided highly valuable spatial information for assessing and characterizing current hydrological status in this large remote ecosystem (Wolfe et al., 2007; Yi et al., 2008). Such information is very difficult, if not impossible, to obtain via conventional hydrometric monitoring. More importantly, it is the temporal insight gained from collecting isotope samples over many years that would be necessary to gauge the response and resilience of the PAD to various environmental stressors. As shown by the Global Network for Isotope in Precipitation, the value of a long term high-quality isotopic dataset can be far beyond the scope of initial research design, with the increasing "isotopic craving" in addressing a wide range of issues related to atmospheric circulation, bird migration and food source certification (Aggarwal et al., 2007).

Isotopic composition in atmospheric moisture (δ_A) is the least constrained parameter in the exercise of quantitative analysis of water isotope data. A priority for further research should clearly be improving the modelling and measurement of δ_A. Although most studies generally treat the atmospheric moisture as homogenous to some extent, several important processes such as mixing of different vapour sources, post-condensation evaporation and recycling moisture from terrestrial environment, make atmospheric moisture heterogeneous at local, regional and global scales (Birks, 2003; Worden et al., 2007). An attempt to quantify mixing of different vapour sources is in progress for Slave River Delta, Northwest Territories. The delta is located in the leeward direction to Great Slave Lake (GSL, 28,400 km^2 in area), hence advective moisture from northern inland area and evaporated vapour from Great Slave Lake present two possible sources of atmospheric moisture. A systematic sampling of water bodies in the delta will be used to investigate the spatio-temporal pattern of mixing, by coupling $\delta^{18}O$ and $\delta^{2}H$ in water balance modelling (Brock et al., in preparation). On the other hand, the coupled isotope tracer approach certainly holds the opportunity to investigate recycling of moisture in terrestrial environments. An "effective relative humidity" that is proportional to the intensity of recycling can be derived by coupling oxygen and deuterium signals in data analysis. Thus, the proportion of moisture recycled from local evaporation (even transpiration) can be quantified. But, there is a difficulty in simultaneously accounting for mixing of different vapour sources and recycling of local evaporated vapour. Nonetheless, all of these relatively simple data

analyses will provide a basis for validating and refining more complicated circulation models, such as REMOiso (Sturm et al., 2005), or even incorporated into it.

Besides the modelling potential for δ_A, techniques for measuring the isotopic composition of atmospheric moisture are also evolving very quickly. Novel optical-based techniques are emerging for *in-situ* measurement of gaseous molecules including water (Bowling et al., 2003; Lee et al., 2005). Such new analytical techniques are not only going to provide abundant real-time measurements to benefit modelling studies, but also have great potential to revolutionize field-oriented monitoring programs such as the on-going PAD project. Eventually, integrating modelling, field studies and advanced analytical technology for the purpose of mutual discovery is the true frontier in water sciences.

Interpretation of lake water $\delta^{18}O$ history would certainly benefit from the availability of lake water δ^2H. With quantitative knowledge of both tracers, the primary isotopic effects caused by change in the isotopic composition of meteoric water can be easily separated from those associated with secondary hydrological processes such as evaporative enrichment. In $\delta^{18}O$-δ^2H space, this translates into LMWL-parallel shifts, which are commonly T-dependent or circulation related, and LEL-parallel shifts, which are generally associated with changes in relative humidity and water balance. The application of the concept of coupled isotope approaches in paleo-archives is very promising. Current techniques for δ^2H analysis in cellulose require large samples and tedious laboratory pretreatments. This largely hampers the availability of δ^2H from sedimentary cellulose. However, compound-specific isotopic (δ^2H) analysis of sedimentary lipid is a promising new research direction to acquire lake water δ^2H history (Huang et al., 2004). Via combining $\delta^{18}O$ analysis of sedimentary cellulose and δ^2H analysis of sedimentary lipids, the advantage of coupled isotope investigation in modern isotope hydrology can be readily transferred into paleo-studies.

As for the PAD project, total extractable lipids from the PAD12 sediment core, which were obtained in the procedure of sedimentary cellulose pretreatment and subsequently archived, could provide an appropriate testing ground for pioneering δ^2H and $\delta^{18}O$ coupled investigation in paleolimnology. On the other hand, multiple-year isotopic monitoring of PAD lakes, part of which have been presented and discussed in Chapter 1, would provide critical baseline and framework to validate and evaluate the application of $\delta^{18}O$-δ^2H coupling in paleo-studies.

Previous studies in the PAD focused on flow regime and hydrological processes in the Peace River and its major distributary channels. However, recent studies have concluded that the hydroecology of the Athabasca sector of the PAD is far more sensitive to change in Athabasca River flow compared to the Peace sector, which appears to be remarkably resilient to changes in Peace River flow regimes (Wolfe et al., 2008). In consideration of the expected expansion of the tar sands projects a few hundred kilometers upstream of the PAD, future research attention should be shifted to the Athabasca sector. More lakes along the lower reaches of the Athabasca River (within and outside of Athabasca sector) should be monitored and studied. Improved spatial resolution along the Athabasca River will help to identify the most susceptible zones in the Athabasca drainage system to human-induced disturbance.

Overall, there is still much more to learn from the PAD, and much more to be improved in management practices of this productive ecosystem. A systematic view of the hydrosphere-biosphere-atmosphere continuum with a dual-isotope approach is the key to significant breakthroughs in understanding the past, present and the future.

References

Chapter 1

Bailey JNL, 2008. Reconstruction of paleoclimate time-series in the Peace-Athabasca Delta, northern Alberta, from stable isotope in tree-rings. MSc thesis, University of Waterloo, Waterloo 193 pp.

Diefendorf AF, and Patterson WP, 2005. Survey of stable isotopes values in Irish surface waters. *Journal of Paleolimnolgy*, 34: 257-269.

Edwards TWD, Birks SJ, Luckman BH, MacDonald GM, 2008. Climatic and hydrologic variability during the past millennium in the eastern Rocky Mountains and Northern Great Plains of western Canada. *Quaternary Research*, doi:10.1016/j.yqres.2008.04.013.

Groisman PY, and Easterling DR, 1994. Variability and trends of total precipitation and snowfall over the United States and Canada. *Journal of Climate* 7:184–205.

Gummer WD, Cash KJ, Frederick JW, Prowse TD, 2000. The Northern River Basins Study: context and design. *Journal of Aquatic Ecosystem Stress and Recovery* 8: 7-16.

Hall RI, Wolfe BB, Edwards TWD, Karst-Riddoch TL, Vardy SR, McGowan S, Sjunneskog C, Paterson A, Last WM, English M, Sylvestre F, Leavitt PR, Warner BG, Boots B, Palmini R, Clogg-Wright KP, Sokal MA, Falcone M, van Driel P and Asada T, 2004. A multicentury flood, climatic, and ecological history of the Peace-Athabasca Delta, northern Alberta, Canada. Final report. Published by BC Hydro, 163 pp + Appendices.

Henderson AK, and Shuman BN, 2008. Hydrogen and oxygen isotopic compositions of lake water in the western United States. *Geological Society of America Bulletin*, in review.

Jones MD, and Roberts CN, 2008. Interpreting lake isotope records of Holocene environmental change in the Eastern Mediterranean. *Quaternary International* 181: 32-38.

Jones PD, Osborn TJ, Briffa KR, 2001. The evolution of climate over the last millennium. *Science* 292: 662-667.

Junk WJ, 2005. Flood pulsing and the linkages between terrestrial, aquatic and wetland systems. *Verh Internat Verein Limnol* 29: 11-38.

Leng MJ, and Anderson NJ, 2003. Isotopic variation in modern lake waters from western Greenland. *The Holocene* 13: 605-611.

Leng MJ, and Marshall JD, 2004. Paleoclimate interpretation of stable isotope data from lake sediment archives. *Quaternary Science Reviews* 23: 811-831.

Mayr C, Lücke A, Stichler W, Trimborn P, Ercolano B, Oliva G, Ohlendorf C, Soto J, Fey M, Haberzettl T, Janssen S, Schäbitz F, Schleser GH, Wille M, Zolitschka B, 2007. Precipitation origin and evaporation of lakes in semi-arid Patagonia (Argentina) inferred from stable isotopes ($\delta^{18}O$, $\delta^{2}H$). *Journal of Hydrology* 334: 53-63.

Nilsson C, Reidy CA, Dynesius M, Revenga C, 2005. Fragmentation and flow regulation of the world's large river systems. *Science* 308: 405–408.

Overpeck J, Hughen K, Hardy D, Bradley R, Case R, Douglas M, Finney B, Gajewski K, Jacoby G, Jennings A, Lamoureux S, Lasca A, MacDonald G, Moore J, Retelle M, Smith S, Wolfe A, and Zielinski G, 1997. Arctic environmental change of the last four centuries. *Science* 278: 1251–1256.

PAD-PG (Peace-Athabasca Delta Project Group) 1973. Peace-Athabasca Delta Project, Technical Report and Appendices. Volume 1: Hydrological Investigations, Volume 2: Ecological Investigations.

PAD-IC 1987. Peace-Athabasca Delta Water Management Works Evaluation. Final Report, Appendix A: Hydrological Assessment, Appendix B: Biological Assessment, Appendix C: Ancillary Studies. Peace-Athabasca Delta Implementation Committee, Governments of Alberta, Saskatchewan and Canada. 63 pp.

PAD-TS (Peace-Athabasca Delta Technical Studies) 1996. MacMillan S. (Editor). Final Report. PAD-TS Steering Committee, Fort Chipewyan, Alberta. Word Picture Communications. 106 pp.

Pietroniro A, Leconte R, Toth B, Peters DL, Kouwen N, Conly FM, Prowse T, 2006. Modelling climate change impacts in the Peace and Athabasca catchment and delta: III integrated model assessment. *Hydrological Processes* 20: 4231- 4245.

Prowse TD, and Lalonde V, 1996. Open-water and ice-jam flooding of a northern delta. *Nordic Hydrology* 27: 85-100.

Prowse TD, and Conly, FM, 1998. Impacts of climatic variability and flow regulation on ice-jam flooding of a northern delta. *Hydrological Processes* 12: 1589-1610.

Sinnatamby RN, 2006. An Assessment of hydro-ecological changes at two closed-drainage basins in the Peace-Athabasca Delta, Alberta, Canada. MSc thesis, University of Waterloo, Waterloo 108 pp.

Sinnatamby RN, Yi Y, Sokal M, Clogg-Wright K, Vardy SR, Karst-Riddoch T, Last W, Johnston J, Hall RI, Wolfe BB, Edwards TWD, Cartographic and paleolimnological evidence for expansion of Lake Athabasca during the Little Ice Age. *Journal of Paleolimnology*. In preparation.

Schindler DW, and Donahue WF, 2006. An impending water crisis in Canada's western prairie provinces. *PNAS* 109: 7210-7216.

Townsend GH, 1975. Impact of the Bennett dam on the Peace-Athabasca Delta. *Journal of the Fisheries Research Board of Canada* 32: 171-176.

Wetlands International, 2005. Wetlands International: Ramsar Sites Information Service. Website: http://www.wetlands.org.

Wolfe BB, Edwards TWD, Hall RI, 2002. Past and present ecohydrology of the Peace-Athabasca Delta, northern Alberta, Canada: Water isotopes lead the way. *PAGES News*. 10: 16-17.

Wolfe BB, Karst-Riddoch TL, Vardy SR, Falcone MD, Hall RI, Edwards TWD, 2005. Impacts of climate and river flooding on the hydro-ecology of a floodplain basin, Peace-Athabasca Delta, Canada since A.D. 1700. *Quaternary Research* 64: 147-162.

Wolfe BB, Hall RI, Last WM, Edwards TWD, English MC, Karst-Riddoch TL, Paterson A, and Palmini R, 2006. Reconstruction of multi-century flood histories from oxbow lake sediments, Peace-Athabasca Delta, Canada. *Hydrological Processes* 20: 4131-415.

Wolfe BB, Karst-Riddoch TL, Hall RI, Edwards TWD, English MC, Palmini R, McGowan S, Vardy SR, 2007. Classification of hydrologic regimes of northern floodplain basins (Peace-Athabasca Delta, Canada) from analysis of stable isotopes ($\delta^{18}O$, $\delta^{2}H$) and water chemistry. *Hydrological Processes* 21: 151-168.

Wolfe BB, Hall RI, Edwards TWD, Vardy SR, Falcone MD, Sjunneskog C, Sylvestre F, McGowan S, Leavitt PR, and van Driel P, 2008. Hydroecological responses of the Athabasca Delta, Canada, to changes in river flow and climate during the 20th century. *Ecohydrology* 1: doi:10.1002/eco.13.

Chapter 2

Allison GB, Leaney FW, 1982. Estimation of isotopic exchange parameters, using constant feed pans. *Journal of Hydrology* 55: 151-161.

Birks SJ, Edwards TWD, Gibson JJ, Drimmie RJ, Michel FA, 2004. *Canadian Network for Isotopes in Precipitation*. (http://www.science.uwaterloo.ca/~twdedwar/cnip/cniphome.html). Accessed 6 July 2007.

Coleman ML, Shepherd TJ, Durham JJ, Rouse JE, Moore GR, 1982. Reduction of water with zinc for hydrogen isotope analysis. *Analytical Chemistry* 54: 993-995.

Coplen TB, 1996. New guidelines for reporting stable hydrogen, carbon, and oxygen isotope-ratio data. *Geochimica et Cosmochimica Acta* 60: 3359-3360.

Craig H, 1961. Isotopic variations in meteoric waters. *Science* 133: 1702-1703.

Craig H, Gordon LI, 1965. Deuterium and oxygen 18 variations in the ocean and the marine atmosphere. In: Tongiorgi E (Ed.), Stable Isotope in Oceanographic Studies and Paleotemperatures. Pisa, Italy: Laboratorio di Geologia Nucleare, pp 9-130.

Dinçer T, 1968. The use of oxygen-18 and deuterium concentrations in the water balance of lakes. *Water Resources Research* 4: 1289-1305.

Drimmie RJ, Heemskerk RA, 1993. Water ^{18}O by CO_2 equilibration. Technical Procedure 13.0, Rev. 02. Environmental Isotope Laboratory: Department of Earth Sciences, University of Waterloo. 11 pp.

Edwards TWD, Wolfe BB, Gibson JJ, Hammarlund D, 2004. Use of water isotope tracers in high-latitude hydrology and paleohydrology. In: Pienitz R, Douglas MSV, Smol JP (Eds.), Long-term Environmental Change in Arctic and Antarctic Lakes, Developments in Paleoenvironmental Research, vol. 8. Springer, Dordrecht, pp 187-207.

Environment Canada, 2004. *Climate Data Online* (http://www.climate.weatheroffice.ec.gc.ca/climateData/hourlydata_e.html). Accessed 8 April 2007.

Epstein S, Mayeda TK, 1953. Variation of O^{18} content of waters from natural sources. *Geochimica et Cosmochimica Acta* 4: 213-224.

Falcone M, 2007. Assessing hydrological processes controlling the water balance of lakes in the Peace-Athabasca Delta, Alberta, Canada, using water isotope tracers. MSc thesis, University of Waterloo, Waterloo 190 pp.

Ferhi A, Bariac T, Letolle R, 1983. 18O/16O ratios in leaf water and cellulose of aquatic and terrestrial plants. In: IAEA (Eds), Palaeoclimates and Palaeowaters: a Collection of Environmental Isotope Studies. International Atomic Energy Agency, Vienna, pp 85-99.

Gat JR, 1996. Oxygen and hydrogen isotopes in the hydrological cycle. *Annual Reviews in Earth and Planetary Sciences* 24: 225-262.

Gat JR, Levy Y, 1978. Isotope hydrology of inland sabkhas in the Bardawil area, Sinai. *Limnology and Oceanography* 23: 841- 850.

Gat JR, Matsui E, 1991. Atmospheric water balance in the Amazon Basin: an isotopic evapotranspiration model. *Journal of Geophysical Research* 96: 13179-13188.

Gat JR, Bowser CJ, Kendall C, 1994. The contribution of evaporation from the Great Lakes to the continental atmosphere: estimate based on stable isotope data. *Geophysical Research Letters* 21: 557-560.

Gibson JJ, Edwards TWD, Bursey GG, Prowse TD, 1993. Estimating evaporation using stable isotopes: quantitative results and sensitivity analysis for two catchments in northern Canada. *Nordic Hydrology* 24: 79-94.

Gibson JJ, 2002. A new conceptual model for predicting isotope enrichment of lakes in seasonal climates. *PAGES News* 10: 10-11.

Gibson JJ, Edwards TWD, 2002. Regional water balance trends and evaporative-transpiration partitioning from a stable isotope survey of lakes in northern Canada. *Global Biogeochemical Cycles* 16: doi: 10.1029/2001GB001839.

Gibson JJ, Edwards TWD, Prowse TD, 1999. Pan-derived isotopic composition of water vapour and its variability in northern Canada. *Journal of Hydrology* 217: 55-74.

Gibson JJ, Birks SJ, Edwards TWD, in press. Global prediction of δ_A and $\delta^{18}O$- $\delta^{2}H$ evaporation slopes for lakes and soil water accounting for seasonality. *Global Biogeochemical Cycles*.

Gonfiantini R, 1986. Environmental isotopes in lake studies. In: Fritz P, Fontes JC (Eds), Handbook of Environmental Isotope Geochemistry, The Terrestrial Environment, vol. 2. Elsevier, New York, pp 113-168.

Hall RI, Wolfe BB, Edwards TWD, 2004. A Multi-century Flood, Climatic, and Ecological History of the Peace-Athabasca Delta, Nothern Alberta, Canada. Final Report. Published by BC Hydro. 163pp + Appendices.

Horita J, Wesolowski D, 1994. Liquid-vapour fractionation of oxygen and hydrogen isotopes of water from the freezing to the critical temperature. *Geochimica et Cosmochimica Acta* 58: 3425-3437.

Jacob H, Sonntag C, 1991. An 8-year record of the seasonal variation of ^{2}H and ^{18}O in atmospheric water vapour and precipitation at Heidelberg, Germany. *Tellus* 43B: 291-300.

Mayr C, Lücke A, Stichler W, Trimborn P, Ercolano B, Oliva G, Ohlendorf C, Soto J, Fey M, Haberzettl T, Janssen S, Schäbitz F, Schleser GH, Wille M, Zolitschka B, 2007. Precipitation origin and evaporation of lakes in semi-arid Patagonia (Argentina) inferred from stable isotopes ($\delta^{18}O$, $\delta^{2}H$). *Journal of Hydrology* 334: 53-63.

PADPG, 1973. Peace-Athabasca Delta Project, Technical Report and Appendices, Vol 1: Hydrological Investigations, Vol 2: Ecological Investigations. Peace-Athabasca Delta Project Group, Delta Implementation Committee, Governments of Alberta, Saskatchewan and Canada; 176pp.

Peters DL, 2003. Controls on the persistence of water on perched basins of the Peace-Athabasca Delta, northern Canada. PhD thesis, Trent University 194pp.

Peters DL, Prowse TD, Marsh P, Lafleur PM, Buttle JM, 2006. Persistence of water within perched basins of the Peace-Athabasca Delta, northern Canada. *Wetlands Ecology and Management* 14: 221-243.

Rozanski K, Araguas-Araguas L, Gonfiantini R, 1993. Isotopic patterns in modern global precipitation. In: Swart PK, Lohmann KC, McKenzie J, Savin S (Eds.), Climate Change in Continental Isotopic Records. *American Geophysical Union Geophysical Monograph* 78: 1-36.

Vallet-Coulomb C, Gasse F, Robinson L, Ferry L, 2006. Simulation of the water and isotopic balance of a closed tropical lake at a daily time step (Lake Ihotry, South-West of Madagascar). *Journal of Geochemical Exploration* 88: 153-156.

Welhan JA, Fritz P, 1977. Evaporation pan isotopic behaviour as an index of isotopic evaporation conditions. *Geochimica et Cosmochimica Acta* 41: 682-686.

Wolfe BB, Karst-Riddoch TL, Hall RI, Edwards TWD, English MC, Palmini R, McGowan S, Vardy SR, 2007. Classification of hydrologic regimes of northern floodplain basins (Peace-

Athabasca Delta, Canada) from analysis of stable isotopes ($\delta^{18}O$, $\delta^{2}H$) and water chemistry. *Hydrological Processes* 21: 151-168.

Yakir D, Sternberg LSL, 2000. The use of stable isotopes to study ecosystem gas exchange. *Oecologia* 123: 297-311.

Zuber A, 1983. On the environmental isotope method for determining the water balance of some lakes. *Journal of Hydrology* 61: 409-427.

Chapter 3

Abbott MB, Wolfe BB, Wolfe AP, Seltzer GO, Aravena R, Mark BG, Polissar PJ, Rodbell DT, Rowe HD, Vuille M, 2003. Holocene paleohydrology and glacial history of the central Andes using multiproxy lake sediment studies. *Palaeogeography Palaeoclimatology Palaeoecology* 194: 123-138.

Anderson L, Abbott MB, Finney BP, 2001. Holocene climate inferred from oxygen isotope ratios in lake sediments, central Brooks Range, Alaska. *Quaternary Research* 55: 313-321.

Baertschi P, 1976. Absolute 18O content of standard mean ocean water. *Earth and Planetary Science Letters* 31:341-344.

Beuning KRM, Kelts K, Ito E, Johnson TC, 1997. Paleohydrology of lake Victoria, East Africa, inferred from 18O/16Oratios I sediment cellulose. *Geology* 25:1083-1086.

Beuning KRM, Kelts K, Russell J, Wolfe BB, 2002. Reassessment of Lake Victoria - Upper Nile River paleohydrology from oxygen isotope records of lake-sediment cellulose. *Geology* 30: 559-562.

Birks SJ, Edwards TWD, Remenda VH, 2007. Isotopic evolution of Glacial Lake Agassiz: New insights from cellulose and porewater isotopic archives. *Palaeogeography Palaeoclimatology Palaeoecology* 246: 8-22.

Brenninkmeijer CAM, Kraft P, Mook WG, 1983. Oxygen isotope fractionation between CO_2 and H_2O. *Isotope Geosciences* 1: 181-190.

Buhay WM, and Betcher RN, 1998. Paleohydrologic implication of 18O enriched lake Agassiz water. *Journal of Paleolimnology* 19: 285-296.

Cernusak LA, Farquhar GD, Wong CS, Stuart-Williams H, 2004. Measurement and interpretation of the oxygen isotope composition of carbon dioxide respired by leaves in the dark. *Plant Physiology* 136: 3350-3363.

Cooper LW, and DeNiro MJ, 1989. Oxygen-18 content of atmospheric oxygen does not affect the oxygen isotope relationship between environmental water and cellulose in a submerged aquatic plant, *Egeria densa Planch*. *Plant Physiology* 91: 536-541.

Coplen TB, 1996. New guidelines for reporting stable hydrogen, carbon, and oxygen isotope-ratio data. *Geochimica et Cosmochimica Acta* 60: 3359-3360.

DeNiro MJ, and Epstein S, 1979. Relationship between the oxygen isotope ratios of terrestrial plant cellulose, carbon dioxide, and water. *Science* 204: 51-53.

DeNiro MJ, and Epstein S, 1981. Isotopic composition of cellulose from aquatic organisms. *Geochim et Cosmochim Acta* 45: 1885-1894.

Draper NR, and Smith H (eds), 1998. Applied Linear Regression. Wiley, New York, 706pp.

Edwards TWD, and Fritz P, 1986. Assessing meteoric water composition and relative humidity from ^{18}O and ^{2}H in plant cellulose: paleoclimatic implications for southern Ontario, Canada. *Applied Geochemistry* 1: 715-723.

Edwards TWD and McAndrews JH, 1989. Paleohydrology of a Canadian Shield lake inferred from ^{18}O in sediment cellulose. *Canadian Journal of Earth Sciences* 26: 1850-1859.

Edwards TWD, 1993. Interpreting past climate from stable isotopes in continental organic matter. In Swart PK, Lohmann KC, McKenzie J, Savin S (eds), Climatic Change in Continental Isotopic Records. *American Geophysical Union Geophysical Monograph* 78: 333-341.

Epstein S, and Mayeda TK, 1953. Variation of O^{18} content of waters from natural sources. *Geochimica et Cosmichimica Acta* 4: 213-224.

Epstein S., Thompson P, and Yapp CJ, 1977. Oxygen and Hydrogen Isotopic Ratios in Plant Cellulose. *Science* 198: 1209-1215.

Guy RD, Fogel ML, Berry JA, 1993. Photosynthetic fractionation of the stable isotopes of oxygen and carbon. *Plant Physiology* 101: 37-47.

MacDonald GM, Edwards TWD, Moser KA, Pienitz R, Smol JP, 1993. Rapid response of treeline vegetation and lakes to past climate warming. *Nature* 361: 243-246.

Sauer PE, Miller GH, Overpeck JT, 2001. Oxygen isotope ratios of organic matter in arctic lakes as a paleoclimate proxy: field and laboratory investigations. *Journal of Paleolimnology* 25: 43-64.

Sternberg LDLO, and DeNiro MJD, 1983. Biogeochemical implications of the isotopic equilibrium fractionation factor between the oxygen-atoms of acetone and water. *Geochimica et Cosmochimica Acta* 47: 2271-2274.

Sternberg LDL, Deniro MJ, Savidge RA, 1986. Oxygen isotope exchange between metabolites and water during biochemical reactions leading to cellulose synthesis. *Plant Physiology* 82: 423-427.

Sternberg LSL, 1989. Oxygen and hydrogen isotope ratios in plant cellulose: mechanisms and applications in Rundel PW, Ehleringer JR, Nage KA (eds.), Stable Isotopes in Ecological Research. Springer-Verlag, New York: 124-141.

Ruben S, Randall M, Kamen M, Hyde JL, 1941. Heavy oxygen (O^{18}) as a tracer in the study of photosynthesis. *Journal of the American Chemical Society* 63: 877-879.

Werner RA, Komexl BE, Rossmann A, Schmidt HL, 1996. On-line determination of delta O-18 values of organic substances. *Analytica Chimica Acta* 319: 159-164.

Wolfe BB, and Edwards TWD, 1997. Hydrologic control on the oxygen-isotope relation between sediment cellulose and lake water, western Taimyr Peninsula, Russia: implications for the use of surface-sediment calibrations in paleolimnology. *Journal of Paleolimnology.* 18: 183-191.

Wolfe BB, Edwards TWD, Aravena R, Forman SL, Warner BG, Velichko AA, and MacDonald GM, 2000. Holocene paleohydrology and paleoclimate at treeline, north-central Russia, inferred from oxygen isotope records in lake sediment cellulose. *Quaternary Research* 53: 319-329.

Wolfe BB, Edwards TWD, Elgood RJ, Beuning KRM, 2001. Carbon and oxygen isotope analysis of lake sediment cellulose: method and application. In Last WM & Smol JP (eds.) Tracking Environmental Change Using Lake Sediments. Volume 2: pp 375-400 Physical and Geochemical Mehods. Kluwer Academic Publishers, Dordrecht, The Netherlands.

Wolfe BB, Falcone MD, Clogg-Wright KP, Mongeon CL, Yi Y, Mark WA, Edwards TWD, 2007. Progress in isotope paleohydrology using lake sediment cellulose. *Journal of Paleolimnology* 37: 221-231.

Yakir D, and DeNiro MJ, 1990. Oxygen and hydrogen isotope fractionation during cellulose metabolism in *Lemna gibba L. Plant Physiology* 93: 325-332.

Yakir D, 1992. Variation in the natural abundance of oxygen-18 and deuterium in plant carbohydrates. *Plant cell and Environment* 15: 1005-1020.

Yakir D, and Wang XF, 1996.Fluxes of CO_2 and water between terrestrial vegetation and the atmosphere estimated from isotope measurements. *Nature* 380: 515-517.

Zanazzi A, and More G, 2005. Paleoclimatic implication of the relationship between oxygen isotope ratios of moss cellulose and source water in wetlands of Lake Superior. *Chemical Geology* 22: 281-291.

Chapter 4

Artjuschenko Z, 1990. Organographia Illustrata Plantarium Vascularium. Institutum Botanicum Nomina V Kamrovii (In Russian with Latin).

Allison GB, and Leaney FW, 1982. Estimation of isotopic exchange parameters, using constant feed pans. *Journal of Hydrology* 55: 151-161.

Bradbury JP, and Dean WE (eds), 1993. Elk Lake, Minnesota: Evidence for Rapid Climate Change in the North-central United States. *The Geological Society of America, Special Paper* 276, 336p.

Berggren G, 1969. Atlas of seeds and small fruits of Northwest-European plant species: Part 2. Cyperaceae. Swedish Natural Science Research Council, Stockholm.

Berggren G, 1981. Atlas of seeds and small fruits of Northwest-European plant species: Part 3. Salicaceae–Cruciferae. Swedish Natural Science Research Council, Stockholm.

Bertsch K, 1941. Handbucher der praktischen Vorgeschichtsforschung, Band 1: Fruchte und Samen. Verlag, Stuttgart.

Birks SJ, Edwards TWD, Gibson JJ, Drimmie RJ, Michel FA, 2004. *Canadian Network for Isotopes in Precipitation*. (http://www.science.uwaterloo.ca/~twdedwar/cnip/cniphome.html). Accessed 6 July 2007.

Cohen AS, 2003. Paleolimnology: the history and evolution of lake systems. Oxford University Press, New York.

Coplen TB, 1996. New guidelines for reporting stable hydrogen, carbon, and oxygen isotope-ratio data. *Geochimica et Cosmochimica Acta* 60: 3359-3360.

Craig H, 1961. Isotopic variations in meteoric waters. *Science* 133: 1702-1703.

Craig H, and Gordon LI, 1965. Deuterium and oxygen 18 variations in the ocean and the marine atmosphere. In: Tongiorgi E. (Ed.), Stable Isotope in Oceanographic Studies and Paleotemperatures. Pisa, Italy: Laboratorio di Geologia Nucleare, pp 9-130.

Dansgaard W, 1964. Stable isotopes in precipitation. *Tellus* 16: 436–68.

Dinçer T, 1968. The use of oxygen-18 and deuterium concentrations in the water balance of lakes. *Water Resources Research* 4: 1289-1305.

Edwards TWD, Wolfe BB, Gibson JJ, Hammarlund D, 2004. Use of water isotope tracers in high-latitude hydrology and paleohydrology. In: Pienitz R, Douglas MSV, Smol JP (Eds.), Long-term Environmental Change in Arctic and Antarctic Lakes, Developments in Paleoenvironmental Research, vol. 8. Springer, Dordrecht, pp 187-207.

Edwards TWD, Birks SJ, Luckman BH, MacDonald GM, 2008. Climatic and hydrologic variability during the past millennium in the eastern Rocky Mountains and Northern Great Plains of western Canada. *Quaternary Research*, doi:10.1016/j.yqres.2008.04.013.

Environment Canada, 2004. *Climate Data Online* (http://www.climate.weatheroffice.ec.gc.ca/climateData/hourlydata_e.html). Accessed 8 April 2007.

Epstein S, and Mayeda TK, 1953. Variation of O^{18} content of waters from natural sources. *Geochimica et Cosmochimica Acta* 4: 213-224.

Frey DG, 1974. Paleolimnology. *Mitteilungen Internationale Vereinigung Limnologie* 20: 95-123.

Gat JR, 1996. Oxygen and hydrogen isotopes in the hydrological cycle. *Annual Reviews in Earth and Planetary Sciences* 24: 225-262.

Gibson JJ, Edwards TWD, Bursey GG, Prowse TD, 1993. Estimating evaporation using stable isotopes: quantitative results and sensitivity analysis for two catchments in northern Canada. *Nordic Hydrology* 24: 79-94.

Gibson JJ, Edwards TWD, Prowse TD, 1999. Pan-derived isotopic composition of water vapour and its variability in northern Canada. *Journal of Hydrology* 217: 55-74.

Gibson JJ, and Edwards TWD, 2002. Regional water balance trends and evaporation-transpiration partitioning from a stable isotope survey of lakes in northern Canada. *Global Biogeochemical cycles* 16: doi: 10.1029/2001GB001839.

Gonfiantini R, 1986. Environmental isotopes in lake studies. In: Fritz P, Fontes JC, (Eds.), Handbook of Environmental Isotope Geochemistry, The Terrestrial Environment, vol. 2 Elsevier, New York, pp. 113-168.

Gummer WD, Cash KJ, Wrona FJ, Prowse TD, 2000. The Northern River Basins Study: context and design. *Journal of Aquatic Ecosystem Stress and Recovery* 8: 7-17.

Hall RI, and Smol JP, 1996. Paleolimnological assessment of long-term water-quality changes in south-central Ontario lakes affected by cottage development and acidification. *Canadian Journal of Fisheries and Aquatic Sciences* 53: 1-17.

Hall RI, Wolfe BB, Edwards TWD, 2004. A Multi-century Flood, Climatic, and Ecological History of the Peace-Athabasca Delta, Nothern Alberta, Canada. Final Report. Published by BC Hydro. 163pp + Appendices.

Jacob H, and Sonntag C, 1991. An 8-year record of the seasonal variation of ^{2}H and ^{18}O in atmospheric water vapour and precipitation at Heidelberg, Germany. *Tellus* 43B: 291-300.

Jones MD, Leng MJ, Roberts CN, Tüşrkes M, Moyeed R, 2005. A coupled calibration and modelling approach to the understanding of dry-land lake oxygen isotope records. *Journal of Paleolimnology* 34: 391 – 411.

Jones MD, and Roberts CN, 2008. Interpreting lake isotope records of Holocene environmental change in the Eastern Mediterranean. *Quaternary International* 181: 32-38.

Jones PD, Osborn TJ, Briffa KR, 2001. The evolution of climate over the last millennium. *Science* 292: 662-667.

Krammer K, and Lange-Bertalot H, 1986-1991. Susswasserflora von Mitteleuropa, Band 2. Gustav Fischer Verlag.

Leng MJ, and Marshall JD, 2004. Paleoclimate interpretation of stable isotope data from lake sediments. *Quaternary Science Reviews* 23: 811-831.

Leng MJ, Lamb AL, Heaton THE, Marshall JD, Wolfe B, Jones M, Holmes J, Arrowsmith C, 2006. Isotopes in lake sediments. In: Leng M (Ed.), Isotopes in Environmental Research: Developments in Environmental Research Vol. 10.

Martin AC, and Barkley WD, 1961. Seed Identification Manual. University of California Press, Berkley.

Mollard JD, Mollard DG, Penner LA, Cosford JI, Zimmer TAM, 2002. Peace-Athabasca Delta Geomorphology: an Assessment of Geomorphic Change Over Time. Report to B.C. Hydro, 131.

Montgomery F, 1977. Seeds and fruits of plants of Eastern Canada and Northeastern United States. University of Toronto Press, Toronto.

Morrison J, Brockwell T, Merren T, Fourel F, Philips AM, 2001. On-line high precision stable hydrogen isotopic analyses on nanoliter water samples. *Analytical Chemistry* 73: 3570-3575.

Peace-Athabasca Delta Implementation Committee (PADIC), 1987. Peace-Athabasca Delta Water Management Works Evaluation. Final Report, including Appendix A, Hydrological Assessment; Appendix B, Biological Assessment; Appendix C, Ancillary Studies, AB and SK, Canada.

Peace-Athabasca Delta Project Group (PADPG), 1973. Peace-Athabasca Delta Project, Technical Report and Appendices: Volume 1, Hydrological Investigations; Volume 2, Ecological Investigations.

Peace-Athabasca Delta Technical Studies (PADTS), 1996. Final Report. PADTS Steering Committee, Fort Chipewyan, Alberta.

Prowse TD, Conly FM, Church M, English MC, 2002. A Review of hydroecological results of the Northern River Basins Study, Canada. Part 1. Peace and Slave Rivers. *River Research and Applications* 18: 429-446.

Reeves CC, 1968. Introduction to paleolimnology. Elsevier N.Y.

Roberts N, and Jones M, 2002. Towards a regional synthesis of Mediterranean climatic change using lake stable isotope records. *PAGES News* 10: 13-15.

Rozanski K, Araguas-Araguas L, Gonfiantini R, 1993. Isotopic patterns in modern global precipitation. In: Swart PK, Lohmann KC, Mckenzie J, Savin S (Eds.), Climate Change in Continental Isotopic Records. *American Geophysical Union, Geophysical Monograph* 78: 1-36.

Sinnatamby RN, 2006. An assessment of hydro-ecological changes at two closed-drainage basins in the Peace-Athabasca Delta, Alberta, Canada. MSc thesis, University of Waterloo, Waterloo 108 pp.

Sinnatamby RN, Yi Y, Sokal M, Clogg-Wright K, Vardy SR, Karst-Riddoch T, Last W, Johnston J, Hall RI, Wolfe BB, Edwards TWD, Cartographic and paleolimnological evidence for expansion of Lake Athabasca during the Little Ice Age. *Journal of Paleolimnology* In preparation.

Smol JP, 1990. Paleolimnology - Recent advances and future challenges. In: De Bernardi R, Giussani G, and Barbanti L (eds), Scientific Perspectives in Theoretical and Applied Limnology. CNDR, Pallanza. *Memorie dell'Istituto Italiano di Idrobiologia* 47: 253-276.

Stuiver M, Reimer PJ, Bard E, Beck JW, Burr GS, Hughen KA, Kromer B, McCormac FG, van der Plicht J, Spurk M, 1998. INTCAL98 radiocarbon age calibration, 24000-0 cal BP. *Radiocarbon* 40: 1041-1083.

von Grafenstein U, Erlenkeuser H, Trimborn P, 1999. Oxygen and carbon isotopes in modern fresh-water ostracode valves: assessing vital offsets and autecological effects of interest for palaeoclimate studies. *Palaeogeography Palaeoclimatology Palaeoecology* 148: 133-152.

Welhan JA, and Fritz P, 1977. Evaporation pan isotopic behaviour as an index of isotopic evaporation conditions. *Geochimica et Cosmochimica Acta* 41: 682-686.

Werner RA, Komexl BE, Rossmann A, Schmidt HL, 1996. On-line determination of delta O-18 values of organic substances. *Analytica Chimica Acta* 319: 159-164.

Wolfe BB, Edwards TWD, Elgood RJ, Beuning KRM, 2001a. Carbon and oxygen isotope analysis of lake sediment cellulose: methods and applications. In: Last WM, Smol JP (Eds.), Tracking Environmental Change Using Lake Sediments. Volume 2: Physical and Chemical Techniques, Developments in Paleoenvironmental Research. Kluwer Academic Publishers, Dordrecht, pp. 373-400.

Wolfe BB, Aravena R, Abbott MB, Seltzer GO, Gibson JJ, 2001b. Reconstruction of paleohydrology and paleohumidity from oxygen isotope records in the Bolivian Andes. *Palaeogeography, Palaeoclimatology, Palaeoecology* 176: 177-192.

Wolfe BB, Edwards TWD, Hall RI, 2002. Past and present ecohydrology of the Peace-Athabasca Delta, northern Alberta, Canada: Water isotopes lead the way. *PAGES News*. 10: 16-17.

Wolfe BB, Karst-Riddoch TL, Vardy SR, Falcone MD, Hall RI, Edwards TWD, 2005. Impacts of climate and river flooding on the hydro-ecology of a floodplain basin, Peace-Athabasca Delta, Canada since A.D. 1700. *Quaternary Research* 64: 147-162.

Wolfe BB, Karst-Riddoch TL, Hall RI, Edwards TWD, English MC, Palmini R, McGowan S, Vardy SR, 2007a. Classification of hydrologic regimes of northern floodplain basins (Peace-Athabasca Delta, Canada) from analysis of stable isotopes ($\delta^{18}O$, $\delta^{2}H$) and water chemistry. *Hydrological Processes* 21: 151-168.

Wolfe BB, Falcone MD, Clogg-Wright KP, Mongeon CL, Yi Y, Brock BE, St. Amour NA, Mark WA, Edwards TWD 2007b. Progress in isotope paleohydrology using lake sediment cellulose. *Journal of Paleolimnology* 37: 221-231.

Yi Y, Bronwyn BB, Falcone MD, Wolfe BB, Edwards TWD, 2008. A coupled isotope tracer method to characterize input water to lakes. *Journal of Hydrology* 350: 1-13.

Zuber A, 1983. On the environmental isotope method for determining the water balance of some lakes. *Journal of Hydrology* 61: 409-427.

Chapter 5

Aggarwal PK, Alduchov O, Araguás LA, Dogramaci S, Katzlberger G, Kriz K, Kulkarni KM, Kurttas T, Newman BD, Pucher A, 2007. New Capabilities for Studies Using Isotopes in the Water Cycle. *Eos 88*: 537.

Birks SJ, 2003. Water isotope partitioning in aquitards and precipitation on the northern Great Plains. PhD thesis, University of Waterloo 291pp.

Bowling DR, Sargent SD, Tanner BD, 2003. Tunable diode laser absorption spectroscopy for stable isotope studies of ecosystem-atmosphere CO_2 exchange. *Agricultural and Forest Meteorology* 118: 1-19.

Brock BE, Yi Y, Edwards TWD, Wolfe BB, Multi-year landscape-scale assessment of lake water balances in the Slave River Delta, NWT, using water isotope tracers. In preparation

Huang Y, Shuman B, Wang Y, Webb Jr. T, 2004. Hydrogen isotope ratios of individual lipids in lake sediments as novel tracers of climatic and environmental change: a surface sediment test. *Journal of Paleolimnology* 31: 363 – 375.

Lee XH, Sargent S, Smith R, Tanner B, 2005. In situ measurement of the water vapor O-18/O-16 isotope ratio for atmospheric and ecological applications. *Journal of Atmospheric and Oceanic Technology* 22: 555-565.

Sturm K, Hoffmann G, Langmann B, Stichler W., 2005. Simulation of $\delta^{18}O$ in precipitation by the regional circulation model $REMO_{iso}$. *Hydrological Processes* 19: 3425-3444.

Wolfe BB, Karst-Riddoch TL, Hall RI, Edwards TWD, English MC, Palmini R, McGowan S, Vardy SR, 2007. Classification of hydrologic regimes of northern floodplain basins (Peace-Athabasca Delta, Canada) from analysis of stable isotopes ($\delta^{18}O$, $\delta^{2}H$) and water chemistry. *Hydrological Processes* 21: 151-168.

Wolfe BB, Hall RI, Edwards TWD, Vardy SR, Falcone MD, Sjunneskog C, Sylvestre F, McGowan S, Leavitt PR, and van Driel P, 2008. Hydroecological responses of the Athabasca Delta, Canada, to changes in river flow and climate during the 20th century. *Ecohydrology* 1: doi:10.1002/eco.13

Worden J, Noone D, Bowman K, 2007. Importance of rain evaporation and continental convection in the tropical water cycle. *Nature* 445: 528-532

Yi, Y, Brock, B.E., Falcone, M.D., Wolfe, B.B., Edwards, T.W.D., 2008. A coupled isotope tracer method to characterize input water to lakes. Journal of Hydrology, 350, 1-13.

Appendix

Appendix I:

Physical and isotopic characterization of evaporation from Sphagnum moss*

Summary Evaporation from and water transfer within living and dead (but undecomposed) *Sphagnum* mosses is important biologically and hydrologically, but understanding of the internal mass-transfer mechanisms remains incomplete. A column experiment was conducted to characterize liquid and vapour fluxes and the profiles of relative humidity, temperature and the hydrogen- and oxygen-isotope composition of *Sphagnum* pore waters evaporating under controlled conditions. A constant water table at 20 cm depth was established in five identical columns fed by a common water reservoir ($\delta^{18}O$ = -13.0‰; $\delta^{2}H$ = -85.8‰). Evaporation from the columns averaged 4.5 mm d^{-1} at the average chamber temperature and relative humidity of 20.7°C and 27.1%, respectively. The columns developed upward-convex profiles of relative humidity and isotopic composition within the first day that persisted throughout the experiment. Isotopic data from columns sampled after 1, 2, 4, 7 and 15 days were strongly constrained by an evaporation line with the linear relation $\delta^{2}H = 3.8\delta^{18}O - 36.1$ (R^2 = 0.99; n = 25), consistent with the expected evaporative enrichment trajectory under chamber conditions. Calculated vapour flux accounted for only ~1% of the total mass flux within the columns, reflecting the dominance of liquid-phase capillary flow. While this calculated vapour flux was small, it decreased markedly near the surface, suggesting that condensation because of evaporative cooling may enhance the liquid moisture conditions there. The presence of a vapour pressure deficit down to about 15 cm below the surface indicate that both evaporation and upward vapour diffusion were occurring at depth within the *Sphagnum* columns, but modelling shows that *in situ* fractionation alone within the columns cannot explain the extent of the observed enrichment. Rather, the enrichment of the heavy isotopes wherever evaporation is occurring and their consequent downward diffusion are needed to explain the observed profiles. Coupled advection-diffusion modelling of these profiles

yielded estimates of the effective liquid-phase diffusivities in *Sphagnum* pore waters of 2.380 (± 0.020) x 10^{-5} cm^2 s^{-1} for $^1H^1H^{18}O$ and 2.415 (± 0.015) x 10^{-5} cm^2 s^{-1} for $^1H^2H^{16}O$, in good agreement with accepted values.

---

[*] Submitted to *Journal of Hydrology* as: Price J.S., Edwards T.W.D., Yi Y., Whittington P.N., Physical and isotopic characterization of evaporation from *Sphagnum* moss.

Introduction

Water movement in *Sphagnum* mosses is a poorly understood phenomenon, yet it is critically important to peatland evaporation processes (Kellner, 2002), carbon exchanges (McNeil and Waddington, 2003), nutrient translocation (Rydin and Clymo, 1989) and heat flow (Kim and Verma, 1996). Here we refer not to the water exchanges in the peat substrate, for which we have recently gained considerable understanding (e.g. Drexler et al., 1999; Kennedy and Van Geel, 2000; Reeve et al., 2000; Price, 2003; Kellner et al., 2005); rather, we seek to clarify the nature of water fluxes through the matrix of living and dead mosses near the peatland-atmosphere interface.

Mosses comprise a matrix of large pores arising between and within the structure of leaves and branches (Hayward and Clymo, 1982; Clymo and Hayward, 1983) that impart a huge potential range (e.g. ~2 – 95%) of moisture contents (Boelter, 1970). Saturated water flow can be too fast to measure (e.g. Boelter, 1965), but when the moss is dry the liquid flux is negligible (Ingram, 1983). Upward migration of water above the water table in *Sphagnum* mosses is typically attributed to capillary flow (Hayward and Clymo, 1982). When this flow is inadequate to meet the evaporative demand, the moss begins to dry and the water pressure (ψ) falls quickly. Water can be withdrawn from storage within hyaline cells when ψ drops below -100 kPa and then the moss desiccates (Hayward and Clymo, 1982). At this stage capillary water flow is negligible, but vapour diffusion can still occur. Under these conditions, evaporation cannot proceed efficiently, and several studies have noted a sharp drop in the evaporation rate from mosses as they dry (Price, 1991; Kim and Verma, 1996), suggesting a limited ability to move water up from the water table (see also Kellner and Halldin, 2002). However, field studies report that water lost to evaporation is mostly replaced by upward flow (Yakazi et al., 2006). How does this occur?

Typically, evaporation is assumed to occur at the *Sphagnum* surface (e.g. Nichols and Brown, 1980), which would require delivery of water by capillary action to the sites where turbulent and radiant exchanges occur. However, latent heat exchanges can also occur below the soil surface (Cahill and Parlange, 1998), indicating that water moves in both liquid and vapour phases. The vapour flux increases where there are large pores and strong thermal and moisture gradients (Yoshikawa et al., 2002; Williams and Flanagan, 1996), especially when there is a strong surface wind (Ishihara et al., 1992). In dry soils the vapour flux can be comparable to the liquid flux (Rose, 1968) and is typically attributed to diffusion, but in some cases occurs by advection caused by

temperature and pressure changes, and by wind pumping (Stern et al., 1999) and water infiltration (Touma et al., 1984). In forest mosses, Carleton and Dunham (2003) showed that vapour diffusion accompanied by diurnal cooling of the upper moss layers caused "distillation" or condensation of vapour in the upper layers. While physiologically important, this yields a relatively small quantity of water.

Insight into the evaporation process and water flux in the soil can be gained by observing the nature and extent of isotopic fractionation and redistribution in a soil profile. Evaporation from peatlands causes enrichment of ^{18}O and ^{2}H in the near-surface pore waters (Williams and Flanagan, 1996; Flanagan et al., 1997) and signals from this evaporative enrichment are subsequently incorporated into associated plant tissues (Brenninkmeijer et al., 1982; Edwards, 1993). Aravena and Warner (1992) showed that differences in evaporation rates between adjacent hummocks and hollows could be detected in the ^{18}O content of *Sphagnum* cellulose, suggesting that pore water isotopic composition may be a sensitive monitor of water dynamics within peatlands.

Exponentially-declining ^{18}O and ^{2}H abundances occur in saturated and unsaturated soil columns undergoing evaporation (Zimmermann et al., 1967; Munnich et al., 1980; Allison et al., 1983; Allison and Barnes, 1983; Barnes and Allison 1983, 1988; Walker et al., 1988; Barnes and Walker 1989; Hseih et al., 1998; DePaolo et al., 2004). These upward-convex profiles reflect competition between the downward diffusion of $^{1}H^{1}H^{18}O$ and $^{1}H^{2}H^{16}O$ molecules concentrated at the surface and the upward flow of liquid water that sustains the evaporation flux. The profiles can be modelled to estimate evaporation rates under steady and non-steady conditions, assuming knowledge of the liquid-phase diffusivities of the respective isotope species. As highlighted by Barnes and Allison (1988), however, vapour-phase diffusion and vapour-liquid exchange also play key roles in the evaporation process in unsaturated soils by "short-circuiting" across air-filled pores, thus transmitting isotopic signals downward more quickly than liquid-phase diffusion alone would allow in a saturated soil.

Here we report results from similar experiments designed to improve our understanding of water transport in *Sphagnum* moss undergoing evaporation. Specifically, our analysis included (1) quantitative partitioning of the net liquid and vapour fluxes, confirming the overwhelming importance of liquid-phase mass transfer by capillary flow, and (2) advection-diffusion modelling to probe the nature of the pore-water isotopic profiles that were obtained. The latter sheds new light on the

fundamental influence that vapour diffusion and vapour-liquid exchange have on hydrologic and isotopic processes in the unsaturated zone of *Sphagnum*-dominated peatlands.

Methods

Experimental Procedure

Our approach was to allow evaporation from columns of relatively undisturbed *Sphagnum rubellum* moss samples having a constant water table supplied with water from a common isotopic source. During the experiment, we determined depth profiles of water content, relative humidity of pore gas, isotopic composition of pore water and soil properties. A large (45 x 45 x 25 cm) block of hummock peat was extracted from a southern Ontario bog (43^o 90' N, 80^o 40' W) in December 2005. The hummock was frozen during removal and thus compression and disturbance during cutting were minimal. In the laboratory, the frozen sample was subdivided and trimmed to fit snugly into six 15 cm diameter x 25 cm long PVC cylinders; vascular vegetation protruding from the samples was clipped. PVC end caps fitted to the bottom end of each core were connected by a screened flexible manometer hose to a common reservoir. The samples were twice completely filled with deionised water from a reservoir and allowed to drain for 24 hours before commencing the experiment. Tests confirmed that this double-flushing procedure effectively re-sets the $\delta^{18}O$ and $\delta^{2}H$ of *Sphagnum* pore waters to that of the reservoir water.

The six manometer tubes and common water supply reservoir were positioned to hold the water table 5 cm above the base of each core (20 cm below the surface) and a secondary reservoir maintained a constant head in the primary reservoir (Figure 1). The secondary reservoir was covered to prevent any changes in isotopic signature due to evaporation but had a small vent to maintain atmospheric pressure. The apparatus was set up in a darkened chamber (~3 x 4 x 4 m), with a grow light set to a 12-hour cycle. A fan in the chamber directed air away from the samples to maintain air circulation, and a Hobo U10 relative humidity sensor simultaneously logged chamber air temperature (*T*) and relative humidity (*RH*).

One of the six samples in the chamber had thermocouples embedded at the surface (0 to 1 cm), 5, 10, 15, 20, and 25 cm, respectively, connected to a Campbell Scientific 10x logger to record moss temperature (T_0, T_5, etc.) every 30 minutes. Temperature at 2.5 cm depth was linearly interpolated from the 0-1 and 5 cm thermocouples. The remaining columns were left to allow evaporation for 1, 2,

4, 7 and 15 days, respectively. At the designated time, each column was disconnected from the water supply, but prior to disconnection *RH* was measured at 2.5 cm depth increments to 15 cm depth with a Vaisala relative humidity micro probe (HMP42). At the ambient humidity levels (93-100%) its reported accuracy and precision are 3% and 0.1%, respectively. Immediately after removal, the sample was sectioned as follows. The PVC column was gently removed by sliding it upwards out of the end-cap and over the core, leaving the *Sphagnum* core standing undisturbed in the end-cap with the water table maintained 5 cm above the base. First, a 5-cm section was cut from the top of the core and placed immediately into a plastic bag and sealed after removing most of the air, followed sequentially by the four remaining sections. This process was accomplished in less than five minutes so that evaporation from the sides of the sample (briefly exposed to the air) was negligible. The sample was then squeezed inside the plastic bag until water pooled – the elution being decanted into a 30 ml sample bottle and sealed. Two additional samples were taken from the secondary water supply reservoir on Day 1 and Day 15 to confirm that no changes had occurred in the source water isotopic composition. .

The sixth column (instrumented with thermocouples) was similarly sectioned to evaluate the volumetric moisture content, porosity, particle density and bulk density using standard methods (Klute, 1986). The evaporation rate from this and the other columns was determined by the rate of water loss from the secondary reservoir, based on the appropriate time and number of columns left in the series. This assumes that the evaporation rate was identical for all columns at any given time, although fluctuations in chamber humidity (and thus evaporation rate) did occur during the course of the experiment.

Isotopic Analysis

Water samples were analyzed in the Environmental Isotope Laboratory at the University of Waterloo, where $^{18}O/^{16}O$ and 2H/1H ratios were measured using standard methods (Epstein and Mayeda, 1953; Coleman et al., 1982; see Drimmie and Heemskerk, 1993). Results are reported in δ values, representing deviations in per mil (‰) from Vienna - Standard Mean Ocean Water (V-SMOW) on a scale normalized such that Standard Light Antarctic Precipitation (SLAP) has values of -55.5‰ ($\delta^{18}O$) and -428‰ ($\delta^{2}H$) as recommended by Coplen (1996). $\delta^{18}O$ or $\delta^{2}H = 1000\ [(R_{sample}/R_{V\text{-}SMOW}) - 1]$, where R is the ratio of $^{18}O/^{16}O$ or $^{2}H/^{1}H$ in the sample and V-SMOW, respectively. Analytical uncertainties are ±0.2 ‰ for δ18O and ±2.0 ‰ for δ2H.

Partitioning Vapour and Liquid Mass Fluxes

The bulk upward flux of water is a combination of vapour diffusion and liquid advection. Vapour diffusion flux (F_v) in the columns can be calculated according to Fick's first law (Millington, 1959) accounting for the effects of soil porosity (ϕ) and air-filled porosity (ε) (Millington and Quirk, 1961, cited in Moldrup et al., 2000) such that

$$F_v = D_v^* \left(\frac{\varepsilon^{10/3}}{\phi^2} \right) \frac{\partial C_v}{\partial z} \qquad [1]$$

where D_v^* is the diffusion coefficient of water vapour in air, C_v is the concentration of water vapour and z is the depth ordinate. Air-filled porosity is determined as

$$\varepsilon = 1 - \theta - \frac{\rho_b}{\rho_p} \qquad [2]$$

where θ is volumetric moisture content, ρ_b is bulk density and ρ_p is particle density. D_v^* may be calculated as (Gates, 1980)

$$D_v^* = 0.212(1 + 0.0071T) \text{ cm}^2 \text{ s}^{-1} \qquad [3]$$

where T is temperature (°C). Vapour concentration (C_v) can be determined from the ideal gas law using the partial pressure of moisture (e), calculated from measurements of relative humidity (RH), temperature (T) and saturation vapour pressure (e_{sat}), where

$$RH = \frac{e}{e_{sat}} \qquad [4]$$

and

$$e_{sat} = 610.78^{\left(\frac{T}{T+238.3} 17.269 \right)} \text{ kPa} \qquad [5]$$

(Tetens, 1930; see Govardhan and Alex, 2005), so that $C_v = 0.002166\ e\ /\ (\ T + 273.15\ )$ kg/m^3.

Modelling of the Isotopic Profiles

We used advection-diffusion modelling to analyze the observed isotopic profiles, following a similar approach to that of Barnes and Allison (1983; 1988) and Allison et al. (1983), though modified to allow for mass-dependent differences in the liquid-phase diffusivities of the different water-isotope species (*cf.* Mathieu and Bariac, 1996; DePaolo et al., 2004).

According to Darcy's Law:

$$\frac{F_l}{\rho} = -K\frac{dh}{dz} \qquad [6]$$

where F_l is the flux in the liquid phase (g cm^{-2} s^{-1}), ρ is the density of liquid water (g cm^{-3}), K is the hydraulic conductivity of the *Sphagnum* column (cm s^{-1}), h is the water head (cm), and z is the depth (cm). Water is evaporatively enriched in the heavy-isotope species ($^{1}H^{1}H^{18}O$ and $^{1}H^{2}H^{16}O$) at the top of the columns and relatively depleted in these species at the bottom. Under conditions of hydrologic and isotopic steady-state, the net fluxes in heavy-isotope species, which are the respective differences between upward advective flux and downward diffusive fluxes, will also reach a constant value at any given depth within the profile.

The flux of heavy isotope species therefore can be expressed by the equation:

$$F_l^i = F_l \cdot R_L + (-D_l^{*i} \cdot \frac{dC_l^i}{dz}) \qquad [7]$$

where the superscript i indicates water molecules containing the respective heavy isotopes, R_L is the isotopic ratio of liquid water (R_L= $^{18}O/^{16}O$ or $^{2}H/^{1}H$), D_l^* is the effective liquid-phase diffusivity (cm^2 s^{-1}), with D_l^{*i} signifying water molecules containing heavy isotopes, and C_l^i (g cm^{-3}) is the concentration of heavy water molecules in the liquid phase.

By definition, C_l^i is the mass divided by volume, therefore:

$$C_l^i = \frac{M^i}{V} = \frac{M^i}{M}\cdot\frac{M}{V} = \frac{N^i m^i}{Nm}\cdot\rho = \frac{m^i}{m}R_L\rho \qquad [8]$$

where M (g) is the mass of water, V (cm^3) is the volume of the water, m (g mol^{-1}) is the molecular weight of water molecules, N (mol) represents the number of water molecules, and ρ (g cm^{-3}) is the density of the water.

Substituting [8] into [7], and treating ρ as constant because of the small range of temperature, yields the expression:

$$F_l^i = F_l \cdot R_L - D_l^{*i} \frac{m^i}{m} \rho \cdot \frac{dR_L}{dz} \qquad [9]$$

which describes the relationship among isotopic fluxes in the liquid phase (F_l^i and F_l), the isotope ratio of water (R_L) and depth (z).

The respective steady-state fluxes can be described by $F_l + F_v = Inflow$ and $F_l^i + F_v^i = Inflow^i$, which can be combined to give:

$$\frac{F_l^i + F_v^i}{F_l + F_v} = R_{Input} \qquad [10]$$

which is consistent with steady-state quantitative conversion of water from the liquid to vapour phase (i.e., without isotopic fractionation).

This can be simplified to a good first-order approximation knowing $F_l >> F_v$ and $F_l{}^i >> F_v{}^i$ (calculated above), such that:

$$R_{Input} = \frac{F_l^i}{F_l} \qquad [11]$$

Rearranging equation [11] and substituting in equation [9] then yields:

$$F_l \cdot R_{input} = F_l \cdot R_L - D_l^{*i} \cdot \frac{m^i}{m} \rho \cdot \frac{dR_L}{dz} \qquad [12]$$

Rearrangement of [12] gives

$$\frac{dR_L}{R_L - R_{input}} = \frac{mF_l}{m^i \cdot D_l^{*i} \cdot \rho} \cdot dz \qquad [13]$$

which expresses the isotopic ratio of water (R_L) as a function of depth. Integrating [13] from the surface ($z = 0$) to depth z yields:

$$\int_{R_{surface}}^{R_L} \frac{dR_L}{R_L - R_{input}} = \int_0^z \frac{mF_l}{m^i \cdot D_l^{*i} \cdot \rho} \cdot dz \qquad [14]$$

Since R_{input}, ρ and D_l^{*i} are constant, the results of integration can be expressed as:

$$\ln\left(\frac{R_L - R_{Input}}{R_{Surface} - R_{Input}}\right) = \frac{mF_l}{m^i \cdot D_l^{*i} \cdot \rho} \cdot z \qquad [15]$$

Converting equation [15] into δ notation gives:

$$\ln\left(\frac{\delta_L - \delta_{Input}}{\delta_{Surface} - \delta_{Input}}\right) = \frac{mF_l}{m^i \cdot D_l^{*i} \cdot \rho} \cdot z \qquad [16]$$

which expresses the relation between the isotopic composition of pore water (δ_L) and the sampling depth (z). Plotting $\frac{\delta_L - \delta_{Input}}{\delta_{Surface} - \delta_{Input}}$ against z yields an exponential profile, thus affording the opportunity to test whether the measured *Sphagnum* pore water isotopic profiles obtained from the column experiment reflect steady-state conditions and, if so, to determine the effective liquid-phase diffusivities for $^1H^1H^{18}O$ and $^1H^2H^{16}O$ in this porous medium.

Results

Bulk density (ρ_b) increased with depth, but in the unsaturated zone (0 – 20 cm) was fairly constant at 0.15 – 0.20 g cm^{-3} (Table 1). Porosity (ϕ) decreased with depth. The moisture content ranged from 14.0% near the surface to 25.9% near the base of the unsaturated zone.

Chamber temperature (T) was relatively stable during the experiment (average ± standard deviation = 20.7 ± 0.6 °C) (Table 2). Instrument failure meant no *RH* data were available until partway through Day 2 (see Table 2). Variably high *RH* subsequently occurred during the Day 3-10 period (average 31.3%) because of servicing of the laboratory ventilation system, before stabilizing over the Day 11-15 period (average 23.0%). The average evaporation loss from the columns over the span of the experiment was 4.5 mm d^{-1}. Weighting to account for variations in chamber *RH* yielded estimated average daily evaporation ranging from 3.9 mm d^{-1} (Day 7) to 4.8 mm d^{-1} (Day 15).

The columns were distinctly cooler at the surface (Figure 2a), and the temperature gradient above the water table was similar in each column. Relative humidity was lowest near the surface (Figure 2b), thus vapour concentration (C_v) decreased upward (Figure 3a). The vapour concentration gradient ($\partial C_v/\partial z$) was similar in each column. Calculated upward vapour flux in the columns (equation [1]) averaged less than 0.04 mm d^{-1} (Figure 3b).

Relative to the $\delta^{18}O$ and $\delta^{2}H$ values of source water (average -13.0‰ and -85.8‰, respectively) enrichment was greatest near the surface (average -6.6‰ and -61.0‰, respectively) (Figure 4a and b). The enrichment decreased exponentially with depth, converging on the isotopic composition of the reservoir at the base of each column (20-25 cm interval). The profiles exhibited small systematic variations between successive sample days, although nearly identical profiles within analytical uncertainties were obtained on Days 2 and 15. The isotopic data from all columns cluster tightly along a line in $\delta^{18}O$-$\delta^{2}H$ space (Figure 4c) described by:

$$\delta^{2}H = 3.8\delta^{18}O - 36.1 \qquad (r^2 = 0.99) \qquad [17]$$

which exactly matches the expected trajectory of evaporative enrichment for surface waters evaporating under our experimental conditions (see Appendix A).

Discussion

Physical Processes

Evaporation from the samples caused cooling, and consequently temperature gradients developed in each column. Variations in air temperature in the chamber were not large (Table 2). Nevertheless, they caused a shift in the absolute temperature of the samples, although the temperature gradients remained similar on most days (Figure 2a). Evaporation was occurring not just from the moss surface, but the presence of a vapour pressure deficit (RH < 100%), especially in the top 5 cm (Figure 2b), suggests that latent heat exchanges were occurring at depth. That the pore atmosphere remained below vapour saturation (Figure 2b) implies either a water vapour flux (loss), or condensation elsewhere within the sample. Collis-George (1959) noted that RH in soil pores is reduced to 98.5% when the tension is at the wilting point (-15,000 cm or pF 4.2), or where there are highly negative solute potentials (Izbicki et al., 2000), because of condensation effects. Neither of these (very low potentials) was present in this case.

The presence of temperature and vapour concentration gradients indicate that both heat and vapour flowed towards the surface, although the very small calculated vapour diffusive flux (0.04 mm d^{-1}) represented ~ 1% of the evaporative water loss from the columns. The abrupt decrease in the calculated flux near the surface (Figure 3b) is an artifact of the inflection point of the temperature gradient at the same depth (Figure 2a), since RH is related to temperature. Advective vapour exchange can also occur due to the expansion and contraction of gas with temperature change and by atmospheric pressure changes (Stern et al., 1999). Based on the ideal gas law, changes in gas volume can be determined for given changes in temperature and pressure. In the chamber the diurnal temperature changes (± 2 ^{o}C) caused less than 1% gas volume change. Over the duration of the experiment the range of atmospheric pressure changes of 3.66 kPa would result in ~5% gas volume change (daily pressure changes averaged <1 kPa) (University of Waterloo, 2006). Thus we believe that temperature and pressure changes had a negligible effect on vapour exchanges, and conclude that vapour diffusion is more important than advective vapour flow. While this vapour flux is small, it may be important in maintaining sufficiently moist conditions for biological productivity (Carleton and Dunham, 2003).

Isotopic Processes

The presence of a vapour pressure deficit in the Sphagnum columns indicates potential for in situ fractionation. However, calculated steady-state evaporative enrichment using the Craig and Gordon (1965) model (see Appendix A) alone cannot fully account for the observed profiles (Figure 5). Rather, downward heavy-isotope diffusion is also required to magnify the signal.

Simulation of the pore water isotopic profiles on different sampling days was undertaken assuming that the upward advective flux was 99% of the estimated net evaporation rate, and that pore water $\delta^{18}O$ and $\delta^{2}H$ values were constrained to the observed evaporation line (equation [17]). Pairs of exponential curves generated using equation [16] were then compared to the observed profiles, adjusting the respective $\delta_{Surface}$ values and effective liquid-phase diffusion coefficients to explore possible matches. This approach differs somewhat from that taken by Barnes and Allison (1983) and many subsequent authors by not assuming the same liquid-phase diffusion coefficients for the two heavy-isotope species, although the respective values are expected to be very similar.

As shown in Figure 6, an exact overall match for pairs of profiles simulated in this manner could only be obtained for the measured data from Days 2 and 15, whereas pairs of exponential profiles could not be fitted to data from Days 1, 4 or 7 within analytical uncertainties. The resulting pair of

best-fit profiles for Days 2 and 15 yielded $\delta^{18}O_{Surface}$ and $\delta^{2}H_{Surface}$ values of -4.2‰ and -52.0‰ and D_l^{*i} estimates of 2.3 (± 0.1) x 10^{-5} cm^2 s^{-1} for $^1H^1H^{18}O$ and 2.6 (± 0.2) x 10^{-5} cm^2 s^{-1} for $^1H^2H^{16}O$. These D_l^{*i} estimates agree well with values in the range 2.2-2.7 x 10^{-5} cm^2 s^{-1} that are commonly assumed for $^1H^1H^{18}O$ and $^1H^2H^{16}O$ in studies of soil and leaf waters (e.g., Barnes and Allison, 1988; Mathieu and Bariac, 1996; Gan et al., 2003; DePaolo et al., 2004; Farquhar and Cernusak, 2005; Ogée et al., 2007; etc.). As often noted, however, such values are typically higher than would be expected for reported experimental temperatures. Our estimates, for example, correspond to a "best-fit" temperature of 27.6 ± 0.4 °C according to the temperature-dependent relations presented in Braud et al. (2005), versus temperatures of 16-20°C measured in the Sphagnum columns. Notably, this also places slightly tighter constraints on our estimates of the respective D_l^{*i} values in order to maintain the expected mass-dependent D_l^{*18}/D_l^{*2} ratio of 0.9833 (Mathieu and Bariac, 1996; DePaolo et al., 2004), yielding 2.380 (± 0.020) x 10^{-5} cm^2 s^{-1} for $^1H^1H^{18}O$ and 2.415 (± 0.015) x 10^{-5} cm^2 s^{-1} for $^1H^2H^{16}O$ under the conditions of our experiment.

The exact agreement between simulated and measured isotopic profiles on Days 2 and 15 strongly suggest that the Sphagnum columns were in isotopic steady state on these days. There is little doubt that this is the case on Day 15, which had the most stable antecedent conditions, especially with respect to RH (Table 2). Even a fully saturated soil column (i.e., absent the effects of vapour diffusion and exchange) would be expected to attain steady state for both isotopes under these experimental conditions after about ten days, as estimated from the effective liquid-phase diffusivities and evaporation rate (E), based on the equation:

$$\tau = D_l^{*i}/E^2 \qquad [18]$$

where τ is the characteristic time for profile development (Zimmermann et al., 1967; Allison and Barnes, 1983). Interestingly, the prior occurrence of identical profiles on Day 2 suggests that steady state had already been attained, at least briefly, for both isotopes prior to the period of higher and variable chamber RH during Days 3-10. While we have incomplete documentation of antecedent RH for Day 2, its similarity to that of Day 15 suggests RH was similar to that of the Day 11-15 interval. The rapid development of isotopic steady-state is thus consistent with the expected importance of vapour-liquid exchange and vapour diffusion within the air-filled porosity of the Sphagnum moss, promoted by the four orders-of-magnitude higher vapour-phase diffusivities of the heavy-isotope species (similar to that of bulk water, see equation [3] above). That is, liquid-phase diffusion alone cannot explain the rapid establishment of the observed profiles. The relatively high vapour-phase

diffusivities and vapour-liquid exchange thus accelerate the development of the isotopic profiles. These processes also mask the effects of liquid-phase tortuosity in the unsaturated zone by short-circuiting the more tortuous liquid flow paths.

The simulated profiles additionally provide convenient reference lines for assessing the transient behaviour of the profiles on other days. For example, the higher $\delta^{18}O$ and $\delta^{2}H$ values in the 0-5 cm layer on Days 4 and 7 likely reflect "excess" downward diffusion of heavy-isotope species from the surface because of decreased evaporation (and hence advection) rate in response to higher RH, while the slightly lower $\delta^{18}O$ and $\delta^{2}H$ values in the underlying 5-10 cm layer (most clearly apparent on Day 7) reflect associated capillary rise, drawing up isotopically-depleted pore waters from below. Because of incomplete chamber RH data, the similarly-distorted profile on Day 1 is more equivocal, yet it also clearly indicates the existence of non-steady-state for both isotopes only one day (and perhaps much less) prior to sampling on Day 2. This suggests that the behaviour of the Sphagnum moss pore waters is remarkably analogous to that of water in transpiring leaves, which develop isotopic steady-state within hours (e.g., see Gan et al., 2003; Cuntz et al., 2007; Ogée et al., 2007). Indeed, water mass and isotope transport in the Sphagnum columns appears to bear striking similarity to new conceptualizations of how water is transported within transpiring leaves, although the understanding of vapour-phase processes remains incomplete (Cuntz et al., 2007).

Conclusions and Implications

These results confirm that water flux in *Sphagnum* moss undergoing evaporation is predominantly liquid capillary flow. In spite of the large air-filled pore spaces, water vapour transport by diffusion represents a negligible fraction of the net mass flow. On the other hand, vapour-phase processes foster rapid development of isotopic steady state. The dynamic balance between liquid-phase advection and diffusion determines the shapes of the isotopic profiles, while vapour diffusion and vapour-liquid exchange control the rate at which the profiles form and how rapidly they adjust to changing conditions, especially shifts in atmospheric relative humidity. Changes in relative humidity strongly affect upward advection, via changes in evaporation rate, as well as the enrichment of heavy-isotope species near the *Sphagnum* surface, which determines the isotopic concentration gradients within underlying layers. In spite of the rudimentary nature of our experimental set-up, we obtained remarkably robust estimates of the effective liquid-phase diffusivities of $^{1}H^{1}H^{18}O$ and $^{1}H^{2}H^{16}O$ for

Sphagnum pore waters, suggesting that potential also exists for application of water-isotope tracers in field-based studies to probe hydrologic processes in *Sphagnum* dominated wetlands.

These findings have several other important implications. First, they suggest that water flux in mosses can be modelled considering only liquid flow, given the appropriate parameter and boundary conditions. Second, while the change of state from liquid to gas may generate little water volume for vapour flow, it likely results in latent heat exchanges in the profile and thus affects the thermodynamics of the moss system. This has implications for carbon exchange, which is closely tied to moisture and temperature (NcNeil and Waddington, 2003). Finally, it is noteworthy that latent heat exchanges caused by evaporation below the soil surface will also affect the determination of soil heat flux, thus potentially causing error in determining available energy for evaporation. Models of evapotranspiration such as the Penman-Monteith (Monteith, 1965) assume that the radiative and convective fluxes occur at a common surface, which may therefore limit their validity in moss-dominated systems.

In *Sphagnum*-dominated systems, translocation of water and presumably other chemical species occur predominantly as liquid capillary flow, but vapour movement also has several implications: 1) upwardly flowing vapour may condense near the evaporatively cooled surface, providing a quantitatively small but potentially important water source for dry surface mosses; and 2) vapour-phase processes accelerate the development of steady-state isotope profiles. Accordingly, water samples taken from mosses subjected to evaporation may be useful in estimating evaporation rates in field studies. Samples taken simultaneously from different moss species or in a different setting within a given bog that exhibit distinctly different isotopic profiles may be indicative of differing evaporation rates. Further field and lab verification is required.

Acknowledgements

The financial support of the Natural Sciences and Engineering Research Council (NSERC) of Canada is gratefully acknowledged.

References

Allison GB, Barnes CJ, 1983. Estimation of evaporation from non-vegetated surfaces using natural deuterium. *Nature* 301: 143-145.

Allison GB, Barnes CJ, Hughes MW, 1983. The distribution of deuterium and ^{18}O in dry soils 2: Experimental. *Journal of Hydrology* 64: 377–397.

Aravena R, and Warner BG, 1992. O-18 Composition of *Sphagnum* and environmental water relations. *Bryologist* 95: 445–448.

Barnes CJ, and Allison GB, 1983. The distribution of deuterium and ^{18}O in dry soils 1. Theory. *Journal of Hydrology* 60: 141–156.

Barnes CJ, and Allison GB, 1988. Tracing of water movement in the unsaturated zone using stable isotopes of hydrogen and oxygen. *Journal of Hydrology* 100: 143–176.

Boelter DH, 1965. Hydraulic conductivity of peats. *Soil Science* 100: 227–231.

Boelter DH, 1970. Water table drawdown around an open ditch in organic soils. *Journal of Hydrology* 15: 329–340.

Braud I, Bariac T, Gaudet JP, Vauclin M, 2005. SiSPAT-Isotope, a coupled heat, water and stable isotope (HDO and $H_2{}^{18}O$) transport model for bare soil. Part I. Model description and first verifications. *Journal of Hydrology* 309: 277-300.

Brenninkmeijer CAM, van Geel B, Mook WG, 1982. Variations in the D/H and $^{18}O/^{16}O$ ratios in cellulose extracted from a peat bog core. *Earth and Planetary Science Letters* 61: 283-290.

Cahill AT, and Parlange MB, 1998. On water vapor transport in field soils. *Water Resources Research* 34: 731–739.

Carleton TJ, Dunham TMM, 2003. Distillation in a boreal mossy forest floor. *Canadian Journal of Forest Research* 33: 663–671.

Clymo RS, and Hayward PM, 1982. The Ecology of *Sphagnum*. In: Smith AJE, (Ed.) Bryophyte Ecology. Chapman and Hall, London: pp. 229-288.

Coleman ML, Shepherd TJ, Durham JJ, Rouse JE, Moore GR, 1982. Reduction of water with zinc for hydrogen isotope analysis. *Analytical Chemistry* 54: 993–995.

Collis-George N, 1959. The Physical Environment of Soil Animals. *Ecology* 40: 550-557.

Coplen TB, 1996. New guidelines for reporting stable hydrogen, carbon, and oxygen isotope-ratio data. *Geochimica et Cosmochimica Acta* 60: 3359–3360.

Craig H, and Gordon LI, 1965. Deuterium and oxygen 18 variations in the ocean and marine atmosphere. In: Tongiorgi E (Ed.), Stable Isotopes in Oceanographic Studies and Paleotemperatures. Pisa, Italy. Laboratorio di Geologia Nucleare, pp. 9–130.

Cuntz M, Ogée J, Farquhar G, Peylin P, Cernusak LA, 2007. Modelling advection and diffusion of water isotopologues in leaves. *Plant, Cell and Environment* 30: 892-909.

DePaolo DJ, Conrad ME, Maher K, Gee GW, 2004. Evaporation effects on oxygen and hydrogen isotopes in deep vadose zone pore fluids at Hanford, Washington. *Vadose Zone Journal* 3: 220-232.

Drexler JZ, Bedford BL, Scognamiglio R, Siegel DI, 1999. Fine-scale characteristics of groundwater flow in a peatland. *Hydrological Processes* 13: 1341–1359.

Drimmie RJ, and Heemskerk RA, 1993. Water ^{18}O by CO_2 equilibration. Technical Procedure 13.0, Rev. 02. Environmental Isotope Laboratory: Department of Earth Sciences, University of Waterloo. 11 pp.

Edwards TWD, 1993. Interpreting past climate from stable isotopes in continental organic matter. *In* Climate Change in Continental Isotopic Records. *Edited by* Swart PK, McKenzie J, Lohmann KC, Savin S, *American Geophysical Union, Geophysical Monograph* 78: 333-341.

Epstein S, and Mayeda TK, 1953. Variations in the O^{18} content of waters from natural sources. *Geochimica et Cosmichimica Acta* 4: 213 - 224.

Farquhar G, and Cernusak LA, 2005. On the isotopic composition of leaf water in the non-steady state. *Functional Plant Biology* 32: 293-303.

Flanagan LB, Brooks JR, Varney GT, Ehleringer JR, 1997. Discrimination against $C^{18}O^{16}O$ during photosynthesis and the oxygen isotope ratio of respired CO_2 in boreal forest ecosystems. *Global Biogeochemical Cycles* 111: 83–98.

Gan, KS, Wong SC, Yong JWH, Farquhar GD, 2003. Evaluation of models of leaf water 18O enrichment using measurements of spatial patterns of vein xylem, leaf water and dry matter in maize leaves. *Plant, Cell and Environment* 26: 1479-1495.

Gates DM, 1980. Biophysical Ecology. Springer-Verlag, New York, Heidelberg, Berlin.

Gonfiantini R, 1986. Environmental isotopes in lake studies. In: Fritz, P. and Fontes, J.C. (Eds.) Handbook of Environmental Isotope Geochemistry, 2. Elsevier, New York, pp. 113–168.

Govardhan K, Alex ZC, 2005. Mems Based Humidity Sensor. Proceedings of the International Conference on Smart Materials Structures and Systems. Institute for Smart Structures and Systems ISSS-2005/SE-04, July 28-30, 2005, Bangalore, India, pp. SE20-SE27.

Hayward PM, and Clymo RS, 1982. Profiles of water-content and pore-size in *Sphagnum* and peat, and their relation to peat bog ecology. *Royal Society of London Series B – Biological Sciences Conference Proceedings* 215: 299–325.

Hsieh JCC, Chadwick OA, Kelly EF, Savin SM, 1998. Oxygen isotopic composition of soil water: Quantifying evaporation and transpiration. *Geoderma* 82: 269-293.

Horita J, Wesolowski D, 1994. Liquid-vapour fractionation of oxygen and hydrogen isotopes of water from the freezing to the critical temperature. *Geochimica et Cosmochimica Acta* 58: 3425–3497.

Ingram HAP, 1983. Hydrology. In: Gore AJP (Ed), Ecosystems of the World 4A, Mires: swamp, bog, fen and moor. Elsevier, Amsterdam, pp. 67–158.

Ishihara Y, Shimojima E, Harada H, 1992. Water vapor transfer beneath bare soil where evaporation is influenced by a turbulent surface wind. *Journal of Hydrology* 131: 63–104.

Izbicki JA, Radyk J, Michel RL, 2000. Water movement through a thick unsaturated zone underlying an intermittent stream in the western Mojave Desert, Southern California, USA. *Journal of Hydrology* 238: 194–217.

Kellner E, 2002. Surface energy fluxes and control of evapotranspiration from a Swedish *Sphagnum* mire. *Agricultural and Forest Meteorology* 110: 101–123.

Kellner E., and Halldin S., 2002. Water budget and surface-layer water storage in a *Sphagnum* bog in central Sweden. *Hydrological Processes* 16: 87–103.

Kellner E, Waddington JM, Price JS, 2005. Dynamics of biogenic gas bubbles in peat: Potential effects on water storage and peat deformation. *Water Resources Research* 41: doi.org/10.1029/2004WR003732.

Kennedy P, and van Geel PJ, 2000. Hydraulics of peat filters treating septic tank effluent. *Transport in Porous Media* 41: 47–60.

Kim J, and Verma SB, 1996. Surface exchange of water vapour between an open *Sphagnum* fen and the atmosphere. *Boundary-Layer Meteorology* 79: 243–264.

Klute A, 1986. Methods of Soil Analysis. Part 1. Physical and Mineralogical Methods, 2nd edn. American Society of Agronomy, Madison, WI.

Larson DW, and Kershaw KA, 1976. Studies on lichen dominated ecosystems. XVIII. Morphological control of evaporation in lichens. *Canadian Journal of Botany* 54: 2061–2073.

Mathieu R, Bariac T, 1996. A numerical model for the simulation of stable isotope profiles in drying soils. *Journal of Geophysical Research D* 101: 12685-12696.

McNeil P, and Waddington JM, 2003. Eco-hydrological controls on *Sphagnum* growth and CO2 exchange on a cutover bog surface. *Journal of Applied Ecology* 40: 354–367.

Millington RJ, 1959. Gas diffusion in porous media. *Science* 130 : 100-102.

Millington R, and Quirk JP, 1961. Permeability of porous solids. *Transactions of the Faraday Society* 57: 1200.

Mills R, 1973. Self-diffusion in normal and heavy water in the range 1-45^{o}C. *Journal of Physical Chemistry* 77: 685–688.

Moldrup P, Olesen T, Schjonning P, Yamaguchi T, Rolston DE, 2000. Predicting the gas diffusion coefficient in undisturbed soil from soil water characteristics. *Soil Science Society of America Journal* 64: 94–100.

Monteith JL, 1965. Evaporation and the environment. *Proceedings of the 19th Symposium of the Society of Experimental Biology* 205-234.

Münnich KO, Sonntag C, Christmann D, Thoma G, 1980. Isotope fractionation due to evaporation from sand dunes. *ZFI – Mitteilungen, Zentralinstitut für Isotopen und Strahlenforschung* 29: 319-322.

Nichols DS, and Brown JM, 1980. Evaporation from a *Sphagnum* moss surface. *Journal of Hydrology* 48: 289–302.

Ogée J, Cuntz M, Peylin P, Bariac T, 2007. Non-steady-state, non-uniform transpiration rate and leaf anatomy effects on the progressive stable isotope enrichment of leaf water along monocot leaves. *Plant, Cell and Environment* 30: 367-387.

Price JS, 1991. Evaporation from a blanket bog in a foggy coastal environment. *Boundary-Layer Meteorology* 57: 391–406.

Price JS, 2003. Role and character of seasonal peat soil deformation on the hydrology of undisturbed and cutover peatlands. *Water Resources Research* 39: doi:10.1029/2002WR001302,2003.

Reeve AS, Siegel DI, Glaser PH, 2000. Simulating vertical flow in large peatlands. *Journal of Hydrology* 227: 207–217.

Rose CW, 1968. Water transport in soil with a daily temperature wave I: Theory and experiment. *Australian Journal of Soil Research* 6: 31–44.

Rydin H, Clymo RS, 1989. Transport of carbon and phosphorus compounds about *Sphagnum*. *Proceedings of the Royal Society of London B* 237: 63-84.

Shurbaji AM, Phillips FM, Campbell AR, Knowlton RG, 1995. Application of a numerical model for simulating water flow, isotope transport, and heat transport in the unsaturated zone. *Journal of Hydrology* 171: 143–163.

Stern L, Baisden WT, Amundson R, 1999. Processes controlling the oxygen isotope ratio of soil CO_2: Analytic and numerical modelling. *Geochimica et Cosmochimica Acta* 63: 799–814.

Tang K, and Feng W, 2001. The effect of soil hydrology on the oxygen and hydrogen isotopic compositions of plants' source water. *Earth and Planetary Science Letters* 185: 355–367.

Tetens O, 1930. Uber Einige Meterologische Begriffe. *Zeitschrift fur Geophysik* 6: 297–309.

Touma J, Vachaud G, Parlange JY, 1984. Air and water-flow in a sealed pond vertical soil columns – experiment and model. *Soil Science* 137: 181–187.

Walker GR, Hughes MW, Allison GB, Barnes CJ, 1988. The movement of isotopes of water during evaporation from a bare soil surface. *Journal of Hydrology* 97: 181-197.

Williams TG, Flanagan LB, 1996. Effect of changes in water content on photosynthesis, transpiration and discrimination against (CO2)-C-13 and (COO)-O-18-O-16 in Pleurozium and Shagnum. *Oecologia* 108: 38–46.

Yazaki T, Urano SI, Yabe K, 2006. Water balance and water movement in unsaturated zones of *Sphagnum* hummocks in Fuhrengawa Mire, Hokkaido, Japan. *Journal of Hydrology* 319: 312–327.

Yoshikawa K, Bolton WR, Romanovsky VE, Fukuda M, Hinzman LD, 2002. Impacts of wildfire on the permafrost in the boreal forests of Interior Alaska, *Journal of Geophysical Research* 107: doi:10.1029/2001JD000438.

Zimmermann U, Ehhalt D, Münnich KO, 1967. Soil water movement and evapotranspiration: changes in the isotopic composition of the water. In: Isotopes in Hydrology, IAEA, Vienna, 567-584.

List of Figures

List of Tables

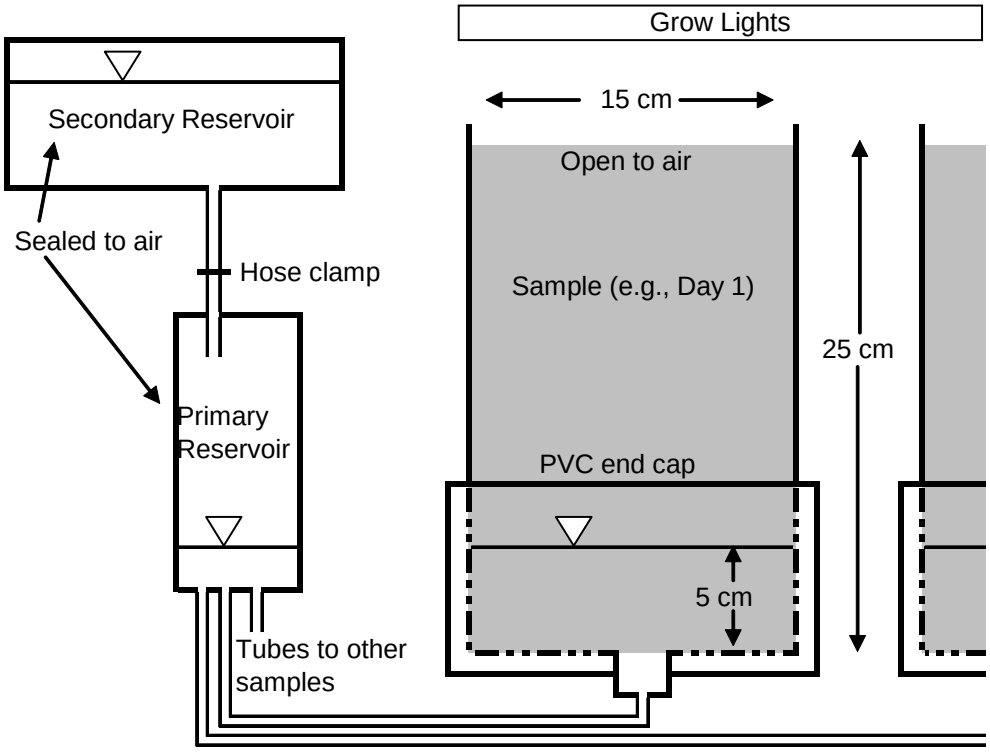
Grow Lights
15 cm
Secondary Reservoir
Open to air
Sealed to air
Hose clamp
Sample (e.g., Day 1)
25 cm
Primary
Reservoir
PVC end cap
5 cm
Tubes to other
samples

Figure 1.

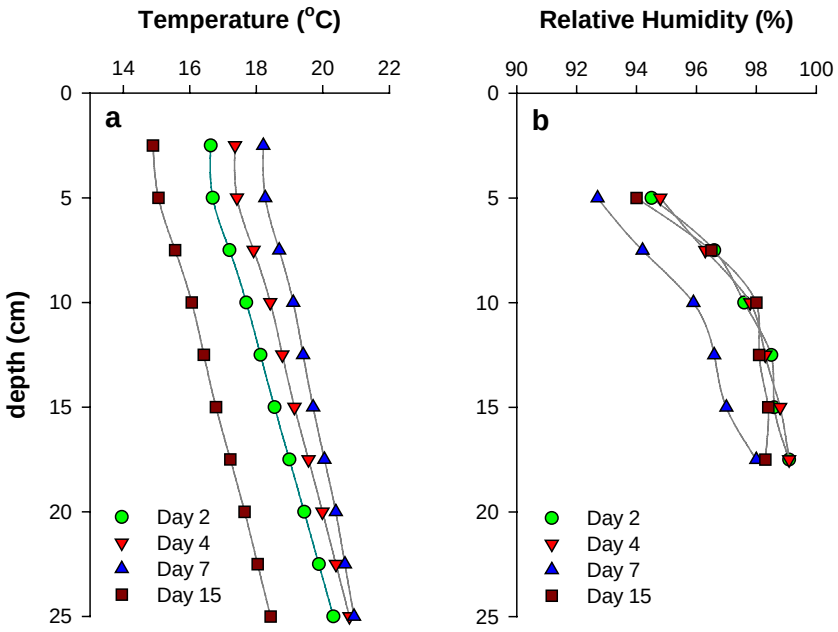
Temperature (°C)
Relative Humidity (%)
depth (cm)
a
b
Day 2
Day 4
Day 7
Day 15

Figure 2.

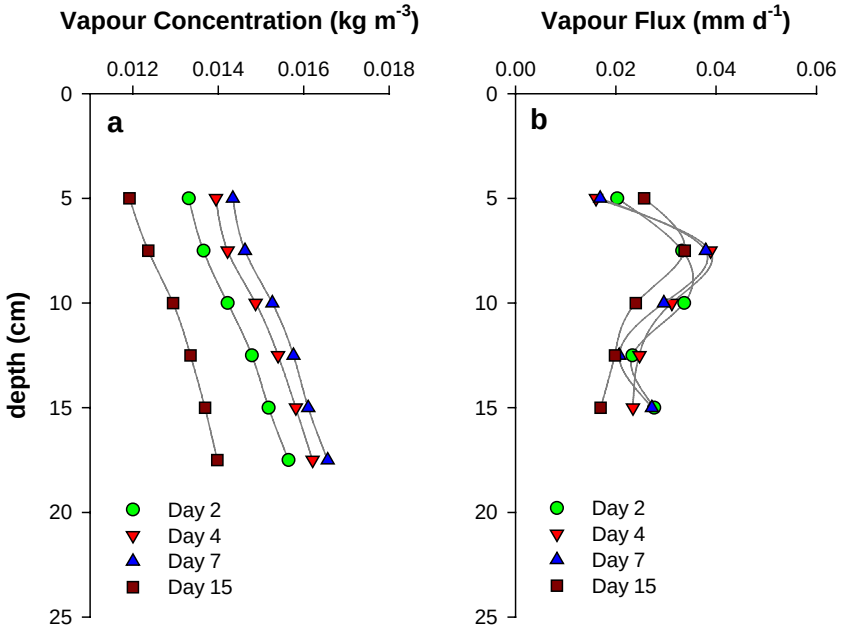
Vapour Concentration (kg m-3)
0.012
0.014
0.016
0.018
0
5
10
15
20
25
depth (cm)
a
Day 2
Day 4
Day 7
Day 15
Vapour Flux (mm d-1)
0.00
0.02
0.04
0.06
b
Day 2
Day 4
Day 7
Day 15

Figure 3.

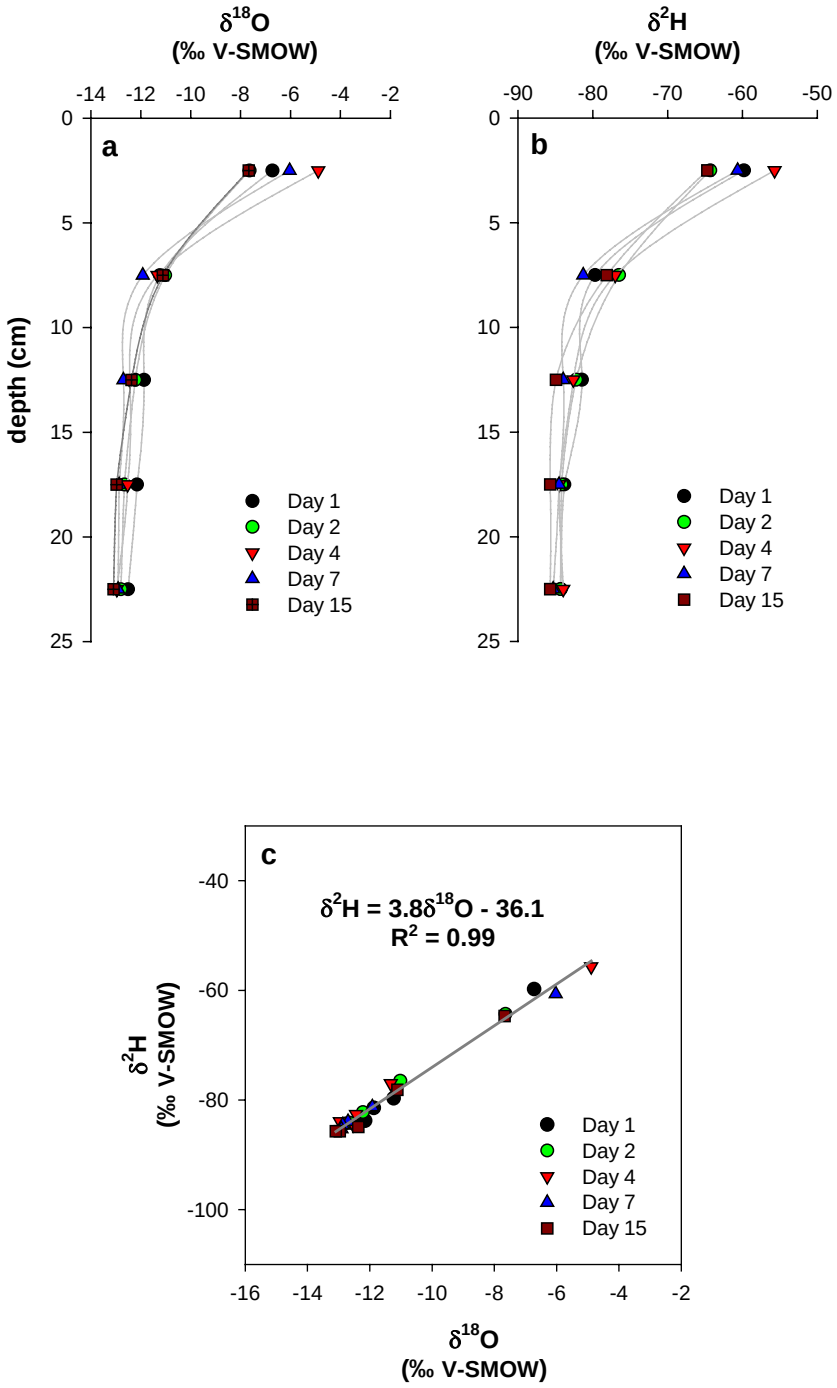
δ18O
(‰ V-SMOW)
δ2H
(‰ V-SMOW)
depth (cm)
a
b
c
Day 1
Day 2
Day 4
Day 7
Day 15
δ2H = 3.8δ18O - 36.1
R2 = 0.99

Figure 4.

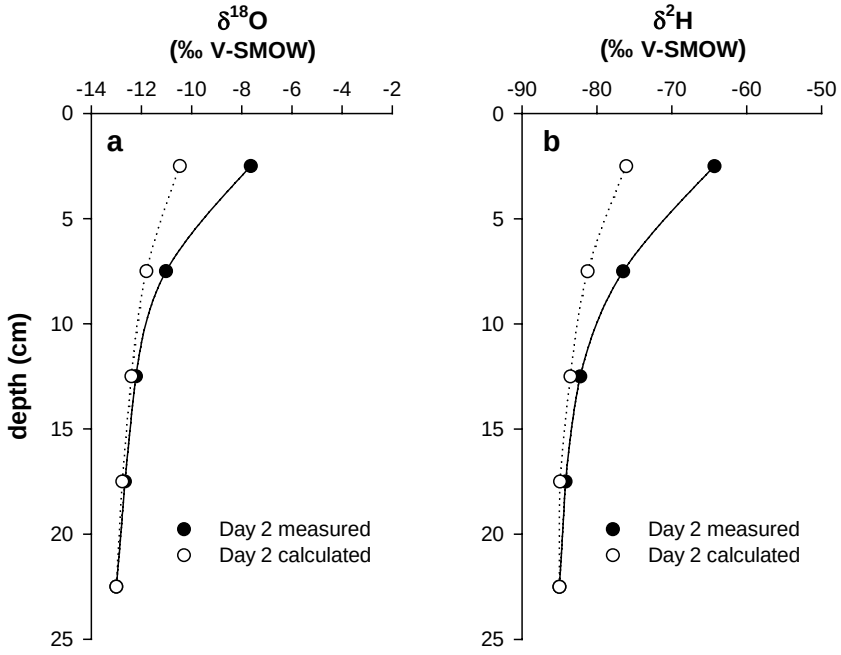
δ18O
(‰ V-SMOW)
-14
-12
-10
-8
-6
-4
-2
0
5
10
15
20
25
depth (cm)
a
Day 2 measured
Day 2 calculated
δ2H
(‰ V-SMOW)
-90
-80
-70
-60
-50
b
Day 2 measured
Day 2 calculated

Figure 5.

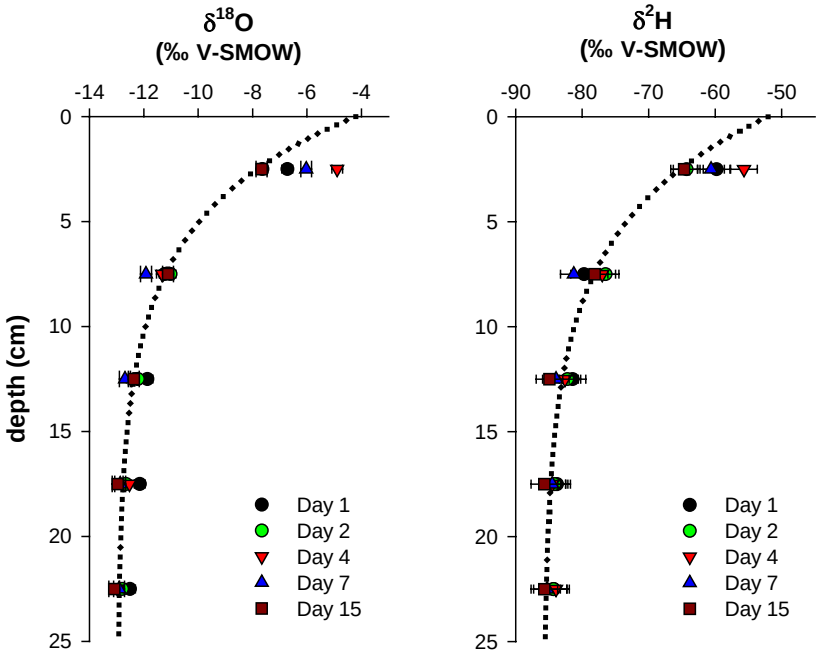
δ18O
(‰ V-SMOW)
-14
-12
-10
-8
-6
-4
0
5
10
15
20
25
depth (cm)
Day 1
Day 2
Day 4
Day 7
Day 15
δ2H
(‰ V-SMOW)
-90
-80
-70
-60
-50
0
5
10
15
20
25
Day 1
Day 2
Day 4
Day 7
Day 15

Figure 6.

Table 1. Physical properties of *Sphagnum.*

Depth (cm)	Bulk Density (g/cm^3)	VMC
0-5	0.018	14.1
5-10	0.017	13.0
10-15	0.015	13.7
15-20	0.020	25.9
20-25	0.037	77.4

Average particle density (ρ_p) 1.2 g cm^{-3}

Table 2. Daily average chamber air temperature (*T*), relative humidity (*RH*) and estimated evaporation rate (*E*) from the *Sphagnum* columns during the experiment.

	T	***RH***	***E***
day	**(°C)**	**(%)**	**(mm d^{-1})**
1	20.8	-	-
2	21.0	-	-
3	20.9	28.4	4.4
4	21.1	32.8	4.1
5	21.1	31.4	4.2
6	21.1	33.7	4.1
7	21.1	36.6	3.9
8	21.4	33.0	4.1
9	21.1	27.9	4.4
10	20.9	26.3	4.5
11	20.8	24.1	4.7
12	20.5	22.9	4.7
13	20.2	23.5	4.7
14	19.8	23.2	4.7
15	19.0	21.4	4.8
average	**20.7**	**28.1**	**4.5**

Appendix A

The evaporative-enrichment response of the *Sphagnum* pore waters can be assessed by considering the special case of the Craig and Gordon (1965) model describing the isotopic composition of a terminal reservoir evaporating in isotopic and hydrologic steady-state:

$$\delta_{Water} = \alpha_e \alpha_k (1 - RH)(\delta_{Input} + 1000) + \alpha_e RH(\delta_{Air} + 1000) - 1000 \qquad [A1]$$

where α_e represents the respective temperature-dependent liquid-vapour equilibrium fractionation factors of 1.0097 and 1.0835 for ^{18}O and ^{2}H at mean experimental temperature of 20.7°C (calculated from equations reported by Horita and Wesolowski, 1994); α_k represents the respective kinetic fractionations of 1.0142 and 1.0125 for open-water evaporation (see Gonfiantini, 1986); *RH* represents mean relative humidity in decimal notation (0.271); δ_{Input} represents the respective $\delta^{18}O$ and $\delta^{2}H$ values of input water (-13.0‰ and -85.8‰) and δ_{Air} represents the respective $\delta^{18}O$ and $\delta^{2}H$ values of ambient atmospheric moisture (-20.5‰ and -149.1‰; based on isotopic equilibrium with local tap water used to humidify the laboratory ventilation system).

The slope of the evaporation line (S_{EL}) is then given by:

$$S_{EL} = (\delta^2 H_{Water} - \delta^2 H_{Input})/(\delta^{18} O_{Water} - \delta^{18} O_{Input}). \qquad [A2]$$

Appendix II:

Progress in isotope paleohydrology using lake sediment cellulose*

Summary Recent advances in sample preparation techniques and mass spectrometry have fostered more routine oxygen isotope analysis of aquatic cellulose in lake sediment cores, a proxy for lake water oxygen isotope history. These methodological developments have significantly increased the feasibility of incorporating this approach into high-resolution, multi-site, and multiproxy studies, which are frequently necessary to answer complex hydrological, hydroecological and hydroclimatic questions requiring a paleoenvironmental perspective. Direct translation of lake sediment aquatic cellulose oxygen isotope composition into lake water oxygen isotope composition offers appreciable opportunity for quantitative paleohydrological reconstructions, as evidenced by studies conducted over the past 15 years that span Holocene and pre-historical time scales.

* Published as: Wolfe B.B., Falcone M.D., Clogg-Wright K.P., Mongeon C.L., Yi Y., Brock B.E., St. Amour N.A., Mark W.A., Edwards T.W.D., Progress in isotope paleohydrology using lake sediment cellulose. *Journal of Paloelimnology* 37: 221-231.

J Paleolimnol (2007) 37:221–231
DOI 10.1007/s10933-006-9015-8

ORIGINAL PAPER

Progress in isotope paleohydrology using lake sediment cellulose

Brent B. Wolfe · Matthew D. Falcone · Ken P. Clogg-Wright · Cherie L. Mongeon · Yi Yi · Bronwyn E. Brock · Natalie A. St. Amour · William A. Mark · Thomas W. D. Edwards

Received: 28 September 2005 / Accepted: 14 April 2006 / Published online: 9 August 2006

Abstract Recent advances in sample preparation techniques and mass spectrometry have fostered more routine oxygen isotope analysis of aquatic cellulose in lake sediment cores, a proxy for lake water oxygen isotope history. These methodological developments have significantly increased the feasibility of incorporating this approach into high-resolution, multi-site, and multi-proxy studies, which are frequently necessary to answer complex hydrological, hydroecological and hydroclimatic questions requiring a paleoenvironmental perspective. Direct translation of lake sediment aquatic cellulose oxygen isotope composition into lake water oxygen isotope composition offers appreciable opportunity for quantitative paleohydrological reconstructions, as evidenced by studies conducted over the past 15 years that span Holocene and pre-historical timescales.

B. B. Wolfe (✉) · C. L. Mongeon
Department of Geography and Environmental Studies, Wilfrid Laurier University, 75 University Avenue West, Waterloo, Ontario, Canada, N2L 3C5
e-mail: bwolfe@wlu.ca

M. D. Falcone · K. P. Clogg-Wright · Y. Yi · B. E. Brock · N. A. St. Amour · W. A. Mark · T. W. D. Edwards · B. B. Wolfe
Department of Earth Sciences, University of Waterloo, Waterloo, Ontario, Canada, N2L 3G1

Keywords Cellulose · Oxygen isotope composition · Lake sediments · Paleohydrology · Heavy liquid density-separation · CF-IRMS

Introduction

Organic compounds provide a useful substrate for tracing lake water oxygen isotope composition history due to the ubiquitous nature of organic material in lake sediments. Oxygen isotope analysis of aquatic cellulose has been the target of most studies over the past 15 years beginning with the seminal work of Edwards and McAndrews (1989). Application of this technique has undergone rapid growth in recent years largely due to improved sample preparation methods and enhanced analytical capability with the advent of on-line continuous flow isotope-ratio mass spectrometry (CF-IRMS). Numerous investigations have provided both qualitative (e.g., MacDonald et al. 1993; Duthie et al. 1996; Wolfe et al. 1996, 2000, 2003; Beuning et al. 1997, 2002; Buhay and Betcher 1998; Abbott et al. 2000, 2003; Anderson et al. 2001; MacDonald et al. 2004) and quantitative (e.g., Edwards and McAndrews 1989; Edwards et al. 1996, 2004; Wolfe et al. 2001a, 2005) insight into various aspects of past hydrology, hydroecology and hydroclimatology.

A fundamental basis for these studies is the assumption that the oxygen isotope composition

of aquatic cellulose deposited in sediments over time records and preserves the oxygen isotope composition of the lake water from which it formed. The following general equation can be used to quantitatively relate the oxygen isotope composition of aquatic cellulose to the source water (Edwards and McAndrews 1989; Wolfe et al. 2001b):

$$\delta^{18}O_{cell} = \delta^{18}O_{mw} + \varepsilon^{18}_{hydro} + \varepsilon^{18}_{cell-lakewater} \quad (1)$$

where $\delta^{18}O_{cell}$ is the oxygen isotope composition of aquatic cellulose (i.e., $\delta^{18}O_{cell} = [(R_{cell}/R_{VSMOW})-1] \times 10^3$ where R is the $^{18}O/^{16}O$ ratio in the cellulose sample and the standard, VSMOW), $\delta^{18}O_{mw}$ is the oxygen isotope composition of local meteoric water, ε^{18}_{hydro} is the oxygen isotope separation between lake water and local meteoric water due to hydrological factors and which is commonly dominated by evaporation, and $\varepsilon^{18}_{cell\text{-}lakewater}$ is the oxygen isotope separation that occurs during synthesis of aquatic cellulose. Thus, decoding paleoenvironmental information from stratigraphic records of $\delta^{18}O_{cell}$ depends on the ability to characterize or constrain $\delta^{18}O_{mw}$, ε^{18}_{hydro}, and $\varepsilon^{18}_{cell\text{-}lakewater}$.

Numerous field and laboratory studies have shown that $\varepsilon^{18}_{cell\text{-}lakewater}$ averages about 28‰ and is independent of water temperature and plant species (see Sternberg 1989; Yakir 1992; Wolfe et al. 2001b; Sternberg et al. 2003), affording the opportunity to directly transform stratigraphic records of $\delta^{18}O_{cell}$ into cellulose-inferred lake water $\delta^{18}O$ profiles (i.e., $\delta^{18}O_{mw}+\varepsilon^{18}_{hydro}$). Interpretation of these profiles have, thus, generally involved separating primary isotopic effects caused by shifts in the oxygen isotope composition of meteoric water (i.e., $\delta^{18}O_{mw}$) from those associated with secondary hydrological processes such as evaporative ^{18}O-enrichment (i.e., ε^{18}_{hydro}). In δ^2H–$\delta^{18}O$ space, this translates to distinguishing MWL-parallel shifts, which are commonly temperature-dependent but can also reflect selective recharge or air mass circulation characteristics, from LEL-parallel shifts, which are generally associated with relative humidity and water balance (Fig. 1; also see Edwards et al. 2004). Direct inference of lake water oxygen isotope composition without complicating temperature- and species-dependent fractionation effects is an especially convenient aspect of this technique, as paleohydrological reconstructions can be generated providing $\delta^{18}O_{mw}$ or ε^{18}_{hydro} are known or can be constrained using other information.

Various approaches have been utilized to separate cellulose-inferred lake water $\delta^{18}O$ histories into $\delta^{18}O_{mw}$ and ε^{18}_{hydro} components, such as incorporation of independently-derived records of paleoprecipitation isotope composition history (e.g., Edwards and McAndrews 1989; Wolfe et al. 2000, 2001a, 2005) and comparison of lake water isotopic records from several lakes in the same region with varying hydrological sensitivities to evaporation (e.g., Edwards et al. 1996). Information from other isotopic records (e.g., $\delta^{13}C$, $\delta^{15}N$) or other proxies (diatoms, pollen, mineralogy, etc.), as well as assessment of modern isotope hydrology of the study lake have also been used to constrain both qualitative and quantitative interpretations (e.g., Wolfe et al. 1996, 2001a, 2005).

Reviews on methods and applications of lake sediment cellulose (C, O) isotope composition for reconstructing past hydrological conditions and nutrient cycling (Wolfe et al. 2001b) and on use of water isotope tracers in hydrological and paleohydrological investigations of lakes at high latitudes (Edwards et al. 2004) have recently been published as part of the *Developments in Paleoenvironmental Research* book series. In this companion article to these chapters, we describe recent technological improvements in sample preparation and oxygen isotope analysis of lake sediment cellulose. This is followed by synopses of selected case studies, each representing a major step in the methodological evolution of this paleohydrological technique and which collectively demonstrate the capacity for quantitative reconstructions.

Recent advances in sample preparation techniques and analysis

Sample preparation

Methods for preparing lake sediment samples for cellulose oxygen isotope analysis have routinely

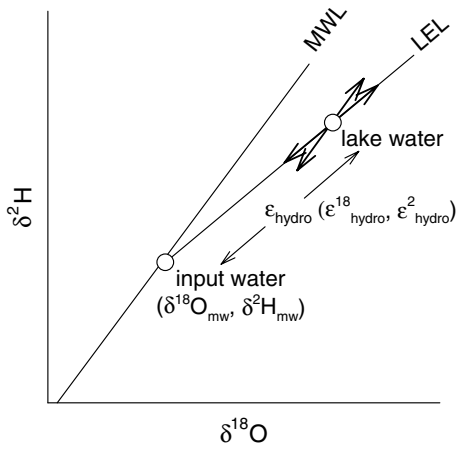

Fig. 1 Interpretation of cellulose-inferred lake water $\delta^{18}O$ records is generally a function of distinguishing trajectories parallel to the Meteoric Water Line (MWL) versus trajectories parallel to the Local Evaporation Line (LEL). The former is linked to changes in input water oxygen isotope composition (i.e., $\delta^{18}O_{mw}$), whereas the latter is most often associated with changes in ^{18}O enrichment due to evaporation (i.e., ε^{18}_{hydro}). Note that similar notation applies to hydrogen isotope parameters

followed those of Green (1963) and Sternberg (1989) for extracting cellulose from wood powder with modifications to accommodate the much finer grain size typical of sediments and for removal of other potentially interfering geochemical fractions (Wolfe et al. 2001b). Preliminary sample treatment involves acid-washing to dissolve carbonate material and dry sediment sieving to remove macrofossil debris (which may be of terrestrial origin) after which analysis of bulk carbon and nitrogen elemental and isotope composition is generally conducted. These data commonly provide insight into past carbon and nitrogen cycling in lakes and their watersheds, including indication of the source of the organic matter (see Meyers and Teranes 2001; Talbot 2001). A dominantly aquatic origin is a key criterion for using lake sediment cellulose $\delta^{18}O$ for paleohydrological reconstruction (see Wolfe et al. 2001b; Sauer et al. 2001).

Sediment cellulose preparation on the fine-grained acid-washed residue is generally a four-part process involving sequential extraction of non-cellulose organic and inorganic components, as described in Wolfe et al. (2001b). Briefly, this involves (1) solvent extraction to remove lipids, resins, and tannins, (2) bleaching to remove lignin, (3) alkaline hydrolysis to remove xylan, mannan, and other polysaccharides and (4) leaching to remove Fe- and Mn-oxyhydroxides.

In recent years, purification and separation of cellulose from lake sediment has been enhanced by employing heavy-liquid density separation after Fe- and Mn-oxyhydroxide leaching. This additional sample preparation step effectively removes remaining and potentially interfering minerogenic constituents. Sodium polytungstate (SPT), a highly soluble inorganic salt, is used to produce a heavy liquid with a specific gravity of 1.9–2.0, which we find is effective for suspending cellulose (~1.5 sg; Vincent 1999) in the supernatant from heavier mineral matter following centrifugation. A similar purification step using SPT is also utilized for preparing diatom samples from highly minerogenic deposits for species identification (e.g., Hay et al. 1997) and for oxygen isotope analysis (Morley et al. 2004). Details of methods are as follows (Fig. 2):

1. Freeze-dried Fe/Mn-leached sediment is transferred to 50 ml centrifuge-safe plastic tubes.
2. Thirty millilitres of 1.9–2.0 sg SPT are added to sediment sample in 50 ml centrifuge-safe plastic tubes. Cap is tightened securely. Sample tube is then shaken vigorously to suspend cellulose fraction.
3. Sample tube is centrifuged at 1800 rpm for 20 min. Typically, sample tube is left to stand for 2–3 h or overnight if notable mineral matter is visibly in the supernatant.
4. Suspended fraction (i.e., cellulose) is aspirated using a glass pipette and transferred from 50 ml centrifuge-safe plastic tube to a 200 ml glass bottle.
5. Two hundred-millilitre bottle is filled with deionized (DI) water.
6. Solution from 200 ml glass bottle is filtered using 0.45 μm Gelman Supor Membrane Filter (one per sample) using a hand or electric pump. A total of at least 500 ml DI water is used for each sample to ensure all SPT is flushed through to the filtrate. Note that early attempts to centrifuge diluted supernatant in 200 ml glass bottles were unsuccessful in

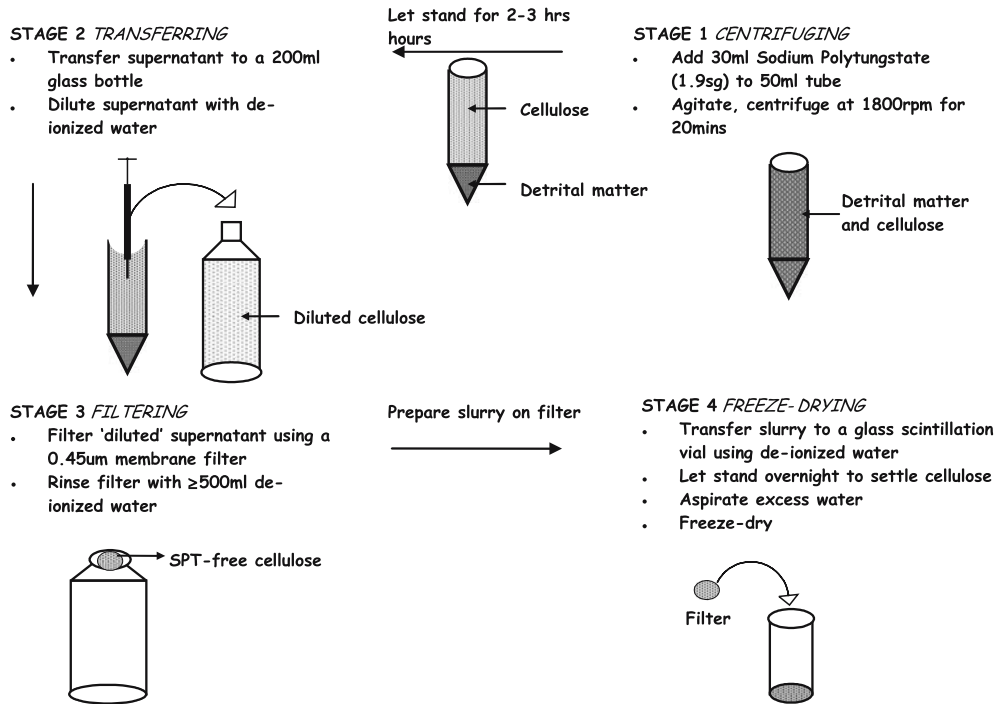

Fig. 2 Procedure for density-separation of lake sediment cellulose from detrital mineral matter using sodium polytungstate

removing SPT, as was also found by Morley et al. (2004).

7. A slurry on the filter is created by releasing pressure of vacuum and adding a small amount of DI water. This is then transferred by disposable pipette to a labelled scintillation vial. Additional residue is washed-off the filter into the scintillation vial with DI water.
8. Vial is capped, left to sit overnight and excess water is removed carefully to reduce the possibility of breakage during subsequent freezing and freeze-drying.
9. Sample is frozen and freeze-dried in scintillation vial.

Fibrous cellulose is commonly visible in the freeze-dried residue. While a small amount of minerogenic material may also be present, this is easily avoided when weighing and loading samples into tin capsules for oxygen isotope analysis using CF-IRMS (see below). Interested readers can access the full description of the technical procedure for lake sediment cellulose extraction on the University of Waterloo—Environmental Isotope Laboratory (UW-EIL) website (http://www.science.uwaterloo.ca/research/eilab/Methodology/; see TP 28).

Oxygen isotope analysis

Determination of $\delta^{18}O$ from cellulose was initially a labour-intensive and complicated process, requiring off-line quantitative recovery and cryogenic purification of CO_2 using nickel-tube pyrolysis (Thompson and Gray 1977; Edwards et al. 1994; Wolfe et al. 2001b). While design modifications improved sealing and durability of nickel vessels used in the pyrolysis reaction for studies conducted in the mid-late 1990s, more recent advent of CF-IRMS incorporating high-temperature pyrolysis systems have made conversion of organic substances markedly easier and automated (e.g., Farquhar et al. 1997; Saurer et al. 1998). For example, production of sediment cellulose $\delta^{18}O$ results was limited to 6–8 samples per day using the nickel-tube pyrolysis off-line technique, which then still required mass spectrometric analysis on cryogenically purified CO_2. This step has been considerably streamlined using CF-IRMS such that direct $\delta^{18}O$ measurement of

~80 total sediment cellulose samples (in addition to standards) can be performed during an unattended overnight run with all sample analyses generally performed in duplicate. In comparison, analyses of only 10–20% of samples were usually repeated to assess analytical uncertainty using nickel-tube pyrolysis. Substantial reduction in labour and analytical time was essential for the inclusion of cellulose oxygen isotope analyses into a recent multi-proxy paleolimnological investigation that required analysis of hundreds of samples, as described further below.

The analytical arrangement at the UW-EIL consists of a high-temperature furnace (Hekatech, Germany) set at 1300°C configured for oxygen pyrolysis operation, which is connected to a EuroVector EA3028 elemental analyser. The EA is interfaced in continuous flow mode to a GV Instruments (England; previously Micromass) IsoPrime Stable Isotope Ratio Mass Spectrometer (Fig. 3). The reaction tube (19 mm o.d., 14 mm i.d., length 470 mm) is made of ceramic (Al_2O_3). Within the reaction tube, a glassy carbon tube (12.5 mm o.d., 7 mm i.d., length 400 mm) is positioned and isolated from the outer tube to avoid background CO. The inner tube is filled with 130 mm (height) of glassy carbon grit (3,100–4,000 μm) to react with the oxygen from the sample to produce CO. Downstream of the pyrolysis tube, a magnesium perchlorate trap is used to prevent any residual moisture from passing into the mass spectrometer.

Prior to oxygen isotope analysis, density-separated sediment cellulose samples are stored in a desiccator for a period of 48 h to eliminate any traces of atmospheric moisture, which is readily absorbed by the highly hygroscopic cellulose. Using a high-precision electronic balance, subsamples (~1.0 mg) are weighed into tin capsules (4 × 6 mm) and loaded onto the automatic helium-filled autosampler carousel of the pyrolysis reactor. CO generated from the pyrolysis reaction passes through a 1 m, 5 Å molecular sieve-packed GC column held at 100°C and enters the source of the mass spectrometer via a sampling capillary arranged in an open split configuration. The oxygen isotope ratios are obtained by integrating the ion beam areas generated from the CO at atomic mass 30 ($C^{18}O$) and atomic mass 28 ($C^{16}O$) and comparing the ratio with that of a CO reference gas pulse with a known composition. The entire duration of one sample run is

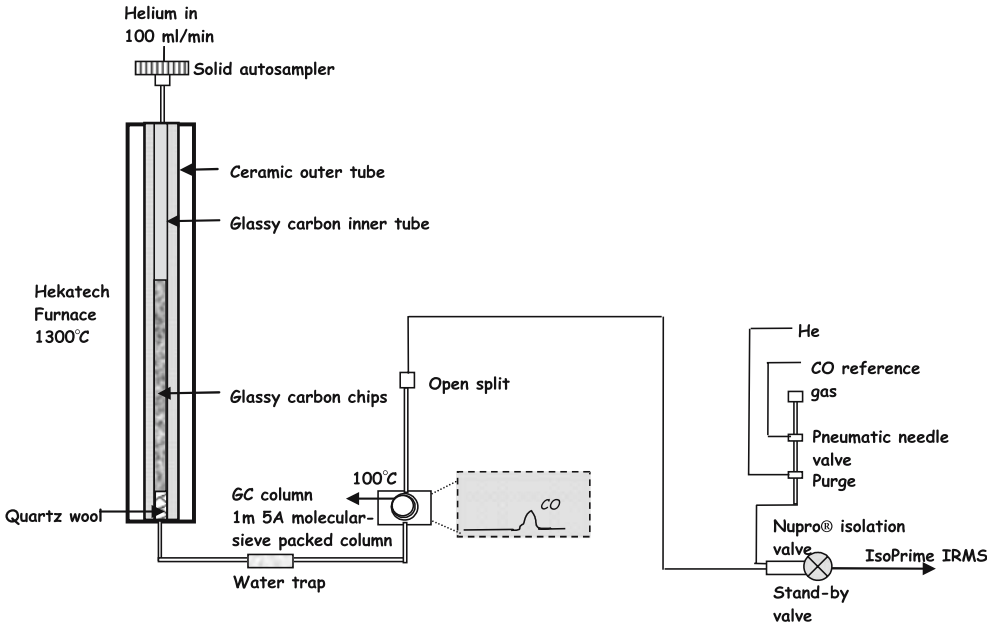

Fig. 3 Continuous flow—isotope ratio mass spectrometry set-up at the University of Waterloo—Environmental Isotope Laboratory

approximately 300 s. Analytical uncertainties on natural samples are typically on the order of ±0.5‰ for $\delta^{18}O$. Final calibration is made to international intercomparison materials with known isotopic composition.

Applications

Below we briefly highlight results from three studies that utilized lake sediment cellulose $\delta^{18}O$ records to quantitatively infer past hydroclimatic conditions at Holocene and pre-historical timescales. Each represents a major methodological development in the application of this technique over the past 15 years.

Weslemkoon Lake, Ontario, Canada (Edwards and McAndrews 1989)

In this inaugural lake sediment cellulose study, sediment cores from Weslemkoon Lake, Ontario, Canada, were analysed for cellulose carbon and oxygen isotope composition to reconstruct Holocene paleohydrology. This study followed a series of investigations utilizing isotopic records from wood and lake sediment carbonate (Edwards et al. 1985; Edwards and Fritz 1986, 1988). These prior studies had identified a four-part post-glacial climate history characterized by a cold and dry early Holocene, warm and dry mid-Holocene, warm and moist mid-late Holocene, and cool and moist late Holocene.

Sediment cellulose was extracted from Weslemkoon Lake cores to (1) test this new method in an area where prior knowledge of paleoclimate history existed and (2) further refine the paleohydrological history. Interpretation of the cellulose-inferred lake water $\delta^{18}O$ record incorporated $\delta^{18}O_{mw}$ as temperature-dependent mean annual oxygen isotope composition of precipitation from prior studies (subsequently elaborated on in Edwards et al. 1996) to semi-quantitatively partition snowmelt-bypass effects as an additional MWL-parallel component in addition to LEL-parallel, evaporative ^{18}O-enrichment from the residual ε^{18}_{hydro} Holocene record. Results were strongly consistent with the earlier studies.

Beyond contributions to southern Ontario paleohydrological and paleoclimatic history, this study confirmed the utility of lake sediment cellulose $\delta^{18}O$ as an archive of lake water $\delta^{18}O$ history and identified that $\delta^{18}O_{mw}$, ε^{18}_{hydro} and $\varepsilon^{18}_{cell\text{-}lakewater}$ control $\delta^{18}O_{cell}$ akin to more established isotopic approaches, namely wood cellulose and lake sediment carbonate. Key findings in support of this newly established technique included (1) surface-sediment cellulose $\delta^{18}O_{cell}$ values were consistent with a $\varepsilon^{18}_{cell\text{-}lakewater}$ value of 28‰, as reported in Edwards et al. (1985) for $\varepsilon^{18}_{cell\text{-}leafwater}$, and (2) close alignment of $\delta^{18}O_{cell}$ values were obtained from cores in two locations in Weslemkoon Lake (Fig. 4), as was the pollen stratigraphy. Importantly, both of these results strongly supported a dominantly aquatic origin for the lake sediment cellulose because cellulose derived from terrestrial sources would be expected to be isotopically enriched compared to aquatic sources due to additional fractionation effects that occur during evapotranspiration. Furthermore, similar relative contributions of terrestrial cellulose to the two widely separated coring sites from two sub-basins was considered highly unlikely given the irregular shape and complex bathymetry of Weslemkoon Lake.

The success of this initial exploratory investigation led to a number of applications in a wide variety of locations and ecological zones including the Bolivian Andes and the Peace-Athabasca Delta, Alberta, Canada, as highlighted below.

Lago Potosi, Bolivia (Wolfe et al. 2001a)

Over the past decade, several multi-proxy studies have been conducted on sediment cores from a number of small lake basins in the eastern Cordillera of the central Andes to document late Pleistocene and Holocene effective moisture history (Abbott et al. 1997, 2000, 2003; Wolfe et al. 2001a). This work has been driven, in part, by the need to more effectively address the potential impacts of changes in water resources on rapidly growing populations that are reliant on glacial meltwater for municipal use and hydroelectricity. Results from other ongoing paleolimnological research (mainly from Lake Titicaca) had recognized that large moisture fluctuations character-

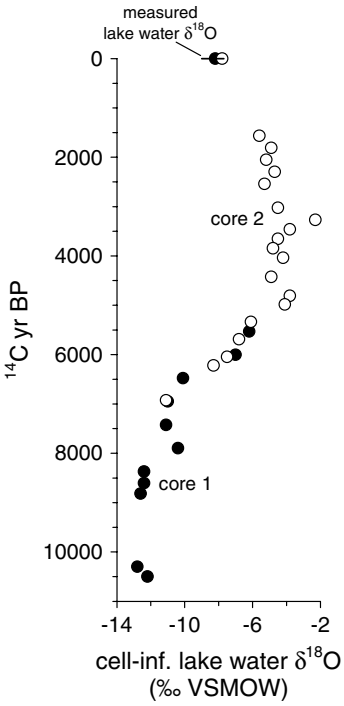

Fig. 4 Holocene cellulose-inferred lake water $\delta^{18}O$ record for Weslemkoon Lake, Ontario, derived from using a $\varepsilon^{18}_{\text{cell-lakewater}}$ value of 28.2‰ on samples from two cores obtained in different parts of the basin. Samples were prepared using methods similar to Wolfe et al. (2001b) excluding the Fe- and Mn-oxyhydroxide leaching step but incorporating heavy-liquid density separation using zinc chloride after the initial solvent extraction. Cellulose oxygen isotope composition was determined using nickel pyrolysis to isolate CO_2 (Thompson and Gray 1977) for analysis by dual-inlet isotope ratio mass spectrometry. Results have analytical uncertainty of ±0.2‰ based on several repeated $\delta^{18}O$ measurements. Error bars are smaller than size of symbol. Also shown is range of measured lake water $\delta^{18}O$ values from Weslemkoon Lake from samples taken in 1984 and 1985 (modified from Edwards and McAndrews 1989)

ized this region, which included marked aridity during the Holocene (e.g., Cross et al. 2000; Baker et al. 2001), but desiccation and discontinuous records had hampered paleoclimatic and paleohydrological reconstruction.

An important component of the multi-proxy studies referred to above was the use of aquatic cellulose oxygen isotope composition to reconstruct past hydroclimatic conditions during the late Pleistocene and Holocene. Improvements in the design of re-sealable nickel vessels (first described in Edwards et al. 1994 with modifications reported in Wolfe et al. 2001b) had simplified offline cryogenic isolation of CO_2, as compared to methodology used by Edwards and McAndrews (1989), permitting increased feasibility of high-resolution paleohydrological reconstructions. Notably, results from a cellulose-inferred lake water $\delta^{18}O$ profile from Lago Potosi, Bolivia, provided the basis for developing a continuous, quantitative, centennial-scale record of Holocene paleoclimate (Wolfe et al. 2001a). Deconvolution of the history of changing evaporative ^{18}O-enrichment (i.e., $\varepsilon^{18}_{\text{hydro}}$ or LEL-parallel shifts) from meteoric water $\delta^{18}O$ (i.e., $\delta^{18}O_{\text{mw}}$ or MWL-parallel shifts) in the lake sediment record was effectively constrained by comparison to an oxygen isotope profile from the Sajama ice core (Thompson et al. 1998). From this comparison, it was evident that variations in the Lago Potosi lake water $\delta^{18}O$ record were dominantly controlled by changes in evaporative ^{18}O-enrichment, which were interpreted to reflect shifts in local effective moisture (Fig. 5a). This record was used to estimate changes in summer relative humidity (and corresponding shifts in water balance) over the past 11,500 cal yr from isotope-mass balance calculations (Fig. 5b).

Model results indicated that the late Pleistocene was moist with summer relative humidity values estimated at 10–20% greater than present. Increasing aridity developed in the early Holocene with maximum prolonged dryness spanning 7,500–6,000 cal yr BP, an interval characterized by summer relative humidity values that may have been 20% lower than present. Highly variable but dominantly arid conditions persisted in the mid- to late Holocene, with average summer relative humidity values estimated at 15% below present, which then increased to about 10–20% greater than present by 2,000 cal yr BP. Slightly more arid conditions characterized the last millennium with summer relative humidity values ranging from 5–10% lower than present. A sensitivity analysis of the isotope-mass balance model provided a concise quantification of the main uncertainties in the paleohumidity reconstruction and was a key feature of this study, although correspondence with other paleohydrological records in the region supported the model results (Wolfe et al. 2001a; also see Abbott et al. 2003).

"Spruce Island Lake," Peace-Athabasca Delta, Alberta, Canada (Wolfe et al. 2005)

Extensive multidisciplinary research is being conducted to gain better understanding of the past and present hydrology, ecology and climate of the Peace-Athabasca Delta, Alberta, Canada, a highly productive northern boreal ecosystem of significant natural heritage (Wolfe et al. 2002). The aim of this ongoing research is to assess the impacts of both natural and anthropogenic factors, ranging from climatic variability and change to the influence of river flow regulation resulting from hydroelectric power generation at the headwaters of the Peace River since 1968. The latter is of particular interest because of the possibility that alteration of Peace River discharge may be affecting the frequency and magnitude of spring ice-jam flooding, which is considered to play an important role in the water balance of many basins that are perched above and disconnected from the complex channel network in the PAD (e.g., see Prowse and Lalonde 1996; Prowse and Conly 1998, 2000). Concerns were heightened in the early 1990s as an extended dry period that followed a major flood in 1974 had resulted in extremely low water levels in many perched basins, which provide important wildlife habitat (Prowse and Conly 1998). Absence of long-term hydrological and ecological records, however, has limited the ability to objectively evaluate the importance of anthropogenic versus natural climatic forcing in regulating hydroecological conditions of the PAD.

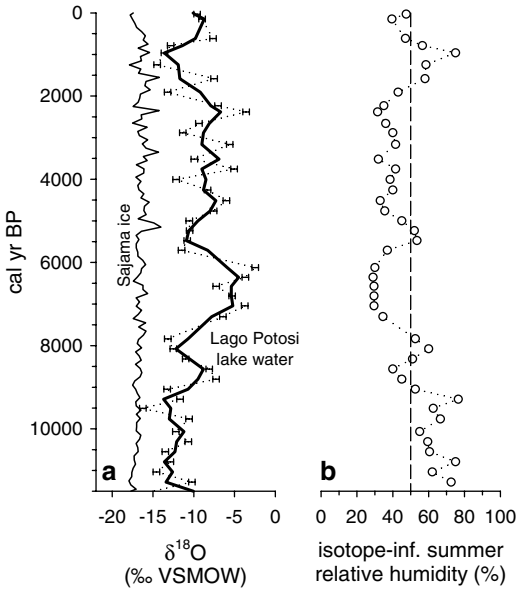

Fig. 5 (**a**) Late Pleistocene and Holocene cellulose-inferred lake water $\delta^{18}O$ record for Lago Potosi, Bolivia, calculated using a $\varepsilon^{18}_{\text{cell-lakewater}}$ value of 28‰. Samples were prepared according to Wolfe et al. (2001b). Cellulose oxygen isotope composition was determined using off-line nickel-tube pyrolysis to isolate CO_2 for analysis by dual-inlet isotope ratio mass spectrometry (Edwards et al. 1994). Error bars represent analytical uncertainty (±0.4‰) determined from repeated $\delta^{18}O$ measurements on 17 of 53 samples. Both raw and three-point running mean profiles are shown. The Sajama ice core $\delta^{18}O$ record is also shown (Thompson et al. 1998). Both records are plotted versus cal yr BP. (**b**) Reconstructed summer relative humidity derived from the cellulose-inferred lake water $\delta^{18}O$ data in (**a**), an isotope-mass balance model assuming steady-state evaporative enrichment fed by source waters of constant isotopic composition (i.e., estimated from the Sajama ice core $\delta^{18}O$ record), and constrained by utilizing multiple water-balance scenarios. Vertical dashed line is modern average summer relative humidity (modified from Wolfe et al. 2001a)

To address this shortcoming, a wide variety of physical, biological and geochemical measurements have been performed on lake sediment cores retrieved from many basins in the PAD to generate hydroecological records spanning the past several hundred years (Hall et al. 2004). In total, nearly 500 sediment cellulose $\delta^{18}O$ measurements (plus an additional ~400 as repeated analyses) were conducted on lake sediment cores between 2001 and 2003 using the latest sample preparation and analytical techniques described above. These methodological and technological improvements were essential for feasible inclusion of the lake sediment cellulose $\delta^{18}O$ approach into this large multi-site, multi-proxy project because high-temporal resolution was required and stringent time constraints were imposed for completion of the study. For most basins studied, changes in water balance (i.e., $\varepsilon^{18}_{\text{hydro}}$ or shifts parallel to the LEL) driven by local hydroclimatic factors (i.e., precipitation + catchment runoff – evaporation) as well as the frequency of flood events were identified as predominant controls on lake water $\delta^{18}O$ history based on extensive sampling and monitoring of lake water isotope composition as well as comparison to other lake sediment proxy indicators. Results from lake

sediment cellulose $\delta^{18}O$ stratigraphic analyses have thus played a central role in assessing quantitative changes in lake water balance history and have been particularly effective in placing the past 35 years of historical observation into a longer-term context as demonstrated below.

High-resolution (sub-decadal) analyses of the oxygen isotope composition of aquatic cellulose extracted from a sediment core from ''Spruce Island Lake,'' a shallow (1 m) perched basin in the PAD, have been especially informative as results illustrated that both wetter and drier conditions have occurred over the past 300 years when compared to recent decades (Wolfe et al. 2005). This included evidence for a period of prominent drought during the 18th century based on strongly enriched cellulose-inferred lake water $\delta^{18}O$ values (Fig. 6a). The cellulose-inferred lake water $\delta^{18}O$ record was quantified into a history of changing water balance, expressed in terms of an evaporation-to-inflow (E/I) ratio, using isotope-mass balance equations. Model results indicated strongly negative water balances ($E \gg I$) characterized much of the 18th century, whereas positive steady-state water balances ($E < I$) dominated for most of the past 230 years (Fig. 6b). Exceptions to the latter included a brief interval between ~1800 and ~1820 when Spruce Island Lake also experienced persistent non-steady-state net evaporation ($E > I$), and recent decade- to multi-decade-long intervals (~1940–1950; ~1965–1985) including the past few years in which the lake appears to have been, on average, close to hydrological balance ($E \approx I$). The E/I reconstruction was consistent with evidence from other indicators including carbon and nitrogen elemental geochemistry, diatom assemblages and plant macrofossils. Furthermore, close correspondence between Spruce Island Lake water balance history with independent records of river flood frequency and climate variability indicated that profound changes in hydrological conditions are a natural feature of the PAD (Wolfe et al. 2005).

Concluding comments

Recent advances in sample preparation and analysis have substantially expedited the use of aquatic cellulose in lake sediments as an isotopic archive of paleohydrological information. As demonstrated elsewhere, the method is best utilized within a broader multi-proxy approach. For example, combination of lake sediment stratigraphic analyses of cellulose oxygen isotope composition and diatom assemblages has proven

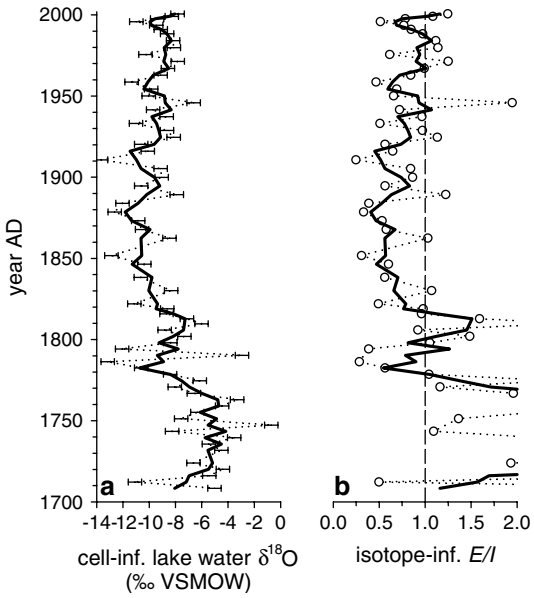

Fig. 6 (**a**) Three hundred-year lake water $\delta^{18}O$ history for Spruce Island Lake, Alberta, inferred from oxygen isotope analysis of aquatic cellulose isolated from a 35-cm sediment core and using a $\varepsilon^{18}_{\text{cell-lakewater}}$ value of 28‰. Samples were prepared according to Wolfe et al. (2001b), with additional purification using heavy-liquid density separation, and analysed using CF-IRMS. Error bars represent analytical uncertainty (±0.51‰) determined from repeated $\delta^{18}O$ measurements on 58 of 68 samples. Both raw and three-point running mean profiles are shown. Chronology is based on ^{210}Pb analyses extrapolated downcore. (**b**) Reconstructed evaporation-to-inflow (E/I) ratio history for Spruce Island Lake estimated using the cellulose-inferred lake water $\delta^{18}O$ profile in (**a**) and an isotope-mass balance model, assuming steady-state evaporative enrichment fed by source waters of constant isotopic composition and parameterization based on contemporary isotope hydroclimatology. Vertical dashed line represents *inflow = evaporation* (δ_{ss}) and approximates average water balance conditions observed between 2000 and 2005 based on isotopic analysis of several lake water samples collected over this period. Data plotting to the right of this line are indicative of drier conditions ($E > I$) compared to present, whereas values to the left reflect wetter conditions ($E < I$) compared to present. Both raw and three-point running mean profiles are shown (modified from Wolfe et al. 2005)

to be a particularly effective approach in our ongoing efforts to further understand the hydro-ecological evolution of the Peace-Athabasca Delta (PAD) ecosystem (Hall et al. 2004; Wolfe et al. 2005). Likewise, extensive isotopic monitoring of basins in the PAD has been particularly useful for constraining quantitative paleohydrological reconstructions, including the record from Spruce Island Lake briefly highlighted here (Wolfe et al. 2005). Significant effort is now being placed on developing and testing potential lake sediment δ^2H archives for direct deconvolution of lake water δ^{18}O and δ^2H histories, and corresponding MWL- versus LEL-parallel shifts through time, which will create additional opportunities for quantitative paleohydrological and paleoclimatic reconstructions (see Fig. 1).

Acknowledgements We would like to extend our thanks to funding agencies which have supported our isotope paleohydrology research over the past two decades. These primarily include the Natural Sciences and Engineering Research Council of Canada, the US National Science Foundation, and the Canada Foundation for Innovation and Ontario Innovation Trust, as well as BC Hydro, our industrial partner in ongoing paleoenvironmental studies of the Peace-Athabasca Delta. We are also especially grateful for the superb technical support provided by the staff of the University of Waterloo—Environmental Isotope Laboratory. Comments from two anonymous reviewers helped to improve the manuscript.

References

Abbott MB, Seltzer GO, Kelts KR, Southon J (1997) Holocene paleohydrology of the tropical Andes from lake records. Quat Res 47:70–80

Abbott MB, Wolfe BB, Aravena R, Wolfe AP, Seltzer GO (2000) Holocene hydrological reconstructions from stable isotopes and palaeolimnology, Cordillera Réal, Bolivia. Quat Sci Rev 19:1801–1820

Abbott MB, Wolfe BB, Wolfe AP, Seltzer GO, Aravena R, Mark BG, Polissar PJ, Rodbell DT, Rowe HD, Vuille M (2003) Holocene paleohydrology and glacial history of the central Andes using multiproxy lake sediment studies. Palaeogeog Palaeoclim Palaeoecol 194:123–138

Anderson L, Abbott MB, Finney BP (2001) Holocene climate inferred from oxygen isotope ratios in lake sediments, central Brooks Range, Alaska. Quat Res 53:313–321

Baker PA, Seltzer GO, Fritz SC, Dunbar RB, Grove MJ, Tapia PM, Cross SL, Rowe HD, Broda JP (2001) The history of South American tropical precipitation for the past 25,000 years. Science 291:640–643

Beuning KRM, Kelts K, Ito E, Johnson TC (1997) Paleohydrology of Lake Victoria, East Africa, inferred from $^{18}O/^{16}O$ ratios in sediment cellulose. Geology 25:1083–1086

Beuning KRM, Kelts K, Russell J, Wolfe BB (2002) Reassessment of Lake Victoria – upper Nile River paleohydrology from oxygen isotope records of lake-sediment cellulose. Geology 30:559–562

Buhay WM, Betcher RN (1998) Paleohydrologic implications of ^{18}O enriched Lake Agassiz water. J Paleolimnol 19:285–296

Cross SL, Baker PA, Seltzer GO, Fritz SC, Dunbar RB (2000) A new estimate of the Holocene lowstand level of Lake Titicaca, central Andes, and implications for Tropical palaeohydrology. The Holocene 10:21–32

Duthie HC, Yang J-R, Edwards TWD, Wolfe BB, Warner BG (1996) Hamilton Harbour, Ontario: 8300 years of limnological and environmental change inferred from microfossil and isotopic analyses. J Paleolimnol 15:79–97

Edwards TWD, Aravena RO, Fritz P, Morgan AV (1985) Interpreting paleoclimate from ^{18}O and ^{2}H in plant cellulose: comparison with evidence from fossil insects and relict permafrost in southwestern Ontario. Can J Earth Sci 22:1720–1726

Edwards TWD, Buhay WM, Elgood RJ, Jiang HB (1994) An improved nickel-tube pyrolysis method for oxygen isotope analysis of organic matter and water. Chem Geol (Iso Geosci Sect) 114:179–183

Edwards TWD, Fritz P (1986) Assessing meteoric water composition and relative humidity from ^{18}O and ^{2}H in wood cellulose: paleoclimatic implications for southern Ontario, Canada. Appl Geochem 1:715–723

Edwards TWD, Fritz P (1988) Stable-isotope paleoclimate records for southern Ontario, Canada: comparison of results from marl and wood. Can J Earth Sci 25:1397–1406

Edwards TWD, McAndrews JH (1989) Paleohydrology of a Canadian Shield lake inferred from ^{18}O in sediment cellulose. Can J Earth Sci 26:1850–1859

Edwards TWD, Wolfe BB, Gibson JJ, Hammarlund D (2004) Use of water isotope tracers in high-latitude hydrology and paleohydrology. In: Pienitz R, Douglas M, Smol JP (eds) Long-term environmental change in Arctic and Antarctic lakes, developments in paleoenvironmental research, vol 7. Springer, Dordrecht, pp 187–207

Edwards TWD, Wolfe BB, MacDonald GM (1996) Influence of changing atmospheric circulation on precipitation δ^{18}O-temperature relations in Canada during the Holocene. Quat Res 46:211–218

Farquhar GD, Henry BK, Styles JM (1997) A rapid on-line technique for determination of oxygen isotope composition of nitrogen-containing organic matter and water. Rapid Commun Mass Spectrom 11:1554–1560

Green JW (1963) Wood cellulose. In: Whistler RL (ed) Methods in carbohydrate chemistry, vol III. Academic Press, New York, pp 9–20

Hall RI, Wolfe BB, Edwards TWD, 17 others (2004) A multi-century flood, climatic, and ecological history of the Peace-Athabasca Delta, northern Alberta, Canada. Final Report. Published by BC Hydro. 163 pp + Appendices

Hay MB, Smol JP, Pipke KJ, Lesack LFW (1997) A diatom-based paleohydrological model for the Mackenzie Delta, Northwest Territories. Arc Alp Res 29: 430–444

MacDonald GM, Edwards TWD, Gervais B, Laing TE, Pisaric MFJ, Porinchu DF, Snyder JA, Solovieva N, Tarasov P, Wolfe BB (2004) Recent paleolimnological research from northern Russian Eurasia and Siberia. In: Pienitz R, Douglas M, Smol JP (eds) Long-term environmental change in Arctic and Antarctic lakes, developments in paleoenvironmental research, vol 7. Springer, Dordrecht, pp 349–380

MacDonald GM, Edwards TWD, Moser KA, Pienitz R, Smol JP (1993) Rapid response of treeline vegetation and lakes to past climate warming. Nature 361:243–246

Meyers PA, Teranes, JL (2001) Sediment organic matter. In: Last WM, Smol JP (eds) Tracking environmental change using lake sediments: physical and chemical techniques, developments in paleoenvironmental research, vol 2. Kluwer Academic Publishers, Dordrecht, pp 239–269

Morley DW, Leng MJ, Mackay AW, Sloane HJ, Rioual P, Batterbee RW (2004) Cleaning lake sediment samples for diatom oxygen isotope analysis. J Paleolimnol 31:391–401

Prowse TD, Conly FM (1998) Impacts of climatic variability and flow regulation on ice-jam flooding of a northern delta. Hydrol Proc 12:1589–1610

Prowse TD, Conly FM (2000) Multiple-hydrologic stressors of a northern delta ecosystem. J Aquat Ecosyst Str Recov 8:17–26

Prowse TD, Lalonde V (1996) Open-water and ice-jam flooding of a northern delta. Nord Hydrol 27:85–100

Sauer PE, Miller GH, Overpeck JT (2001) Oxygen isotope ratios of organic matter in arctic lakes as a paleoclimate proxy: field and laboratory investigations. J Paleolimnol 25:43–64

Saurer M, Robertson I, Siegwolf R, Leuenberger M (1998) Oxygen isotope analysis of cellulose: an interlaboratory comparison. Analyt Chem 70:2074–2080

Sternberg LSL (1989) Oxygen and hydrogen isotope ratios in plant cellulose: mechanisms and applications. In: Rundel PW, Ehleringer JR, Nagy KA (eds) Stable isotopes in ecological research. Springer-Verlag, New York, pp 124–141

Sternberg LSL, Anderson WT, Morrison K (2003) Separating soil and leaf water ^{18}O isotopic signals in plant stem cellulose. Geochem Cosmo Acta 67:2561–2566

Talbot MR (2001) Nitrogen isotopes in paleolimnology. In: Last WM, Smol JP (eds) Tracking environmental change using lake sediments: physical and chemical techniques, developments in paleoenvironmental research, vol 2. Kluwer Academic Publishers, Dordrecht, pp 401–439

Thompson LG, Davis ME, Mosley-Thompson E, Sowers TA, Henderson KA, Zagorodnov VS, Lin P-N, Mikhalenko VN, Campen RK, Bolzan JF, Cole-Dai J, Francou B (1998) A 25,000-year tropical climate history from Bolivian ice cores. Science 282:1858–1864

Thompson P, Gray J (1977) Determination of $^{18}O/^{16}O$ ratios in compounds containing C, H, and O. Internat J App Rad Isot 28:411–415

Vincent JF (1999) From cellulose to cell. J Exp Biol 202:3263–3268

Wolfe BB, Aravena R, Abbott MB, Seltzer GO, Gibson JJ (2001a) Reconstruction of paleohydrology and paleohumidity from oxygen isotope records in the Bolivian Andes. Palaeogeog Palaeoclim Palaeoecol 176:177–192

Wolfe BB, Edwards TWD, Aravena R, Forman SL, Warner BG, Velichko AA, MacDonald GM (2000) Holocene paleohydrology and paleoclimate at treeline, north-central Russia, inferred from oxygen isotope records in lake sediment cellulose. Quat Res 53:319–329

Wolfe BB, Edwards TWD, Aravena R, MacDonald GM (1996) Rapid Holocene hydrologic change along boreal treeline revealed by $\delta^{13}C$ and $\delta^{18}O$ in organic lake sediments, Northwest Territories, Canada. J Paleolimnol 15:171–181

Wolfe BB, Edwards TWD, Elgood RJ, Beuning KRM (2001b) Carbon and oxygen isotope analysis of lake sediment cellulose: methods and applications. In: Last WM, Smol JP (eds) Tracking environmental change using lake sediments: physical and chemical techniques, developments in paleoenvironmental research, vol 2. Kluwer Academic Publishers, Dordrecht, pp 373–400

Wolfe BB, Edwards TWD, Hall RI (2002) Past and present ecohydrology of the Peace-Athabasca Delta, northern Alberta, Canada: water isotope tracers lead the way. PAGES News 10:16–17

Wolfe BB, Edwards TWD, Jiang H, MacDonald GM, Gervais BR, Snyder JA (2003) Effect of varying oceanicity on early to mid-Holocene palaeohydrology, Kola Peninsula, Russia: isotopic evidence from treeline lakes. Holocene 13:153–160

Wolfe BB, Karst-Riddoch TL, Vardy SR, Falcone MD, Hall RI, Edwards TWD (2005) Impacts of climate and river flooding on the hydro-ecology of a floodplain basin, Peace-Athabasca Delta, Canada: A.D. 1700-present. Quat Res 64:147–162

Yakir D (1992) Variations in the natural abundance of oxygen-18 and deuterium in plant carbohydrates. Pl Cell Environ 15:1005–1020

Appendix III:

Climate-driven shifts in quantity and seasonality of river discharge at the hydrographic apex of North America*

Summary Availability of water is a major economic, environmental and societal concern in western North America. Runoff generated from high elevations is the primary source of freshwater for this vast region, yet this declining resource is managed on the basis of short instrumental records that capture an insufficient range of climatic conditions. Here we probe the effects of climate change over the past 1000 years on the quantity and seasonality of river discharge in the upper Mackenzie River system based on paleoenvironmental information from the Peace-Athabasca Delta. These data reveal that recent climate-driven hydrological change has taken a trajectory which is unprecedented in the context of the past millennium. Increasingly prudent allocation of water resources is needed to satisfy human demands while maintaining the integrity of downstream ecosystems.

* Manuscript in preparation as: Wolfe B.B., Hall R.I., Edwards T.W.D., Jarvis S.R., Sinnatamby R.N., Yi Y., Johnston J.W., Climate-driven shifts in quantity and seasonality of river discharge at the hydrographic apex of North America.

Availability of water is a major economic, environmental and societal concern in western North America. Runoff generated from high elevations is the primary source of freshwater for this vast region, yet this declining resource is managed on the basis of short instrumental records that capture an insufficient range of climatic conditions. Here we probe the effects of climate change over the past 1000 years on the quantity and seasonality of river discharge in the upper Mackenzie River system based on paleoenvironmental information from the Peace-Athabasca Delta. These data reveal that recent climate-driven hydrological change has taken a trajectory which is unprecedented in the context of the past millennium. Increasingly prudent allocation of water resources is needed to satisfy human demands while maintaining the integrity of downstream ecosystems.

Many regions of western North America are experiencing critical water shortages, suggesting we have entered a new hydrological regime that will challenge society to respond effectively (*1-3*). Shrinking headwater glaciers, decreasing alpine snowmelt runoff, and declining river discharges in the northern Cordillera, the so-called hydrographic apex of North America (*4*), have largely unknown consequences for natural resource development and downstream watersheds (*5-6*). Like other streams that drain this part of the continent and flow across the northern Great Plains, where seasonal and extended intervals of water deficit are a natural element of the landscape, the Peace and Athabasca rivers provide water that is crucial for societal needs (*7*). Climate variability and exponentially increasing industrial development are, however, raising concerns over the future availability of water resources for continued economic growth in these watersheds and to maintain the integrity of aquatic ecosystems, including the internationally-renowned Peace-Athabasca Delta. This is particularly acute for the Athabasca River because the Alberta oil sands industry remains dependent on its water for bitumen extraction. Water consumption at current and projected rates could have undesirable downstream ecological consequences (*5,6,8*). Assessment of contemporary relations between climate and river discharge is limited by the short duration of meteorological and hydrometric records (generally <100 years; *4,9*). Longer hydrological records are needed to evaluate the responses of river discharge to a range of natural climatic conditions - knowledge that is essential for informed management of water resources (*10*).

Here, we assemble high-resolution paleohydrological records from multiple proxies measured in lake sediment cores obtained from an oxbow lake ('PAD15'), an upland perched basin (PAD 5), and two lowland basins (PAD 9, PAD 12) in the Peace-Athabasca Delta (PAD), as well as from a lagoonal pond on nearby Bustard Island in Lake Athabasca, to examine the effects of changing climate and runoff

generation on the quantity and seasonality of river discharge in western Canada (Fig. 1). Located in the Boreal Plains ecozone at the convergence of the Peace and Athabasca rivers, the PAD is a large (3900 km^2), lake-rich floodplain landscape recognized by international conventions (UNESCO World Heritage Site; Ramsar Wetland) for its ecological significance. Our hydrological reconstructions span the past millennium, a time frame that includes a broad range of climatic conditions during the medieval (~1000 to 1530 CE), Little Ice Age (LIA; ~1530 to 1890) and post-LIA intervals in the Athabasca headwater region (*11*).

Results (Fig. 2; *12*) show that during medieval times the upland site (PAD 5) and one of the lowland basins (PAD 12) were persistently influenced by river floodwater as indicated by cellulose-inferred lakewater ^{18}O values ($^{18}O_{lw}$ for PAD 5: ~ -19 to -16 ‰; PAD 12: ~ -22 to -19 ‰) that are similar to modern-day values of local Peace River ^{18}O during spring break-up (-20.1 to -19.0 ‰). Presence of diatom taxon *Gyrosigma acuminatum* (3-40% abundance) at PAD 12 is consistent with frequent flooding because *Gyrosigma* is tolerant of river-borne sediment influx (*13*). The paleohydrological record for the oxbow lake (PAD 15) only extends to ~1418, but persistently high magnetic susceptibility and C/N ratios also indicate that frequent high-magnitude ice-jam floods from the Peace River occurred during this time. In contrast, the other lowland site (PAD 9) did not receive substantial river flooding and diatom assemblages are reflective of closed-drainage hydrological conditions. Likewise, Lake Athabasca water levels were low based on high C/N ratios at Bustard Island North Pond.

Pronounced corresponding changes in Peace River flood frequency and magnitude and upland lake hydrology occurred during the transition into the LIA (Fig. 2). Peace River flood frequency and magnitude, recorded by magnetic susceptibility and C/N ratios at PAD 15, declined precipitously at ~1600 and remained variable until ~1850. At PAD 5, $^{18}O_{lw}$ values rose correspondingly by ~10 ‰ between ~1550 and 1600, attaining values that may reflect periodic to seasonal dessication of the basin between ~1600 and 1700. Between ~1700 and ~1900, $^{18}O_{lw}$ values at PAD 5 fluctuated between ~-12 and -7 ‰, which are typical of closed-drainage conditions in this ecosystem and are similar to those measured from lakewater samples obtained directly from PAD 5 (-13.4 to -3.4 ‰) over the course of several years of recent monitoring.

Marked changes in lowland hydrology at PAD 9 and Lake Athabasca water levels also occurred between ~1600 and 1900, but proxy indicators reflect higher, rather than lower, water levels (Fig. 2). These data, supported by evidence from historical maps, indicate that Lake Athabasca expanded westward into low-lying areas of the delta and generated elevated discharge along some outflow channels

leading to the frequent flooding of PAD 9 (*14*). At the other lowland site, PAD 12, stratigraphic changes at ~1600 are similar to both PAD 5 and PAD 9. Like PAD 5, PAD 12 $^{18}O_{lw}$ values rapidly increased ~1600 and remained high until ~1650 (~ -15 ‰), although not as high as at PAD 5, indicating the lake did not approach dessication. Instead, PAD 12 received Lake Athabasca outflow waters at this time based on the rise in the abundance of open-drainage diatoms, similar to PAD 9.

Hydrological conditions during the 20th century are characterized by complacent magnetic susceptibility and C/N ratio records at PAD 15, suggesting low frequency and magnitude of floods; increasing but moderate $^{18}O_{lw}$ values at PAD 5, indicating increasing importance of evaporation; and, closed-drainage conditions at PAD 9 and PAD 12 with the lowering of Lake Athabasca water levels.

Multi-centennial records of Peace River flood frequency and magnitude, perched basin upland and lowland hydrology in the PAD, and Lake Athabasca water level closely correlate with the three-phase climate history at the headwaters of the Athabasca River (*11*; Fig. 2). As we discuss below, the site-specific paleohydrological trajectories, which are complex at the landscape scale, can be reconciled by considering the quantity and seasonality of river discharge originating in the eastern Rocky Mountains in the context of climate and glacier mass balance variability over the past 1000 years.

Glaciers advanced in the Rocky Mountains during the early millennium (mainly between ~1150-1380 and ~1450-1505; Fig. 2) because of increased snowfall at high elevations (*11,15*). The earlier time interval includes the "Medieval Megadrought" (~1000-1300) when widespread hydrological drought occurred throughout western North America (*16*), although our results indicate that lakes in the northern portion of the PAD were frequently flooded. Lowland areas in the central part of the delta did not receive floodwater because of low levels in Lake Athabasca. The latter is supported by high C/N ratios at Bustard Island North Pond and agrees with low mean annual streamflow reconstructed for the adjacent North Saskatchewan River watershed (*17*; Fig. 1). These results suggest that warmer conditions during the Medieval Megadrought, and for perhaps two centuries thereafter, continued to cause early and rapid melt of the annual snowpack in the headwater region of rivers draining the eastern Rocky Mountains. These are hydroclimatic conditions conducive for frequent, severe ice-jam flooding downstream (*18-20*) but are less favourable for sustaining river discharge, and Lake Athabasca water levels, beyond the spring melt period (*9*).

Several documented glacier advances also occurred during the LIA in the Rocky Mountains, including ~1585-1615, ~1695-1720 and ~1815-1860 (Fig. 2), in response to colder conditions between the 16th and 19th centuries (*11,15*). These are associated with decreases in flood frequency and magnitude recorded in the magnetic susceptibility and C/N ratios in the sediment record from PAD 15, likely

because of increased glacial storage of water. General decline in flood frequency and magnitude over this time interval is consistent with the transition to colder conditions during the LIA because slow melting during the spring thaw tends to suppress dynamic ice break-up downstream in the vicinity of the PAD (*18-20*). Reduction in flood frequency and magnitude caused the water balance of PAD 5 to switch rapidly from being controlled by river flooding to local climate. Under drier hydroclimatic conditions of the LIA, PAD 5 underwent extreme evaporation similar to elsewhere in the prairie region (*21-22*). While local atmospheric conditions created low water levels at PAD 5, rising Lake Athabasca water levels clearly reflect a different hydrological response to prevailing climatic conditions. Based on these reconstructions, we suggest that delayed generation of snowmelt runoff in the Peace and Athabasca river headwaters reduced the frequency and magnitude of ice-jams downstream but sustained greater summer river discharge and higher water levels in Lake Athabasca during the LIA. In contrast, upland areas in the northern Peace sector of the delta beyond the reach of low-magnitude floods and rising Lake Athabasca waters experienced net evaporative drawdown as a result of locally arid conditions and reduced contributions from local precipitation.

The assemblage of 20th century hydrological conditions recorded at these sites in the PAD, which includes low flood frequency and magnitude, and closed-drainage conditions at both upland and lowland basins, are unlike any other time interval during the past 1000 years (Fig. 2). These reconstructions indicate that the combined influence of the Peace and Athabasca rivers has contributed less to maintaining the hydrological status of lakes in some parts of the PAD during this century than during any other over the past millennium - a probable outcome of shrinking headwater glaciers and decreasing alpine snowmelt runoff since the conclusion of the LIA (*23*). Consequently, drying trends at the lowland basins of the past 100 years reflect declining fluvial input, consistent with gauged records of the Athabasca River (*5*), but are likely also a response to locally decreasing relative humidity over this same time period (*8*). The latter is mainly responsible for the corresponding drying trend at PAD 5 (*8,24*). While continued warming might be expected to generate hydrological conditions experienced during the early millennium, a comparable return of elevated flood frequency and magnitude is unlikely because of diminishing meltwater sources needed to trigger dynamic break-up events downstream (*25*). Thus, the ecological integrity of the PAD may well be at a crossroads. Further drying appears inevitable because declining alpine snowpack and river discharge trends are expected to continue (*1,4,9,26*).

The temporal perspective offered by these paleohydrological reconstructions indicates that climatic changes over the past millennium have led to characteristic responses in the quantity and seasonality of streamflow generated from the hydrographic apex of North America (Fig. 3). For water

resource managers, a key feature that emerges from these results is that the hydrograph of the 20th century is unprecedented over the past 1000 years. Continuing reduction in both peak and total discharge clearly underscores the need for stringent allocation of freshwater resources in these watersheds, and in others reliant on alpine snowmelt runoff (*1*).

References and Notes

1. T. P. Barnett, J. C. Adam, D. P. Lettenmaier, *Nature* **438**, 303 (2005).
2. T. P. Barnett *et al.*, *Science* **319**, 1080 (2008).
3. P. C. D. Milly *et al.*, *Science* **319**, 573 (2008).
4. S. B. Rood, G. M. Samuelson, J. K. Weber, K. A.Wywrot, *J. Hydrol.* **306**, 215 (2005).
5. D. W. Schindler, W. F. Donahue, *Proc. Natl. Acad. Sci. U.S.A.* **103**, 7210 (2006).
6. D. W. Schindler, J. P. Smol, *Ambio* **35**, 160 (2006).
7. D. Sauchyn, S. Kulshreshtha, in *From Impacts to Adaptation: Canada in a Changing Climate 2007*, D. S. Lemmen, F. J Warren, J. Lacroix, E. Bush, Eds. (Government of Canada, Ottawa, 2008). chap 7, 275-328.
8. B. B. Wolfe *et al.*, *Ecohydrology* **1**, 131 (2008).
9. S. B. Rood *et al.*, *J. Hydrol.* **349**, 397 (2008).
10. D. A. Sear, N. W. Arnell, *Catena* **66**, 169 (2006).
11. T. W. D. Edwards, S. J. Birks, B. H. Luckman, G. M. MacDonald, *Quat. Res.*in press (2008).
12. Paleohydrological reconstructions from the lake sediment records are derived from physical, geochemical and biological analytical results, and are constrained temporally by radiometric measurements. Information on materials and methods is available on Science Online.
13. L. S. Fore, C. Grafe, *Freshwater Biol.* **47**, 2015 (2002).
14. R. N. Sinnatamby, thesis, University of Waterloo (2006).
15. B. H. Luckman, R. J. S. Wilson, *Clim. Dyn.* **24**, 131 (2005).
16. E. R. Cook, C. A. Woodhouse, C. M Eakin, D. M. Meko, D. W. Stahle, *Science* **306**, 1015 (2004).
17. R. A. Case, G. M. MacDonald, *J. Am. Water Res. Assoc.* **39**, 703 (2003).
18. T. D. Prowse, V. Lalonde, *Nord. Hydrol.* **27**, 85 (1996).
19. T. D. Prowse, F. M. Conly, *Hydrol. Proc.* **12**, 1589 (1998).
20. S. Beltaos, *Hydrol. Proc.* **17**, 3685 (2003).
21. S. A. Wolfe *et al.*, *Can. J. Earth Sci.* **38**, 105 (2001).
22. S. St. George, E. Nielsen, *Quat. Res.* **58**, 103 (2002).
23. M. N. Demuth, R. Keller, in *Peyto Glacier: One Century of Science*, M. N. Demuth, D. S. Munro, G. J Young, Eds. (National Hydrology Research Institute Science Report #8, Saskatoon, 2006). 83-134.
24. B. B. Wolfe *et al.*, *Quat. Res.* **64**, 147 (2005).
25. S. Beltaos *et al.*, *Hydrol. Proc.* **20**, 4031 (2006).

26. S. Lapp, J. Byrne, I. Townshend, S. Kienzle, *Int. J. Climatol.* **25**, 521 (2005).
27. Financial support was received from the Natural Sciences and Engineering Research Council of Canada (Northern Research Chair, Collaborative Research and Development Grant, and Discovery Grant programs), British Columbia Hydro and Power Authority, Government of Ontario (Premier Research Excellence Awards), the Polar Continental Shelf Project and the Northern Scientific Training Program of Indian and Northern Affairs Canada. Wood Buffalo National Park provided logistical support. Matthew Falcone, Michael Sokal, Florence Sylvestre and Paige Harms analyzed samples from lakes PAD 5, 9, 12 and Bustard Island North Pond, respectively.

Figures

Figure 1. The watersheds of the Peace and Athabasca rivers are located near the hydrographic apex of western North American drainage and are major headwater contributors to the Mackenzie River. Also shown is the adjacent North Saskatchewan River to the south. Identified sites are locations of study basins in the Peace-Athabasca Delta (PAD 5, 9, 12, 15) and on Bustard Island (North Pond; BINP) in western Lake Athabasca, Alberta, Canada.

Figure 2. Multi-centennial records of Athabasca River headwater climate (winter temperature [T_{win}) and growth season relative humidity [RH_{grs}]) (*11*), Peace River flood frequency and magnitude (PAD 15 magnetic susceptibility and weight C/N ratios), Peace-Athabasca Delta upland (PAD 5 cellulose-inferred lakewater ^{18}O) and lowland hydrology (PAD 12 cellulose-inferred lakewater ^{18}O; PAD 9, PAD 12 closed- and open-drainage indicator diatoms, and diatom taxon *Gyrosigma acuminatum*), and Lake Athabasca water level (Bustard Island North Pond weight C/N ratios). Athabasca headwater climate and PAD 15 magnetic susceptibility records are plotted using z-scores, a dimensionless quantity that indicates the number of standard deviations relative to the mean value. Shaded intervals identify known periods of glacier advance in the eastern Rocky Mountains (*11,15*). Hatched lines mark the three-phase paleoclimate sequence identified in the text (*11*).

Figure 3. Schematic river discharge hydrographs for the Medieval Period (solid red line), Little Ice Age (LIA; solid blue line), 20th century (solid black line) and the anticipated future (dashed black line) (*1,8,9*). Analysis of hydrometric data indicates transition to the future scenario, characterized by reduced river discharge during the spring freshet (which will continue to discourage ecologically important ice-jam flooding) and low summer discharge (which is important to sustain economically important industrial activities such as the Alberta oil sands development), is well underway (*9*).

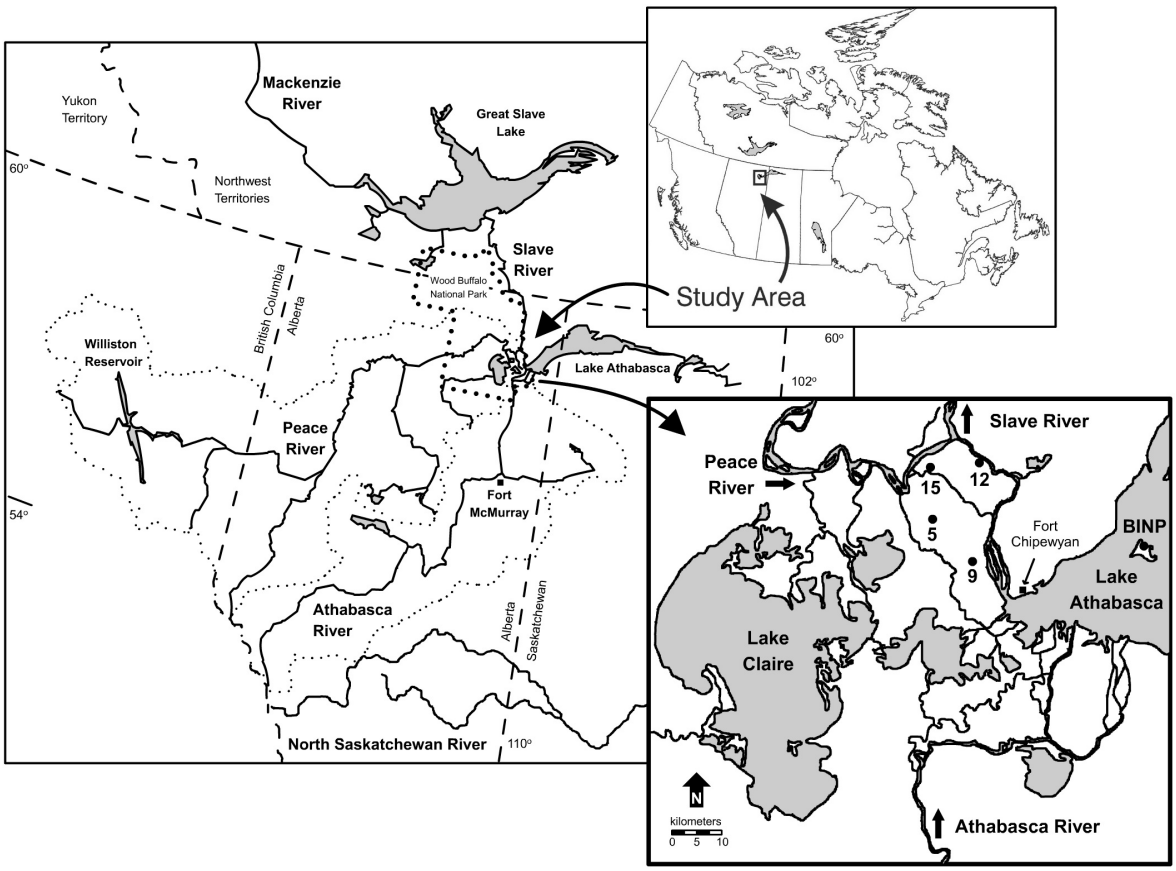
Yukon Territory
Mackenzie River
Great Slave Lake
60°
Northwest Territories
Slave River
Wood Buffalo National Park
British Columbia
Alberta
Williston Reservoir
Lake Athabasca
102°
Peace River
Fort McMurray
54°
Athabasca River
Alberta
Saskatchewan
North Saskatchewan River
110°
Study Area
Slave River
Peace River
15
12
5
9
Fort Chipewyan
BINP
Lake Athabasca
Lake Claire
N
kilometers
0 5 10
Athabasca River

Figure 1.

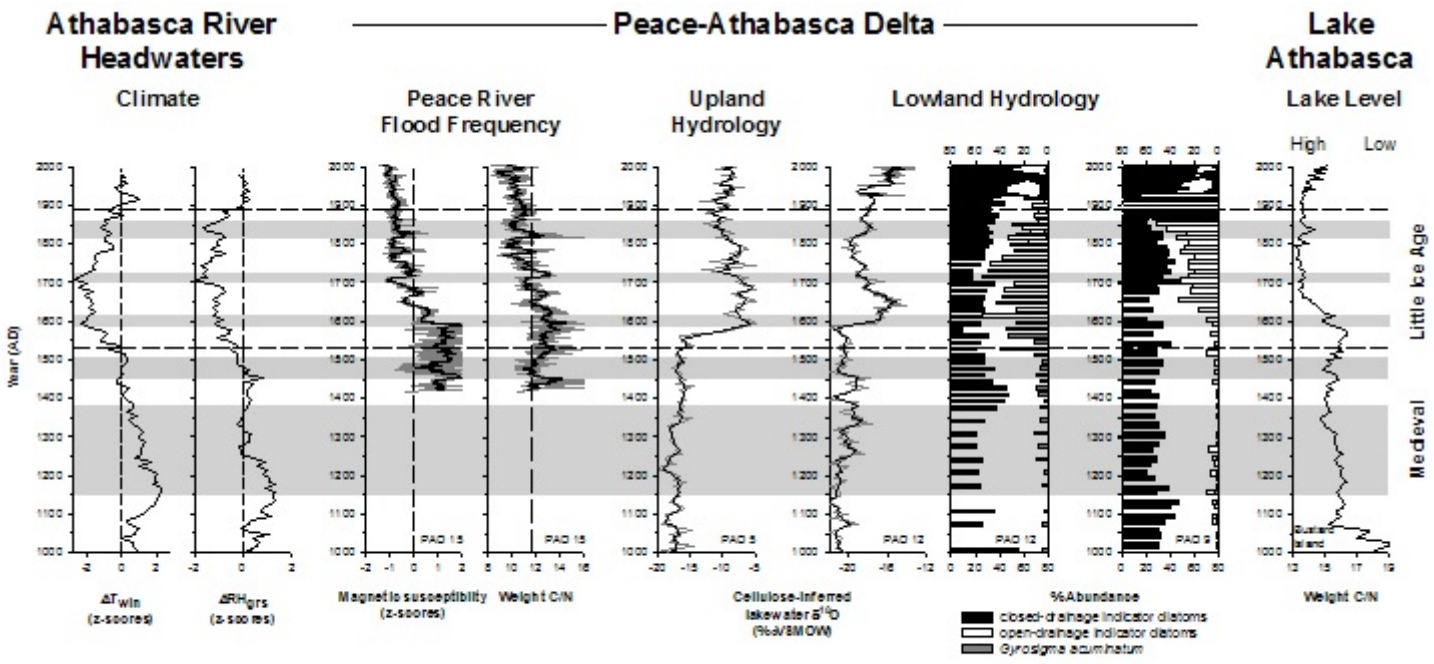
Athabasca River Headwaters
Peace-Athabasca Delta
Lake Athabasca
Climate
Peace River Flood Frequency
Upland Hydrology
Lowland Hydrology
Lake Level
High
Low
Little Ice Age
Medeval
Year (AD)
ΔT_win (z-scores)
ΔRH_grs (z-scores)
Magnetic susceptibility (z-scores)
Weight C/N
Cellulose-Inferred lakewater δ18O (‰VSMOW)
%Abundance
closed-drainage indicator diatoms
open-drainage indicator diatoms
Gyrosigma acuminatum
PAO 15
PAO 5
PAO 12
PAO 9

Figure 2.

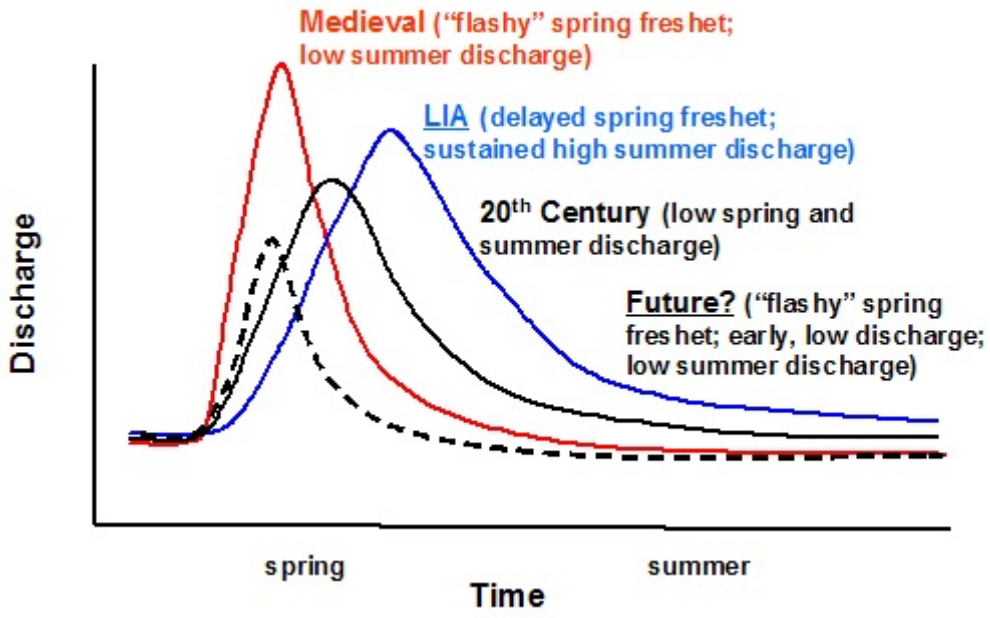
Medieval ("flashy" spring freshet; low summer discharge)
LIA (delayed spring freshet; sustained high summer discharge)
20th Century (low spring and summer discharge)
Future? ("flashy" spring freshet; early, low discharge; low summer discharge)
Discharge
spring
summer
Time

Figure 3.

Supplemental materials and methods

Sediment cores were collected in June 2001 (PAD 5, 9, 12) and July 2004 (Bustard Island North Pond) from a floating platform, and in March 2005 (PAD 15) from lake ice. A gravity corer was used to collect the upper ~30 cm of sediment from all basins. Overlapping 1-m core sequences of lake sediment were retrieved from PAD 5, 9, 12 and Bustard Island North Pond using a Russian peat corer with extension rods. A continuous 5.3-m sediment core was collected from PAD 15 using a vibra-corer system. All sediment cores were sectioned at 0.5-cm intervals for chronological and multi-proxy analyses.

Results from radiometric (^{137}Cs, ^{210}Pb, ^{14}C) analyses are used to establish the lake sediment chronologies (Table S1; Fig. S1). For PAD 5, 9, 12 and Bustard Island North Pond, sediment ages to ~1850 CE are calculated from ^{210}Pb measurements using the Constant Rate of Supply model (*S1*). Depth-age relationships for older sediment are based on results from ^{14}C analyses on plant macrofossils and organic sediment. Results generate similar average sedimentation rates for these basins over the past 1000 years (0.69, 0.56, 0.82 and 0.69 mm yr^{-1} for PAD 5, 9, 12 and Bustard Island North Pond, respectively). Much more rapid sedimentation rates (0.99 cm yr^{-1} from 1418-1595 and 0.92 cm yr^{-1} from 1595-2005) and consequent dilution of unsupported ^{210}Pb preclude its use at PAD 15; the sediment chronology for the upper strata is estimated using an average sedimentation rate determined from a peak in ^{137}Cs concentration, interpreted to reflect maximum atmospheric fallout in 1964. Minor adjustment in average sedimentation rate downcore is constrained by stratigraphic correlation to another core from the basin where additional ^{14}C measurements on macrofossils were performed (*S2*).

Reconstruction of Peace River flood frequency and magnitude is derived from magnetic susceptibility and carbon-to-nitrogen weight ratio measurements on laminated sediments of PAD 15. The same analyses on a previously collected Russian core sequence showed that peaks in these measurements were due to the introduction of detrital material to the oxbow lake and corresponded with known ice-jam flood events that have occurred since 1970 (*S3*). These relations were used to develop a 300-year record of flood frequency and magnitude that closely corresponded with a similar flood reconstruction from another nearby oxbow lake as well as the historical ice-jam flood record. Stratigraphic agreement exists between the flood reconstruction for PAD 15 based on the Russian core sequence and the new, longer vibra-core record reported here for the period of overlap (*S2*).

The record of upland hydrology at PAD 5 is based on the reconstruction of lakewater ^{18}O from analyses of aquatic cellulose ^{18}O, utilizing a cellulose-water oxygen isotope fractionation factor of 1.028 (*S4*). Agreement exists between average lakewater ^{18}O from several years of isotopic monitoring and

uppermost cellulose-inferred lakewater ^{18}O from the sediment core. This supports the use of sediment cellulose as a tracer of lakewater oxygen isotope history, which, for this basin, is mainly controlled by local hydroclimatic factors (i.e., precipitation + catchment runoff - evaporation) as well as the input of high-magnitude floods from the Peace River (*S5*).

Variability in lowland hydrology for PAD 9 is inferred from diatom assemblages. Diatom assemblages for PAD 9 were summed into taxa indicative of closed- and open-drainage hydrological categories based on contemporary relationships between these indicators and environmental variables, as determined from a surface-sediment dataset spanning 52 basins along a hydrological gradient in the PAD (*S6,S7*). *Gyrosigma acuminatum* was not well characterized within the surface-sediment surveys. However, the *Gyrosigma* genus is comprised of motile taxa that occupy epipelic habitats and are known to tolerate rapid sedimentation (*S8*) and is thus likely associated with river floodwaters. For the other lowland basin, PAD 12, approaches described above for PAD 5 and PAD 9 were utilized.

Changes in carbon-to-nitrogen (C/N) weight ratios at Bustard Island North Pond are due to changes in the delivery of terrestrial organic matter relative to aquatic organic matter, as commonly applied elsewhere (*S9*). Low C/N ratios are consistent with rising pond water and a reduction in terrestrial organic matter reaching the coring site. Although the pond is separated from Lake Athabasca by a sand barrier, the lake controls the local groundwater table, which provides a hydrological connection between the two water bodies. Thus, Lake Athabasca water levels also likely rose during these times. Conversely, elevated C/N ratios are interpreted to be due to low pond (and lake) levels because of encroachment of the pond's shoreline and increase in delivery of terrestrial organic matter to the coring location.

Table S1. Radiocarbon data for lake sediment cores from PAD 5, 9, 12 and Bustard Island North Pond. Median calibrated ages were used in depth-age calculations.

Lab. number	Material	Sediment core depth (cm)	Reported age (^{14}C yr BP)	Calibrated 2σ age range (Cal yr AD)
PAD 5				
Beta-169362	aquatic seed	42.25	530±40	1320 to 1350; 1390 to 1440
Beta-165112	wood	47.5	890±40	1020 to 1240
Beta-169363	aquatic seed	73.75	1380±40	620 to 690
Beta-169364	aquatic seed	80.5	1470±40	530 to 650
Beta-232443	aquatic seed	116.25	1650±40	260 to 280, 330 to 450, 450 to 460, 480 to 530
Beta-232445	aquatic seed	182.25	2660±40	-900 to -790
Beta-232446	aquatic seed	216.25	3100±40	-1440 to -1280
PAD 9				
Beta-193586	*Sparganium*, *Carex*, *Scirpus* and *Rumex* seeds	74.5	1540±40	420 to 620
PAD 12				
Beta-160220	*Cyperaceae* seeds, wood fragments and spruce needles	119.0	1630±40	350 to 530
Bustard Island North Pond				
Beta-223382	organic sediment	68.0	1030±50	900 to 1050, 1100 to 1140

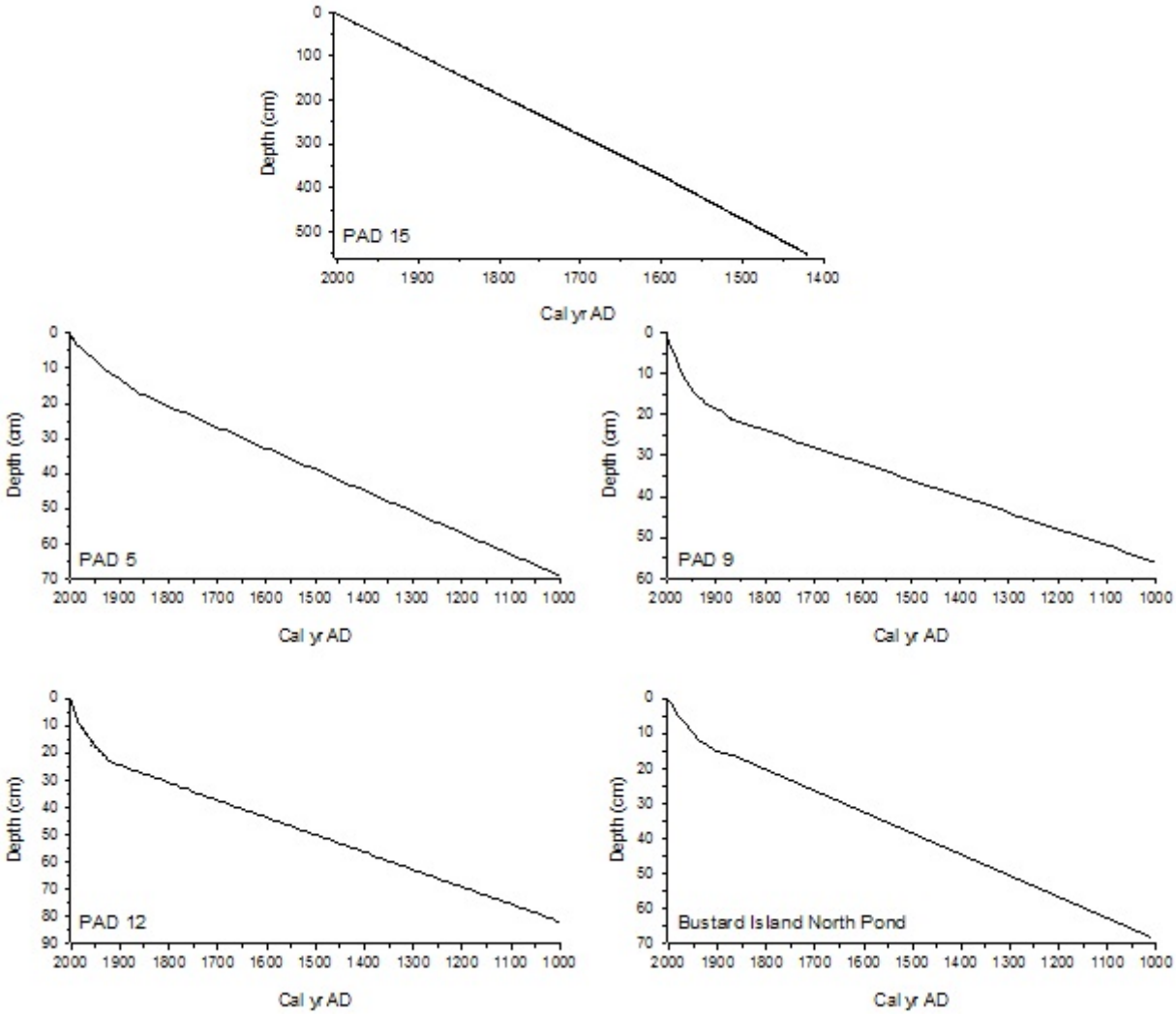

Figure S1. Lake sediment depth-age plots for PAD 15, 5, 9, 12, and Bustard Island North Pond.

References

S1. P. G. Appleby, in *Tracking Environmental Change Using Lake Sediments: Basin Analysis, Coring, and Chronological Techniques*, Developments in Paleoenvironmental Research, vol. 1, W. M. Last, J. P. Smol, Eds. (Kluwer, Dordrecht, 2001). 171-203.

S2. S. R. Jarvis, thesis,Wilfrid Laurier University (2008).

S3. B. B. Wolfe *et al*., *Hydrol. Proc.* **20**, 4131 (2006).

S4. B. B. Wolfe, T. W. D. Edwards, R.J. Elgood, K. R. M. Beuning, in *Tracking Environmental Change Using Lake Sediments: Basin Analysis, Coring, and Chronological Techniques*, Developments in Paleoenvironmental Research, vol. 2, W. M. Last, J. P. Smol, Eds. (Kluwer, Dordrecht, 2001). 373-400.

S5. B. B. Wolfe *et al.*, *Quat. Res.* **64**, 147 (2005).

S6. R. N. Sinnatamby, thesis, University of Waterloo (2006).

S7. R. I. Hall, B. B. Wolfe, T. W. D. Edwards, "A multi-century flood, climatic, and ecological history of the Peace-Athabasca Delta, northern Alberta, Canada" (Final Report, Published by BC Hydro, Burnaby, 2004).

S8. L. S. Fore, C. Grafe, *Freshwater Biol.* **47**, 2015 (2002).

S9. P. A. Meyers, J. L. Teranes, in *Tracking Environmental Change Using Lake Sediments: Basin Analysis, Coring, and Chronological Techniques*, Developments in Paleoenvironmental Research, vol. 2, W. M. Last, J. P. Smol, Eds. (Kluwer, Dordrecht, 2001). 239-270.